AD NUMBER

AD297539

NEW LIMITATION CHANGE

TO

Approved for public release, distribution unlimited

FROM

Distribution authorized to U.S. Gov't. agencies and their contractors; Administrative/Operational Use; Oct 1962. Other requests shall be referred to Aeronautical Systems Division, Wright-Patterson AFB, OH 45433.

AUTHORITY

ASD/USAF ltr, 30 Nov 1989

ASD-TR 61-22
Part II
AD0297539

POLYMER STRUCTURES AND PROPERTIES

TECHNICAL REPORT NO ASD-TR 61-22
PART II

October, 1962

DIRECTORATE OF MATERIALS AND PROCESSES
AERONAUTICAL SYSTEMS DIVISION
AIR FORCE SYSTEMS COMMAND
WRIGHT-PATTERSON AIR FORCE BASE, OHIO

Project No. 7342, Task No. 734203

(Prepared under Contract No. AF 33(616)-6968;
Mellon Institute, Pittsburgh, Pennsylvania;
T. A. Orofino, J. W. Mickey, E. F. Casassa,
G. C. Berry, V. R. Allen, T. G Fox,
C. A. J. Hoeve, and M. O'Brien, authors)

DISCLAIMER NOTICE

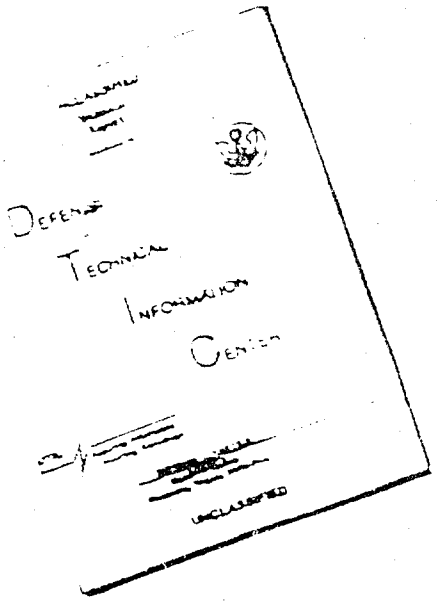

THIS DOCUMENT IS BEST QUALITY AVAILABLE. THE COPY FURNISHED TO DTIC CONTAINED A SIGNIFICANT NUMBER OF PAGES WHICH DO NOT REPRODUCE LEGIBLY.

NOTICES

When Government drawings, specifications, or other data are used for any purpose other than in connection with a definitely related Government procurement operation, the United States Government thereby incurs no responsibility nor any obligation whatsoever; and the fact that the Government may have formulated, furnished, or in any way supplied the said drawings, specifications, or other data, is not to be regarded by implication or otherwise as in any manner licensing the holder or any other person or corporation, or conveying any rights or permission to manufacture, use, or sell any patented invention that may in any way be related thereto.

ASTIA release to OTS not authorized.

Qualified requesters may obtain copies of this report from the Armed Services Technical Information Agency, (ASTIA), Arlington Hall Station, Arlington 12, Virginia.

Copies of this report should not be returned to the Aeronautical Systems Division unless return is required by security considerations, contractual obligations, or notice on a specific document.

FOREWARD

This report was prepared by Mellon Institute under USAF Contract No. AF 33(616)-6968. This contract was initiated under Project No. 7342, "Fundamental Research on Macromolecular Materials and Lubrication Phenomena," Task No. 734203, "Fundamental Principles Determining the Behavior of Macromolecules." The work was administrered under the direction of the Directorate of Materials and Processes, Deputy for Technology, Aeronautical Systems Division. Dr. W. E. Gibbs was the project engineer.

This report covers work conducted from 1 May 1961 to 20 April 1962.

We are indebted to Mr. R. E. Kerwin for the numerical computations required in Part I, Section VI.

ABSTRACT

Theoretical studies of the properties of polymers in dilute solution have involved: the effect of heterogeneity in molecular weight on the second virial coefficient; the relation of chain dimensions to the virial coefficient; and the effect of chain branching (for the case of the star molecule with an arbitrary number of branches) upon both dimensions and virial coefficients in poor solvents.

Experimental results on the effects of branching are reported for polystyrene trifunctional molecules in both good and poor solvents. Linear polystyrene has been used in studying specific solvent effects on chain dimensions in media exhibiting very similar values for the Flory temperature.

Some refinements have been made in the design of a light scattering photometer, and calibration procedures for establishing the absolute magnitude of Rayleigh scattering have been critically evaluated.

The melt viscosities of mixtures of polymer fractions of very different molecular weights appear to depend on the viscosity average molecular weight in a theta solvent rather than a higher molecular weight average, as has been suggested.

New characterization data have been obtained for the vinyl acetate polymer obtained by emulsion polymerization in the presence of protein and detergent.

From measurements of swelling of crosslinked polyethylene in solvents of different structure, it is concluded that specific solvent effects on chain dimensions are inappreciable for this polymer.

This technical report has been reviewed and is approved.

William E. Gibbs

William E. Gibbs
Acting Chief, Polymer Branch
Nonmetallic Materials Laboratory
Directorate of Materials and Processes

TABLE OF CONTENTS

PART I DILUTE SOLUTION STUDIES

TABLE OF CONTENTS - continued

PART I DILUTE SOLUTION STUDIES - continued

TABLE OF CONTENTS - continued

PART I DILUTE SOLUTION STUDIES - continued

PART II MOLECULAR MOBILITY AND MECHANICAL BEHAVIOR OF MACROMOLECULES

PART III ELASTICITY OF POLYMERIC NETWORKS

LIST OF FIGURES

LIST OF FIGURES - continued

LIST OF TABLES

LIST OF TABLES - continued

PART I - DILUTE SOLUTION STUDIES

I. Dimensions of Polymers--Specific Solvent Effects[1] — T. A. Orofino and J. W. Mickey

A. Introduction

The dimensions of an isolated polymer coil, as reflected by such measurable quantities as the intrinsic viscosity and light scattering radius of gyration, in a θ-solvent solution where the net segment-solvent interaction is nil,[2] may in general depend upon two factors: (a) the temperature at which the particular polymer-solvent pair is a θ-mixture and (b) the chemical and physical nature of the solvent molecule. The latter, in relation to the structural characteristics of the polymer repeating unit, may impose certain conformational restrictions upon relatively short sections of the polymer chain. We are interested in studying this effect, whose elucidation necessarily involves control or elimination of factor (a) as a variable. On this account, we have endeavored to select a number of solvents for a particular polymer--a single fraction of anionically polymerized polystyrene--each of which exhibits approximately the same θ-temperature with polystyrene, but differs substantially from other members of the series in chemical type or structure. Possible differences in the θ-solvent dimensions of polystyrene in these various media, which it has been our object to assess, could therefore be attributed to the specific short range polymer-solvent interactions, the more general, and obscuring, effect of temperature having been circumvented by selection of θ-temperatures in approximate juxtaposition.

The careful and detailed dilute solution measurements required in the investigation outlined above also provide valuable data on the dependence of polymer dimensions and interactions on temperature.

In the preceding annual report (ASD Technical Report 61-22) we have presented in some detail the theoretical background for our investigation, together with experimental data collected in the initial stages of this work.

B. Light Scattering Studies

We have carried out extensive light scattering studies on three polystyrene-θ-solvent systems. In each case, the primary object of this phase of our investigation has been to determine the temperature at which the second virial coefficient of the polystyrene-solvent system considered vanishes--the operational definition of the θ-temperature adopted in this program. We have completed studies on the systems polystyrene-cyclohexane and polystyrene-diethylmalonate (an analogous, complimentary study of the former system involving osmotic pressure measurements has been described earlier -- see ASD Technical Report 61-22.) Measurements on the system polystyrene-n-chloroundecane are still in progress.

Manuscript released by the authors September 1962 for publication as an ASD Technical Report.

The photometer used in our investigations is a Brice-Phoenix instrument, suitably adapted for our particular requirements. The instrument has been fitted with an efficient thermostat by means of which temperature in the light scattering cell may be maintained constant at any setting in the range 25-45°C.

For each polystyrene-solvent system studied, individually weighed polymer samples were dissolved under controlled conditions, passed through ultrafine glass filters contained in a warm environment at a temperature well above the θ-temperature of the mixture, and transferred to the light scattering cell. Light scattering intensities were measured at fifteen angles, at each of the temperatures selected for the system. The data were treated in accordance with the customary extrapolation procedure. The concentration dependence of the zero-angle scattering is shown for the two systems polystyrene-cyclohexane and polystyrene-diethylmalonate in Figs. 1 and 2. Values* of the second virial coefficient Γ_2 obtained from the limiting slopes of the curves shown in accordance with the relationship

$$Kc/R_0 = 1/\bar{M}_w + 2\Gamma_2 c/\bar{M}_w + \cdots \qquad (1)$$

where R_0 is Rayleigh's ratio at zero angle, K is the optical constant, c is polymer concentration and $\bar{M}_w$ is weight average molecular weight, are listed in Table I and shown plotted versus reciprocal absolute temperature in Fig. 3. From the latter curves, we interpolate at the ordinate value zero the θ-temperatures $34.8 \pm {}^{0.3}_{0.2}$ °C and $35.9 \pm {}^{0.8}_{1.0}$ °C for the cyclohexane[3] and diethylmalonate systems, respectively.

A procedure identical with that described above is currently being utilized in connection with our studies on the system polystyrene-n-chloroundecane. Our measurements are not yet complete, but based on preliminary data, a θ-temperature of about 35°C is indicated for this system.

---

*The radii of the circles surrounding the experimental points in these graphs represent our estimates of the uncertainties in the ordinate values plotted. An accurate assessment of the experimental error associated with a particular measurement is
obtain. In an effort to be as objective as possible, however, we have analyzed carefully our light scattering, concentration and temperature data in a consistent manner, arriving at the tolerances indicated. From the error circles in these plots, a similar analysis of the uncertainty in Γ_2 may be made (indicated by the bars in Fig. 3), from which, finally, an estimate of the experimental error in the θ-temperature may be deduced. A similar procedure has been followed in the analysis of the intrinsic viscosity data (cf. seq.), taking also into account in the specification of $[\eta]_\theta$, the associated uncertainty in θ itself.

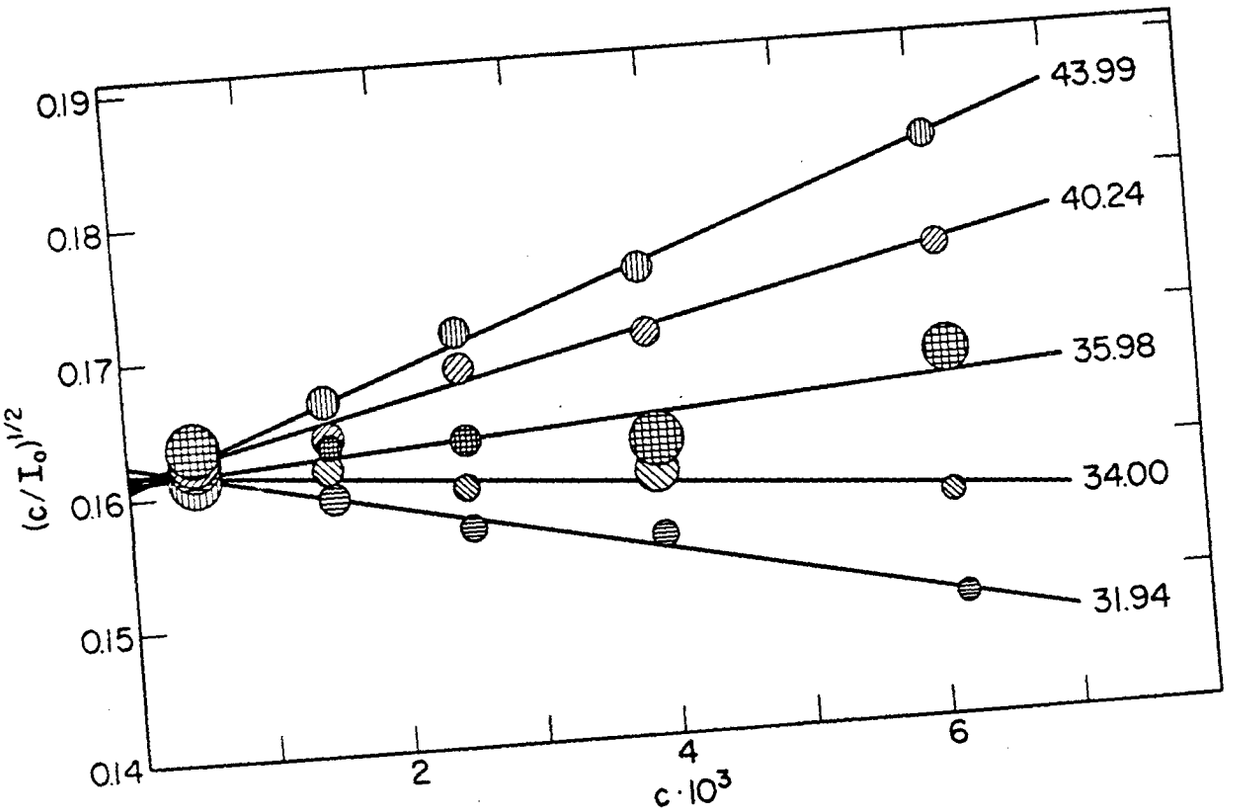

Figure 1 Square Root Plots of Reciprocal Reduced Excess Scattering Intensities as a Function of Temperature and Polymer Concentration for the Polystyrene-Cyclohexane System

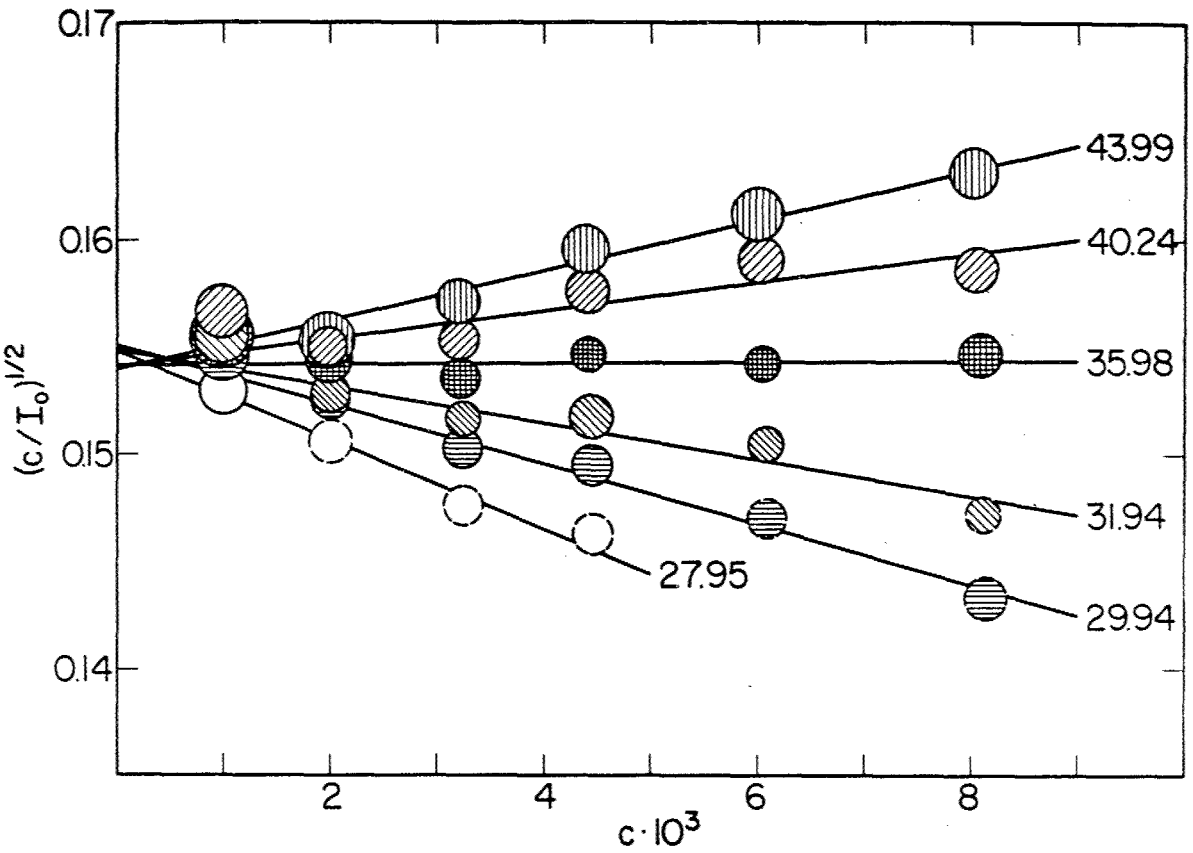

Figure 2 Square Root Plots of Reciprocal Reduced Excess Scattering Intensities as a Function of Temperature and Polymer Concentration for the Polystyrene-diethylmalonate System

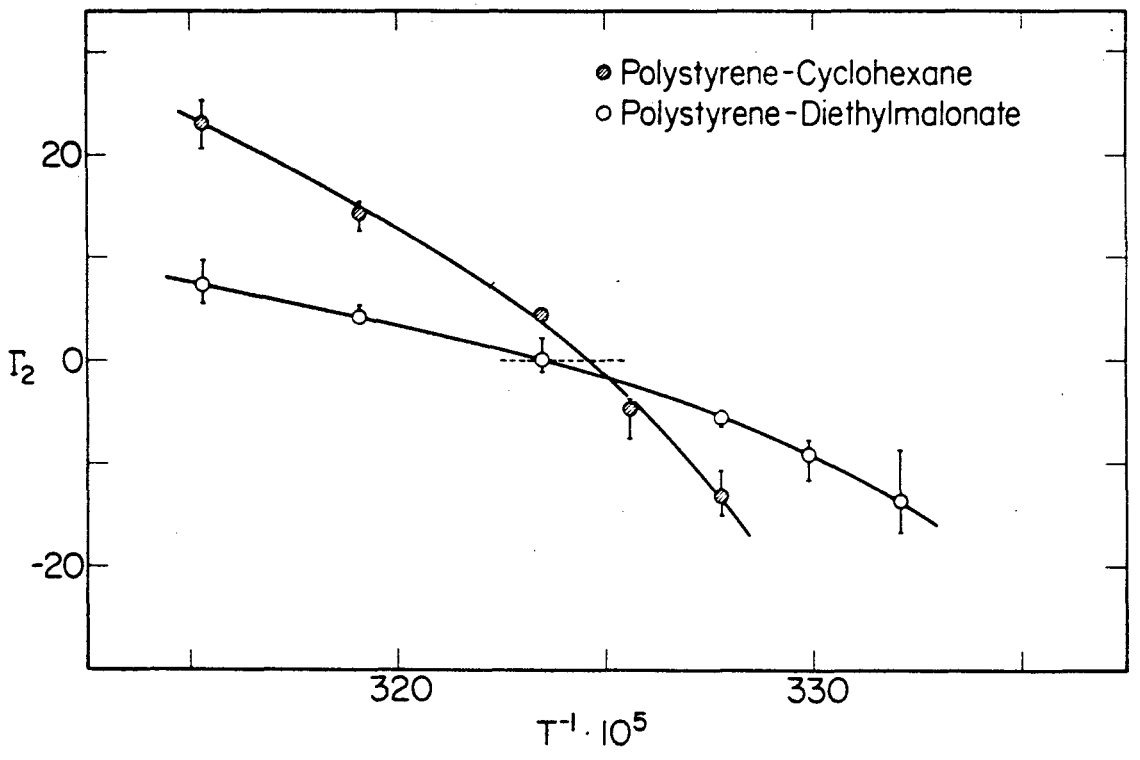

Figure 3 Plots of Second Virial Coefficients Versus Reciprocal Absolute Temperature for Polystyrene-θ-Solvent Systems

Table I

Virial Coefficient Data, Polystyrene-θ-Solvent Systems

	Γ_2, cc/g	
t°C	cyclohexane	diethylmalonate
43.99	23.1	7.4
40.24	14.3	4.3
35.98	4.5	0.1_4
34.00	-4.6	
31.94	-13.1	-5.5
29.94		-9.1
27.95		-13.6
	$\theta = 34.8 \begin{smallmatrix} + 0.3 \\ - 0.2 \end{smallmatrix}$	$\theta = 35.9 \begin{smallmatrix} + 0.8 \\ - 1.0 \end{smallmatrix}$

$dn/dc = 0.181$

$\bar{M}_w = 4.06 \times 10^5$

C. Intrinsic Viscosity Studies

For each of the polystyrene-solvent systems, the accurate determination of whose characteristic θ-temperatures has been described in the preceding section, we have carried out (or plan to carry out) complimentary intrinsic viscosity studies in the vicinity of the respective θ-points. In each case a single lot of solvent, purified and characterized prior to the light scattering measurements, has been set aside for use in all such studies anticipated.

The viscometer used in our work is a Ubbelohde instrument with a flow time t for cyclohexane of ca. 240 sec. at 35°C. The kinetic energy correction is 15/t. The viscometer is contained in a constant temperature bath (±0.002°C) provided with air and vacuum lines and filtering equipment designed for use at elevated temperatures (above the θ-point).

Intrinsic viscosity values $[\eta]$ determined at various temperatures for the cyclohexane and diethylmalonate systems are listed in Table II. Included also are values of the Huggin's constant k' appearing in the viscosity equation

$$\eta_{sp}/c = [\eta] + k'[\eta]^2 c + \cdots \tag{2}$$

where c is polymer concentration. The specific viscosity η_{sp} appearing here is defined through the relationship

$$1 + \eta_{sp} = \eta_{rel} = (\rho/\rho_0)(t/t_0) \tag{3}$$

where t is (corrected) flow time, ρ is density and the subscript zero refers to the solvent. The viscosity data, plotted in accordance with Eq. (2), are shown in Fig. 4 and Fig. 5.

D. Summary. Comparison of Solution Properties

Dilute solution parameters computed from experimental data for two of the polystyrene-solvent systems investigated in the present program are compiled in Table III. In column 4 are listed values of the viscosity constant K, computed from the relationship[2]

$$K = [\eta]_\theta / M^{1/2} \tag{4}$$

applicable to θ-solvent solutions of linear polymers. The effects of temperature on the intrinsic viscosity and second virial coefficient at θ are indicated by the values of the limiting slopes listed in columns 5

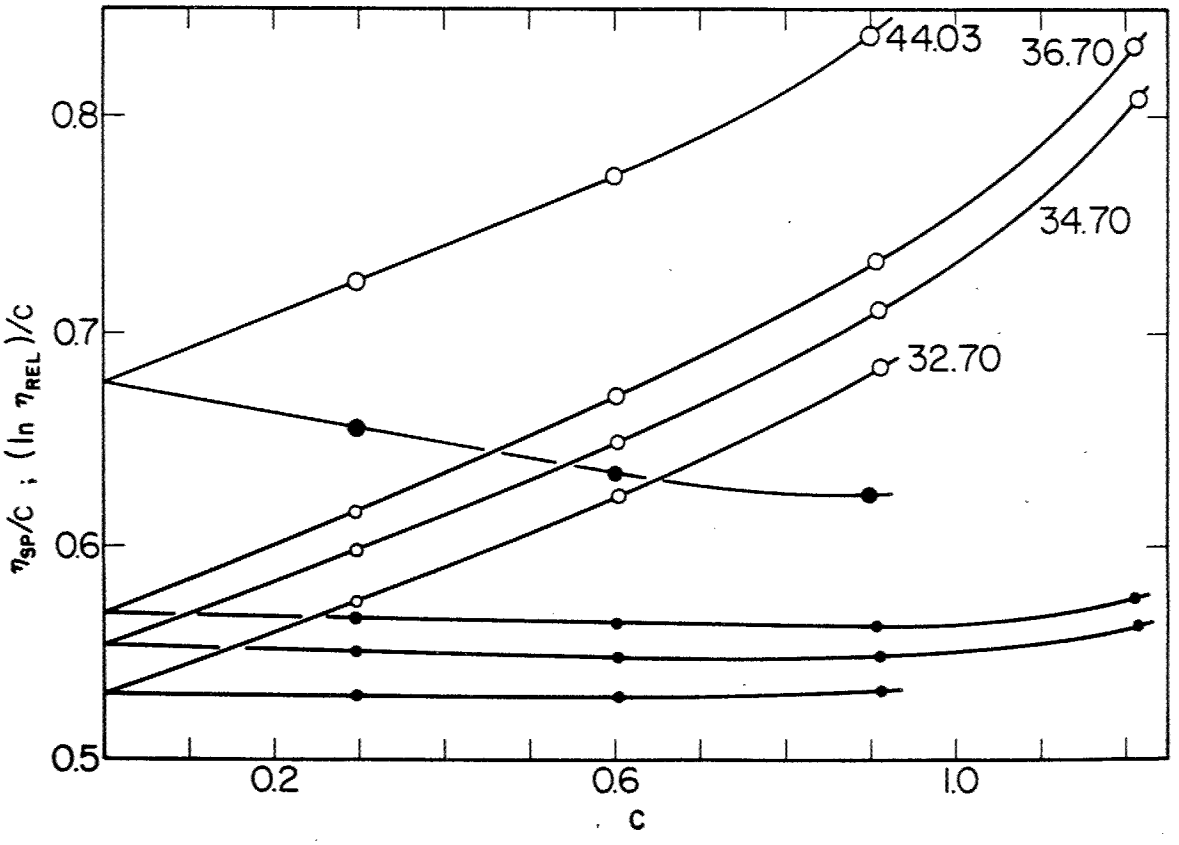

Figure 4 Viscosity Plots for Polystyrene in Cyclohexane at Various Temperatures. Open circles represent values of η_{sp}/c, filled circles $(\ln \eta_{rel})/c$.

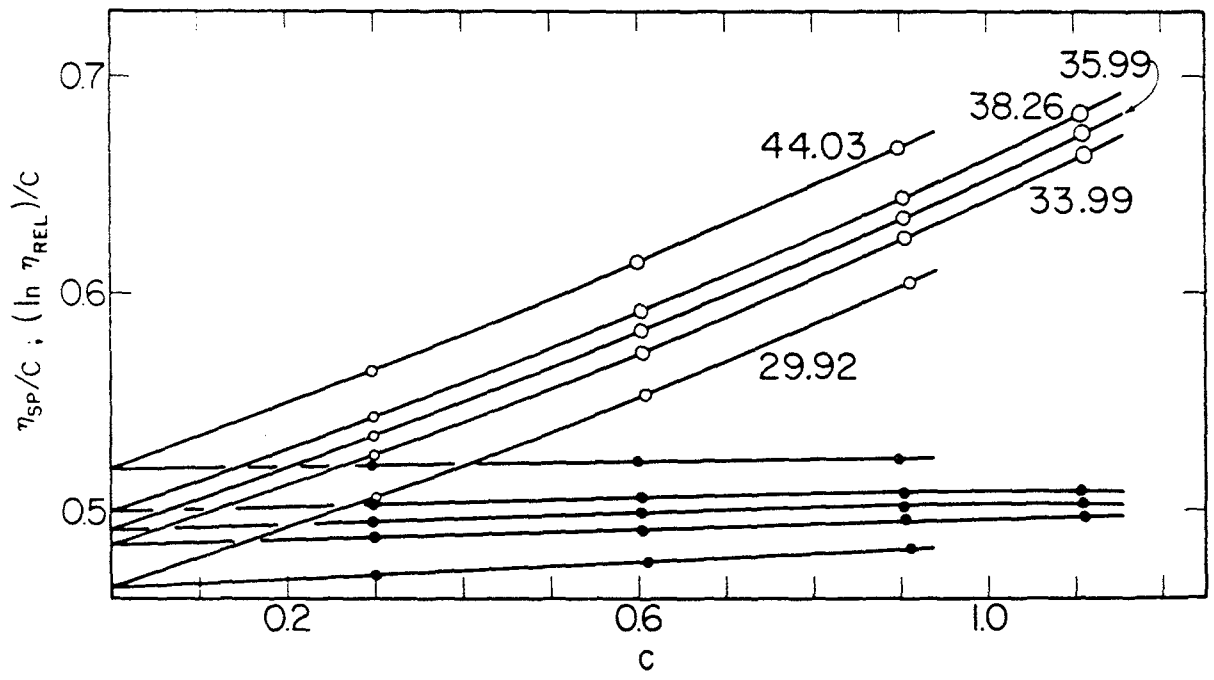

Figure 5 Viscosity Plots for Polystyrene in Diethylmalonate at Various Temperatures. Open circles represent values of η_{sp}/c, filled circles (ln η_{rel})/c.

Table II

Intrinsic Viscosity Data, Polystyrene-θ-Solvent Systems

	cyclohexane		diethylmalonate	
t°C	$[\eta]$, dec/g	k'	$[\eta]$, dec/g	k'
44.03	0.677	0.35	0.519	0.57
38.26			0.500	0.58
36.70	0.563	0.51		
35.99			0.491	0.61
34.70	0.554	0.49		
33.99			0.484	0.60
32.70	0.531	0.51		
29.92			0.468	0.59
	$^{*}[\eta]_\theta = 0.552 \begin{smallmatrix} +0.004 \\ -0.003 \end{smallmatrix}$		$[\eta]_\theta = 0.490 \begin{smallmatrix} +0.004 \\ -0.003 \end{smallmatrix}$	

*The tolerances designated take into account the uncertainties in the respective θ-temperatures noted in Table I.

Table III

Comparison of Parameters, Polystyrene-θ-Solvent Systems

$$\bar{M}_w = 4.06 \times 10^5$$
$$\bar{M}_n = 4.04 \times 10^5$$
$$\bar{M}_w/\bar{M}_n \text{ (fractionation)} = 1.05$$

1	2	3	4	5	6	7	8	9	10	11
						$10^{16}(\overline{r_0^2}/M)$				
Solvent	θ°C	$[\eta]_\theta$	$10^4 K$	$10^3\left(\frac{d[\eta]}{dT}\right)_\theta$	$\left(\frac{d\Gamma_2}{dT}\right)_\theta$	from β	from K	obs.	k'_θ	$\delta-\delta_{PS}$
Cyclohexane	34.8	0.552	8.66	12.6	3.7	0.57	0.54	0.50	0.50	- 1.0
Diethylmalonate	35.9	0.490	7.69	3.6	1.1	0.55	0.50	0.47	0.60	+ 0.3

and 6. In regard to the latter, the difference observed for the two solvent systems may also be expressed in terms of the parameter ψ_1 appearing in the Flory-Krigbaum theory[2,4] for the second virial coefficient

$$\Gamma_2 = M\psi_1(1 - \theta/T)(\bar{v}^2/V_1)F(x) \qquad (5)$$

where $\bar{v}$ is the partial specific volume of the polymer, V_1 the molar volume of solvent and $F(x)$ is an interaction function which assumes the value unity at T equal to θ. We compute from our data in accordance with Eq. (5) the ψ_1 values 0.38 and 0.17 for the cyclohexane and diethylmalonate systems, respectively.

In columns 7-9 of Table III are listed values of the ratio of mean square end-to-end separation of the polymer chain ends to molecular weight, $\overline{r_0^2}/M$ (for linear chains, independent of molecular weight). The entries in column 9 were derived directly from our light scattering dissymmetry data. Owing to the small size of the molecular species involved, and the associated low dissymmetry ratios displayed by the solutions, the values of $\overline{r_0^2}/M$ computed in this manner are subject to considerable uncertainty. In column 8 are listed values of $\overline{r_0^2}/M$ calculated from the theoretical definition of the viscosity constant K (see Eq. (4))

$$K = \Phi(\overline{r_0^2}/M)^{3/2} \qquad (6)$$

taking for Φ, a supposedly universal constant, the value 2.2×10^{21}. The entries for $\overline{r_0^2}/M$ in column 7 were derived from a treatment of our data in accordance with the combined "exact" series relationships for intra- and intermolecular interactions applicable to solutions characterized by small polymer excluded volumes. A detailed discussion of the procedure constitutes the subject matter of a separate section of this report (see Section V).

Values of the Huggin's constant k', interpolated at T equal to θ for each system, are listed in column 10.

In the last column of Table III are listed values of the Hildebrand solubility parameter difference $\delta - \delta_{PS}$, where δ_{PS} refers to polystyrene. The numerical value of this quantity provides in each case a semi-quantitative measure of the degree to which the polymer segment and the solvent molecule differ in chemical characteristics; the disparity in the two sets of values listed may in turn be taken as an indication of substantial differences between the solvents considered. It is the comparison of such differences in solvent characteristics with corresponding differences (or similarities) in observable solution properties which comprises one of the ultimate objectives of the present studies.

In summarizing the results of our dilute solution investigations to date, we may conclude: (1) our comparative studies of the two θ-solvent systems polystyrene-cyclohexane and polystyrene-diethylmalonate have revealed a small, but significant, difference in the intrinsic viscosities of polystyrene in the two media; (2) because of the close proximity of the θ-temperatures, the effect noted cannot be attributed to the influence of temperature per se on the viscometric properties of the polymer. Thus, although in each system the net effect of segment-solvent interactions at θ is nil, the specific interrelations among the chemical and physical factors through which this thermodynamic equivalence is attained are determined by more detailed considerations than mere juxtaposition of the θ-temperatures. We may further conclude: (3) the disparity in intrinsic viscosities observed primarily reflects concomitant differences in the coil dimensions of the dissolved polystyrene molecules and, accordingly, manifests itself in other observable physical properties in which size of the polymer molecule plays a dominant role. Our data show, for example, that the second virial coefficients, when compared for the two systems, display a relationship similar to that observed for the intrinsic viscosity values. It is interesting to note that the coil dimensions of this polystyrene sample, as reflected by the ratios $\overline{r_o^2}/M$ in Table III, are likewise in accord with the notion of an overall dimunition in the size of the molecular domain of the polymer in the diethylmalonate medium.

II. Dilute Solution Properties of Branched Polymers. Polystyrene Trifunctional Star Molecules[5] * — T. A. Orofino and J. W. Mickey

A. Introduction

During the past year we have been engaged in various dilute solution studies of a model branched polymer of the trifunctional star structure. A thorough investigation, recently completed, has revealed that, to varying degrees, the fractions studied in our initial work contained some linear polystyrene mixed with the trifunctional material originally believed to constitute the entire sample.** We have since repeated and extended our studies, employing in the new investigation, a single polystyrene trifunctional star sample whose homogeneity in regard to molecular weight distribution and functionality has been established from fractionation, ultracentrifuge, and absolute molecular weight studies. The work on this project has now been completed. The results presented here constitute the terminal report on this phase of our activities.

The sample chosen for investigation was isolated from a branched polymer product synthesized by Dr. F. Wenger and Mrs. S.-P. S. Yen The synthesis involves the coupling of essentially monodisperse polystyryl lithium chains with 1,2,4-trichloromethyl benzene, yielding as the principal product trifunctional star molecules consisting of three linear polystyrene chains joined by one end at a common (benzene ring) junction. The skeletal structure of these materials thus involves only carbon-carbon linkages. The virtual chemical identity of the branched chains with linear polystyrene, together with their homogeneity in regard to functionality and molecular weight distribution, make them ideally suited for physical measurements, the results of which may be directly compared with previously established properties of their linear counterparts. In connection with the latter, we have, in addition to our branched polymer studies, carried out pertinent solution measurements on linear polystyrene samples as well.

B. Solution Measurements

The solution measurements carried out on sample 8-III_2 selected for detailed study include: light scattering measurements at four temperatures in cyclohexane and at one temperature in toluene; intrinsic viscosity measurements at one temperature in benzene and in toluene and at three temperatures in cyclohexane; osmotic pressure measurements in cyclohexane at one temperature. The experimental techniques employed were identical with those described in Section I of this report, as was the general treatment of the data obtained. We have, however, omitted the detailed error analysis applied there.

---

*A study carried out in collaboration with Dr. F. Wenger and Mrs. S.-P. S. Yen, Mellon Institute.

**The principal sample used in the earlier studies was designated 10-III (cf. seq.)

The general characterization data for this sample are shown in Table IV. The weight-to-number average ratio and the ratio of molecular weights of branched polymer to the linear starting material observed may be taken as unity and three, respectively, within experimental error.

Table IV

Characterization Data. Polystyrene Star Sample 8-III$_2$

$$\bar{M}_w = 3.48 \times 10^5$$

$$\bar{M}_n = 3.51 \times 10^5 \qquad \bar{M}_{w_{monomer}} = 1.12 \times 10^5$$

$$\bar{M}_w/\bar{M}_n = 0.99(1.00) \qquad \bar{M}_w/\bar{M}_{w_{monomer}} = 3.11$$

Light scattering and virial coefficient data derived for the cyclohexane system are shown graphically in Figs. 6 and 7. The circle radii in Fig. 6 denote 1% of the ordinate values plotted. Data for the toluene system are shown in Fig.8 where again, circle radii are 1% of the ordinate values in the conventional plot (top curve) and 1/2 % in the square root plot (bottom line).

The intrinsic viscosity data for the cyclohexane, benzene, and toluene systems are shown in Figs. 9 and 10.

C. Results

The results of dilute solution studies may be divided into two convenient categories: those pertaining to solution characteristics in poor, or θ-solvent, media (cyclohexane) and those applicable to good solvent mixtures (benzene and toluene). Data obtained from studies of the former are summarized in Tables V and VI and compared with corresponding results for linear polystyrene. In Table VII are listed results for the good solvent media.

Intrinsic viscosity and second virial coefficient data obtained as a function of temperature in cyclohexane are listed in columns 2 and 6 of Table V. From the interpolated intrinsic viscosity at the θ-temperature in cyclohexane (arrived at, in accordance with the procedure detailed in Section I, from the present virial coefficient data--see Fig. 7) we have computed the ratio g' of $[\eta]_b$ for the branched polymer to $[\eta]_\ell$ for linear polystyrene of the same molecular weight. This entry appears in column 3 and may be compared (below Table) with the theoretical values[7,8,19] of the corresponding ratio of root mean square

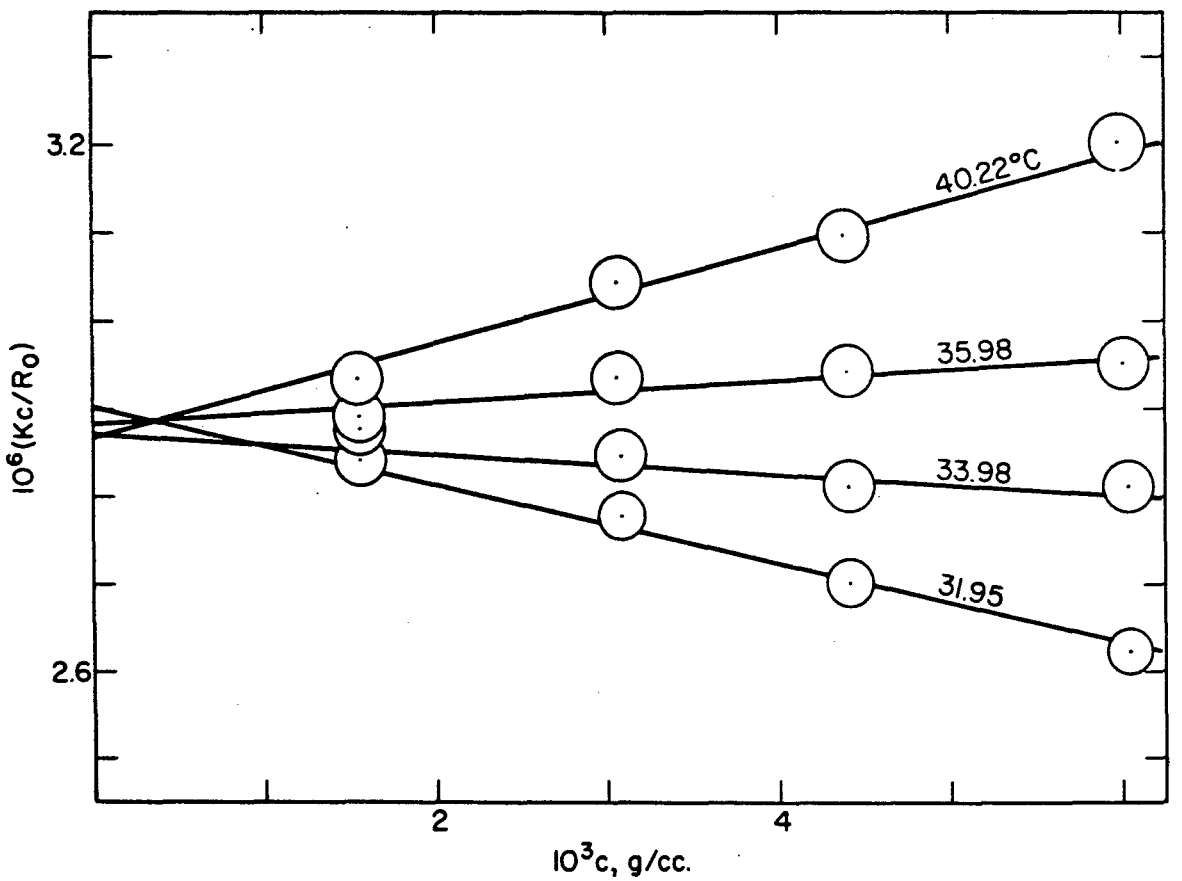

Figure 6 Light Scattering Plots of Polystyrene Star Sample 8-III_2 in Cyclohexane at Various Temperatures

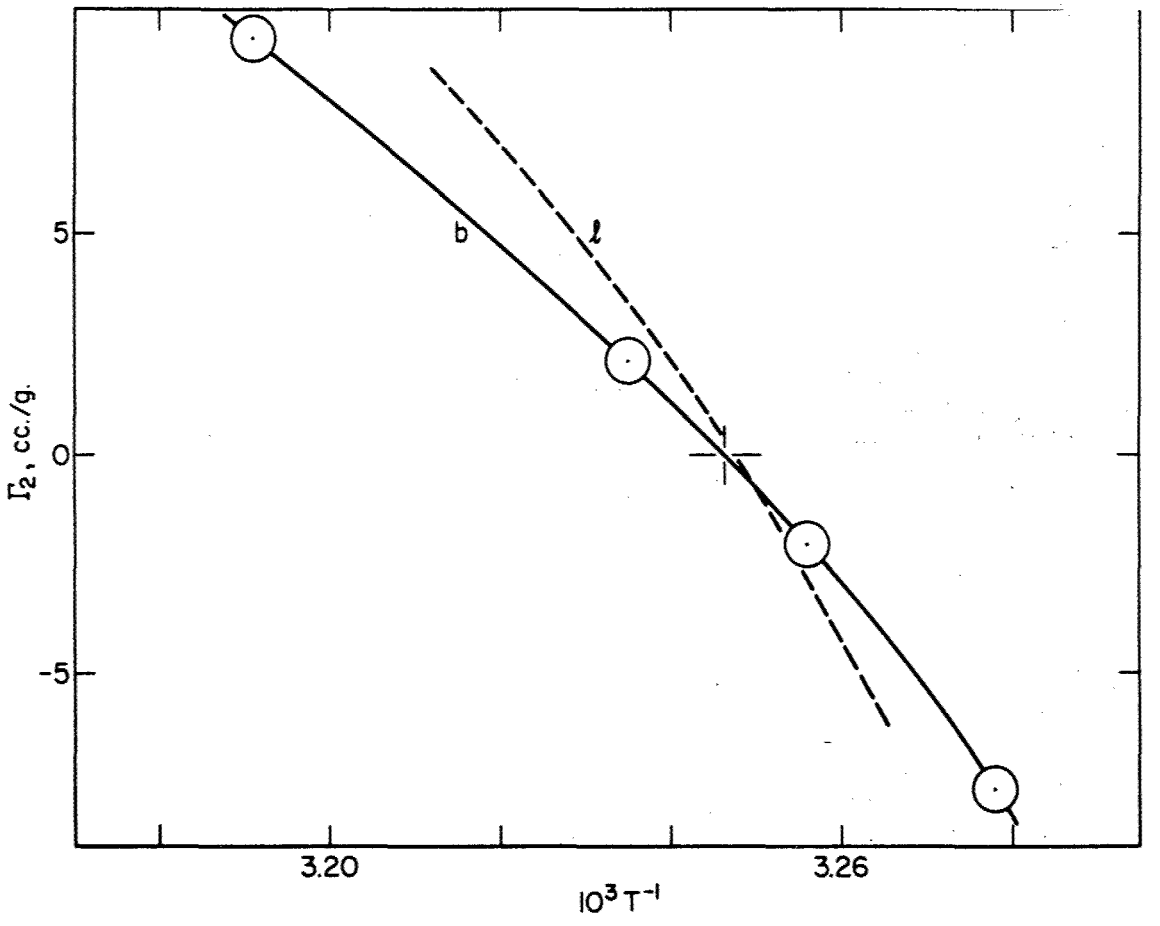

Figure 7 Plot of Second Virial Coefficient Versus Reciprocal Absolute Temperature for Star Sample 8-III$_2$ in Cyclohexane. Dashed curve represents data for linear polystyrene of the same molecular weight.

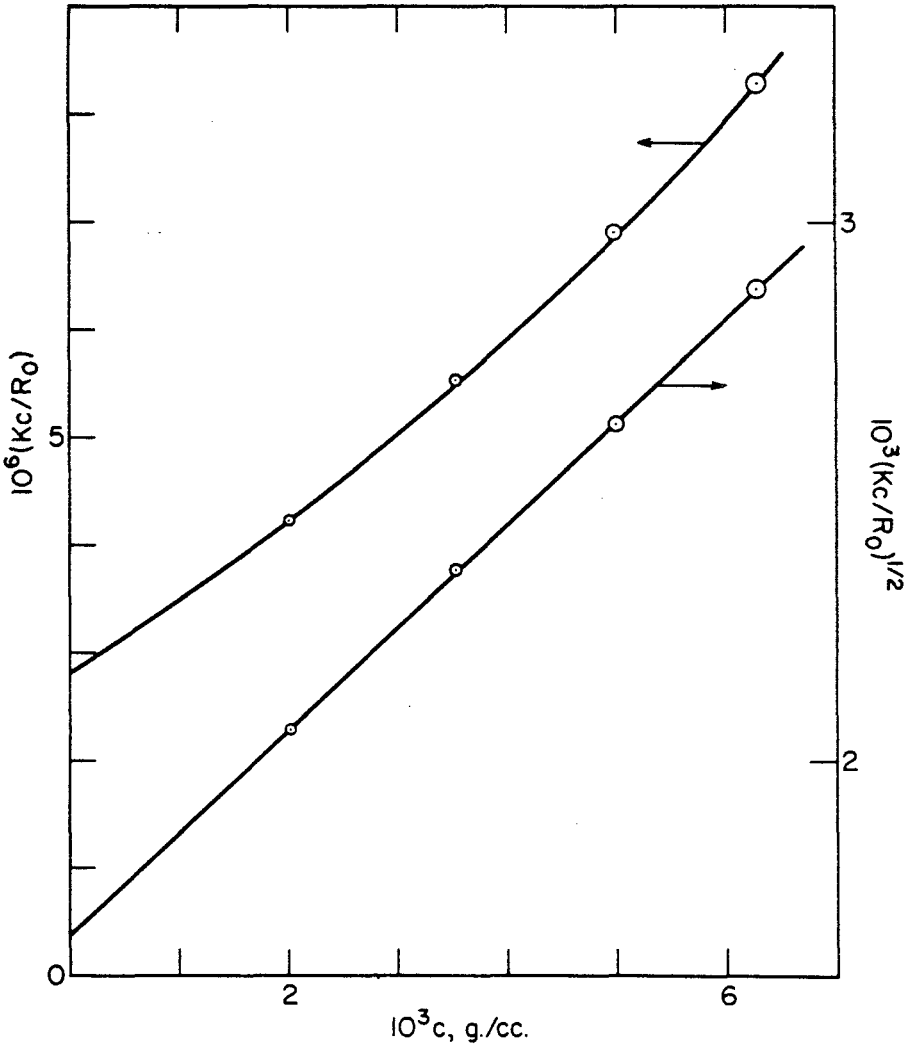

Figure 8 Light Scattering Plots for Star Sample 8-III_2 in Toluene

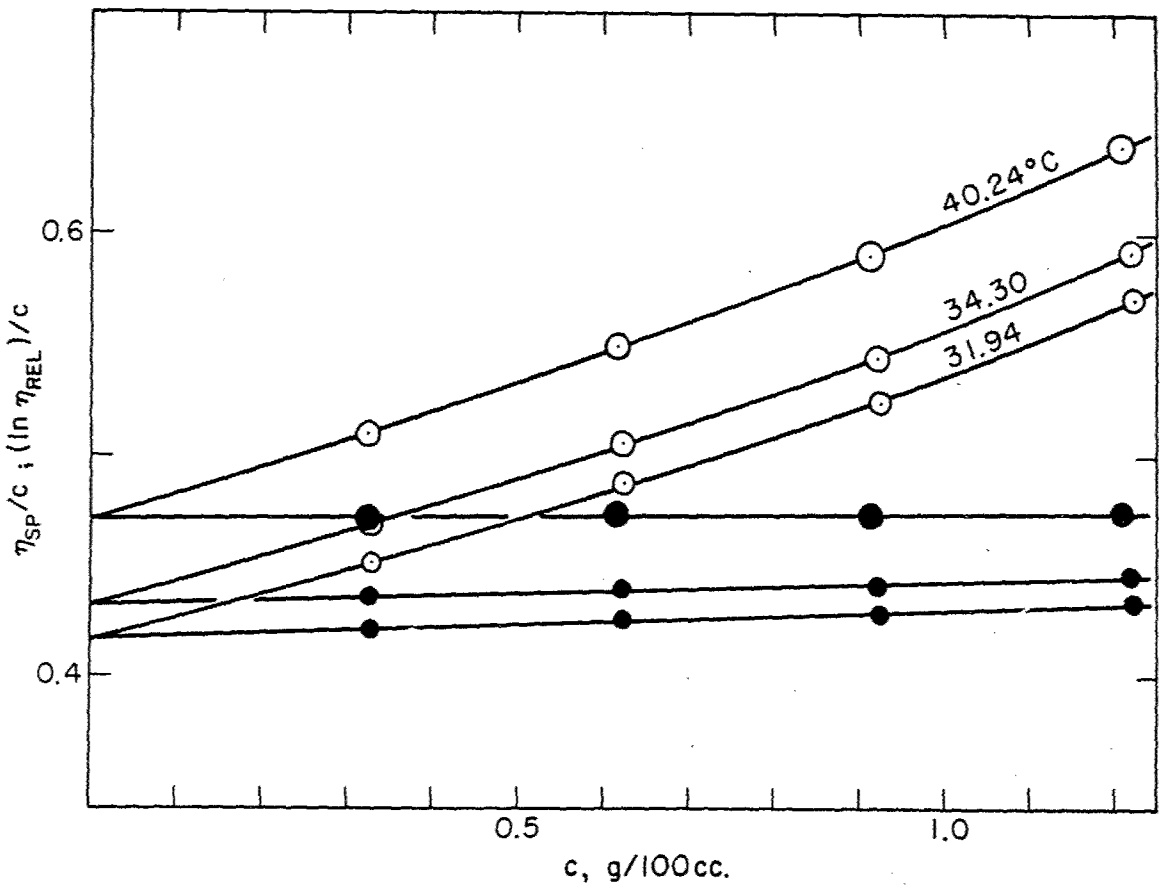

Figure 9 Viscosity Plots for Star Sample 8-III$_2$ in Cyclohexane at Various Temperatures. Open circles represent values of η_{sp}/c, filled circles $(\ln \eta_{rel})/c$.

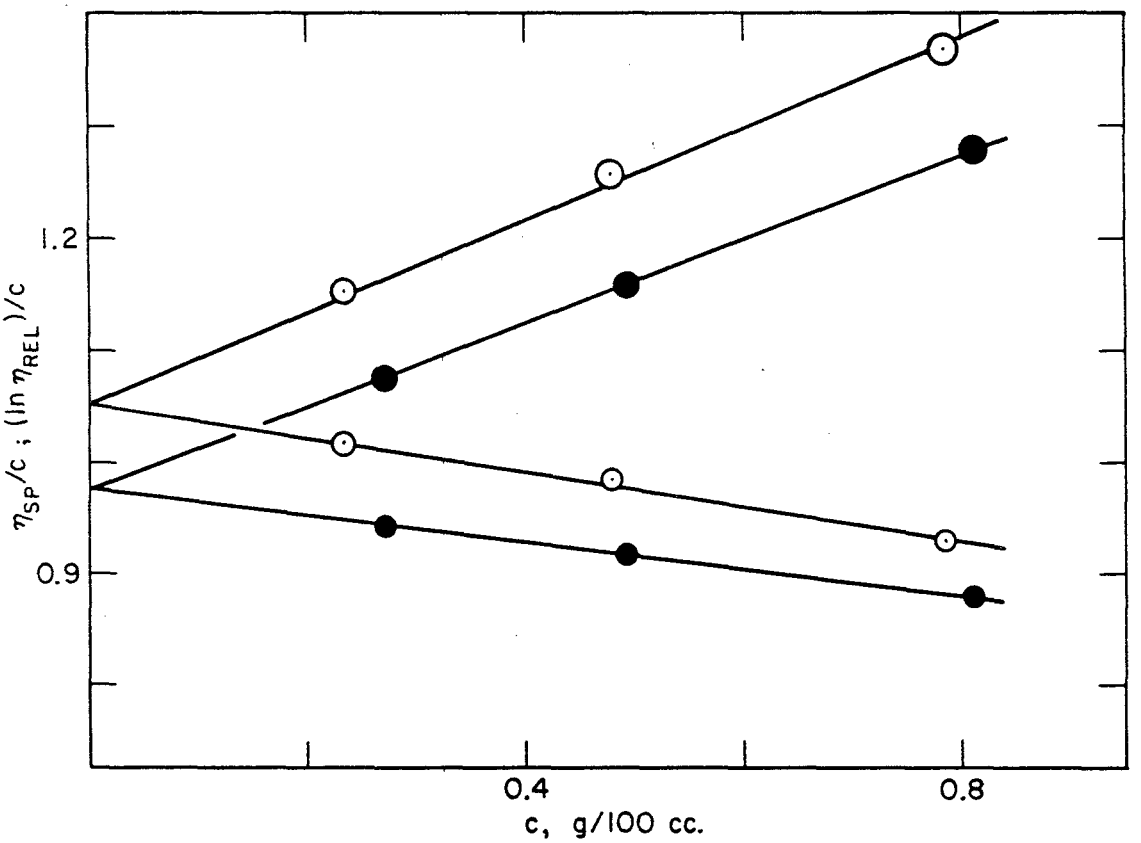

Figure 10 Viscosity Plots for Star Sample 8-III_2 in Benzene at 25°C (open circles) and in Toluene at 30°C (filled circles)

Table V

Dilute Solution Parameters. Star Sample 8-III$_2$ in Cyclohexane

1	2	3	4	5	6	7
t°C	$[\eta]_b$	g'(a)	k'_b	k'_ℓ	Γ_{2_b}	$\Gamma_{2_b}/\Gamma_{2_\ell}$ (c)
40.22	0.471				9.4	0.70
35.98	0.443				2.2	0.63
(34.8)	0.435_θ	0.85_θ	0.59	0.50 (b)	(0)	--
33.98	0.430				-2.0	0.71
31.95	0.416				-7.6	0.67

$$(\overline{s_o^2})_b/(\overline{s_o^2})_\ell = g = 0.778$$

$$g^{1/2} = 0.882$$

$$g^{3/2} = 0.686$$

(a) $[\eta]_\theta$ for the linear molecule calculated from $[\eta]_{\theta,\ell} = KM^{1/2}$, $K = 8.66 \times 10^{-4}$ (see Section I). The parameter g' computed in this way is independent of possible absolute errors in our light scattering calibration.

(b) For the linear molecule, we have taken the k'_θ value reported in Section I.

(c) For the linear molecule, we have utilized data in Section I, corrected for the molecular weight difference.

Table VI

Dilute Solution Parameters. Linear, Star Sample 8-III$_2$ in Cyclohexane

1	2	3	4	5	6
Structure	θ°K	ψ_1	$10^{16}(\overline{r_o^2}/M)_\ell$	$10^{18}(\overline{s_o^2})/M$	g
Linear (a)	308.0	0.38	0.57	9.5	0.76
Star	308.0	0.24	0.56	7.3	

$$g_{theo} = 0.78$$

(a) from results of Section I

Table VII

Dilute Solution Parameters. Star Sample 8-III$_2$ in Good Solvents

1	2	3	4	5	6	7	8
Solvent	$[\eta]_b$	g'(a)	k'_b	k'_ℓ	Γ_{2_b}	$\Gamma_{2_b}/\Gamma_{2_\ell}$ (b)	α_b^3/α_ℓ^3
Toluene (30°)	0.976	0.88	0.39	0.38	115	0.86	1.04
Benzene (25°)	1.052	0.87	0.37	0.38	---	--	1.03

$$(\overline{s_o^2})_b/(\overline{s_o^2})_\ell = g = 0.778$$

$$g^{1/2} = 0.88$$

$$g^{3/2} = 0.69$$

(a) We have computed $[\eta]$ for the linear molecule from $[\eta] - \bar{M}_w$ relationships established in our laboratories for linear polystyrene. The parameter g' calculated in this way is independent of possible absolute errors in our light scattering calibration.

(b) The value of Γ_2 for the linear polymer was calculated from the published relationship of Flory and Krigbaum[6] for polystyrene-toluene.

radii $g^{1/2}$ and the cube of this quantity, $g^{3/2}$, approximations to g' predicted by different theories (cf. seq.). In columns 4 and 5 values of the Huggins constant are compared for the branched and linear polystyrenes in cyclohexane. In the last column of Table V are listed ratios of Γ_2 values for branched and linear polystyrene of the same molecular weight.

A comparison of some thermodynamic parameters for branched and linear polystyrene is shown in Table VI. Values of the θ-temperature, column 2, derived by identical methods applied to this star sample and to linear polystyrene (Section I) were found to be the same within experimental error, facilitating comparisons of other solution parameters. In column 3 are listed values of the Flory-Krigbaum parameter ψ_1 (see Section I). In column 4 are listed values of the parameter $\bar{r}_o^2/M$ for linear polystyrene, derived in each case from analysis of $[\eta]$ and Γ_2 data in accordance with the exact series treatment (cf. subsequent Sections III, V). On the basis of the compatibility of these values, derived independently from data on branched and linear polystyrene, one may compute, from the same data, values of $\bar{s}_o^2/M$ for the two structures. From these, in turn, we have arrived at an "experimental" value of the ratio of

mean square radii of gyration of branched and linear polystyrene of the same molecular weight, g, listed in the last column of Table VI. The theoretical value of g is 0.78. The good agreement, in effect, serves as a check on the consistency of our comparisons of dilute solution data for the branched and linear polymers.

Values of the viscosity ratio g' in the good solvent media benzene and toluene are listed in column 3 of Table VII. Again, they may be compared with $g^{1/2}$ and $g^{3/2}$ listed below for these trifunctional star structures. The Huggins constants are compared in columns 4 and 5, virial coefficients in toluene in columns 6 and 7. In the last column are listed values for the ratio of intrinsic viscosity expansion factors for star and linear polystyrene. Thus, for example, α_b^3 is defined as the ratio of $[\eta]_b$ in a given solvent to $[\eta]_{\theta,b}$ for a star polymer of the same molecular weight in a θ-solvent. The corresponding value of α_ℓ^3 involved in the computation of the ratio listed refers to linear polystyrene of the same molecular weight as that of the branched polymer.

D. Summary and Conclusions

Our pertinent findings in regard to comparisons of the dilute solution properties of trifunctional star polystyrene and linear polystyrene of the same molecular weight may be summarized from the data of Tables V, VI, and VII. These are: (1) the intrinsic viscosities of the branched polymer, in both poor and good solvent media, are less than those of the linear counterpart. Specifically, the ratio g' has been found to more closely approximate the theoretical ratio $g^{1/2}$ predicted by Zimm and Kilb[10] than the quantity $g^{3/2}$ predicted by earlier extensions of the Flory-Fox viscosity equation.[11] The parameter g' is not, however, in precise quantitative agreement with $g^{1/2}$ for the cyclohexane θ-solvent system and, moreover, increases significantly in value in better solvents. The Huggins constant k' in good solvents is unaffected by branching of the type investigated here; in poor solvents, an augmentation of k' with branching has been noted. (2) the second virial coefficient in both poor and good solvents is diminished by branching. Expressed as the ratio $\Gamma_{2b}/\Gamma_{2\ell}$, the effect is more pronounced in poor solvent media. The temperature coefficient of Γ_2 at θ appears to be diminished by branching. (3) the value of the parameter θ in cyclohexane solutions was found to be the same for branched and linear polystyrenes. The Flory-Krigbaum parameter ψ_1, reflecting the observed difference in $d\Gamma_2/dT$ mentioned above, was found to be substantially diminished by branching. (4) the result from our indirect evaluation of the mean square radius of the branched molecule is in accord with the notion that the diminution of $[\eta]$ and Γ_2 in poor and good solvents arises from a substantially reduced coil size of the star polymer. Data on the expansion factor ratio α_b^3/α_ℓ^3 indicate that these coil dimensions become relatively more expanded in good solvents than do those of the linear polymer in the same media.

Finally, it is interesting that, without exception, each of the various solution properties established for sample 10-III, studied earlier and since found to consist of a mixture* of two more or

*As evidenced by sedimentation studies, the sample consisted of about a 50-50 mixture.

Table VIII

Dilute Solution Parameters for Mixtures of Linear and Trifunctional Star Polystyrene Molecules

			Judged Dependent on Branching								Judged Independent of Branching	
Sample	Composition	$10^{-5}\,\bar{M}_w$	$\bar{M}_w/\bar{M}_{w\,monomer}$	g'_θ	$g'_{benzene}$	k'_θ	ψ_{1CH} (c)	$\Gamma_{2,CH,40°}/\Gamma_{2,CH,\ell}$ (d)	$\Gamma_{2,toluene}/\Gamma_{2,toluene,\ell}$ (d)	$\alpha^3/\alpha^3_{\ell\,benzene}$ (d)	θ_{CH}	$k'_{benzene}$
(a) ---	linear	(a) --	1.00	1.00	1.00	0.50	0.38	1.00	1.00	1.00	34.8	0.38
(b) 10-III	star + linear	3.12	2.55	0.91	0.94	0.56	0.25	0.74	--	1.02	34.3	0.36
8-III_2	star	3.48	3.11	0.85	0.87	0.59	0.24	0.70	0.86	1.03	34.8	0.37

(a) Molecular weight insensitive properties listed are those for polystyrene D (Section I), $\bar{M}_w = 4.06 \times 10^5$. Other properties are interpolated from data on polystyrene D.

(b) Trimer molecular weight is ca. 3.7×10^5, dimer, ca. 2.5×10^5.

(c) CH = cyclohexane.

(d) The parameters for the linear counterparts refer in each case to the same molecular weight as that of the mixture.

less distinct components--trifunctional star and (linear) difunctionally coupled polystyrene, is in accord with the findings reported above for star sample 8-III$_2$. That is, those properties ascertained to be essentially unaffected by branching of the type considered here (e.g., θ and k' in good solvents) were found to be in quantitative agreement for samples 10-III and 8-III$_2$. Likewise, those properties for which a significant dependence on branching was observed (e.g. g'_θ, g', and k'_θ) were found to change monotonically in value with progressive changes in the proportion of star component present in the samples. The pertinent comparative data are summarized in Table VIII and provide a measure of the sensitivity of the various parameters to branching.*

In conclusion, we feel that the results reported here represent an internally consistent comparison between the solution properties of polystyrene trifunctional star molecules and linear polystyrene. Qualitatively, and to some degree, quantitatively, our findings should find applicability to branched polymer systems of higher functionality.

*The expected variation of branching dependent properties with percent star component would not be in simple proportion to the latter, inasmuch as the mixture contains species of different molecular weights. Taking this factor into account, we would, for example, calculate a g'_θ value of about 0.90 for mixture 10-III, assuming g'_θ for the pure star material to be 0.85.

III. Initial Dependence of Mean Square Radius of Star Molecules on Segment Excluded Volume — T. A. Orofino

A. Introduction

In connection with experimental branched polymer studies carried out during the past year (Section II) we have also had occasion to consider some of the complementary theoretical aspects of the solution behavior of these materials. Specifically, we have extended the "exact" theoretical computation of the first order interaction coefficient a_1 in the general series expression for the mean square radius

$$\overline{s^2} = \overline{s_0^2} + \overline{s_0^2} a_1 z + O(z^2) + \cdots \tag{7}$$

to the class of p-functional star molecules. In the above equation, applicable in form to linear or branched molecules of any architecture, z is an excluded volume parameter whose value is determined by the extent of thermodynamic interaction between polymer segments and solvent molecules; it is defined through the relationship

$$z = (3/2\pi b_0^2)^{3/2} N^{1/2} \beta \tag{8}$$

where b_0 is the length of one statistical polymer chain segment of excluded volume β and N is the total number of such segments comprising the molecule. The coefficient a_1 is characteristic of a particular, specified geometrical chain structure (e.g., linear molecule) and the subscript zero denotes random flight conditions. A knowledge of the coefficients a_i for a particular structure enables one to calculate the degree to which segment-solvent interactions augment the chain dimensions, relative to those characteristic of random flight (θ-solvent) media. (The principal practical value of Eq. (7), however, perhaps lies in the fact that it may be combined with an analogous series expression for the second virial coefficient--see subsequent Section V).

The formulation of a_1 and higher terms in Eq. (7), equivalent to that used by Zimm, Stockmayer, and Fixman[12,13] in their pioneer work on this general problem, is expressed here in the language of probability theory and lends itself to a more direct physical interpretation of the rather involved computations.

B. Theory

We shall content ourselves with a brief description of the physical nature of the problem and its general mathematical formulation.

To each of the conformations which an idealized polymer chain comprised of freely jointed, non-interacting segments of zero volume can assume, there is associated a statistically definable instantaneous radius of gyration of the molecular mass. The time average of these radii over all conformations which the molecule assumes constitutes the so-called mean square radius of gyration of the polymer chain. The hypothetical restrictions of freely jointed chain segments and absence of interaction or volume exclusion effects cannot, of course, be met by any real polymer chain in solution. Within certain limits, however, the equivalent of these idealized conditions can be realized thermodynamically through judicious choice of the polymer-solvent pair, i.e., at the θ-temperature of the mixture. To the extent that the idealized conditions mentioned above are, in fact, satisfied by θ-solvent systems, polymer molecules dissolved therein may be considered to obey "random flight" statistics. Thus, the observable mean square radius of the molecule may be identified with the corresponding quantity for a suitable defined equivalent random flight chain.

If we accept the correspondence between the real chain in θ-solvent media and the hypothetical random flight chain of zero chain segment volume described above, we may in the same sense associate a real chain dissolved in interacting media with an equivalent mathematical chain model in which each constituent segment occupies a definite volume in space. The latter effect imposes certain restrictions upon the conformational behavior of the model assumed, which restrictions are akin to those experienced by the actual polymer chain in solution.

In arriving at a theory which will adequately take into account the interactions of polymer segments with solvent one may consider, in accord with the analogy drawn above, the dependence of coil dimensions of a mathematical chain model on chain length and the volume "excluded" by one segment to all others. The properties of the model chosen, in turn, may be deduced from the relatively simple and well-known statistical behavior of random flight chains. In effect, the calculations of the kind here considered amount to mathematical deletion of those contributions to a particular property of random flight chains which violate the restrictions of volume exclusion. Thus, in the calculation of the mean square radius of the model chain we include only those conformations of random flight chains, and the associated dimensions which enter into the averaging process, in which all of the specified volumes assigned to the segments in no way overlap.

The enumeration, and subsequent subtraction, of unacceptable random flight conformations defined in accordance with the above conditions proceeds as follows. We formulate first the relatively simple expression for the fraction of all those random flight conformations, characterized by some fixed measure of coil extension, in which <u>at least</u> two chain segments occupy the same volume in space (within defined limits, ultimately analogous to the extent of segment-segment interaction in solution). The number of such conformations may be subtracted from the total for the set, to obtain a revised degenerary factor more nearly appropriate to the

model chain under consideration. The computation described may be repeated for all coil dimensions available to the chain. The calculation at this stage comprises the so-called "single contact" approximation.[14]

The procedure outlined above, however, although eliminating all unacceptable conformations involving segment overlaps, does not properly account for the total number of allowable conformations. The reason for this is that whereas a particular conformation involving, for example, a contact between segments i and j is quite properly eliminated from further consideration, it may at the same time also involve a contact between segments k and ℓ, and is thus subject to duplicate deletion at a further stage of the computation. Accordingly, it is necessary to introduce at this point the "double contact" approximation by means of which the multiplicity of such deletions is corrected. The original conformation considered may, of course, contain three or more contacts which are only properly accounted for by higher and higher orders of approximation. The necessity for such higher terms naturally increases with increase in segment excluded volume; for sufficiently small interactions, however, the single contact calculation provides a useful description of polymer coil size.

The series development of Eq. (7), arising from a detailed treatment of the procedure outlined above, has been applied to linear molecules. Our only new contribution has been to extend the first order calculation to the general class of p-functional star molecules. The principal steps in the mathematical development are outlined below.

C. Computations

The mean square radius of any chain, branched or linear, may be expressed by

$$\overline{s^2} = \frac{1}{2N^2} \sum_{\ell} \sum_{m} \overline{r^2_{\ell m}} \tag{9}$$

where $r^2_{\ell m}$ is the mean square separation of elements ℓ,m in the chain and N is the total number of segments. For a uniform star molecule containing p branches of equal length n = N/p the summations over the indices ℓ and m denoted by Eq. (9) may be resolved to yield the expression

$$2(pn)^2 \overline{s^2_b} = \binom{p}{2} \sum\sum^{A} \overline{r^2_{\ell m}} - p(p-2) \sum\sum^{B} \overline{r^2_{\ell m}} \tag{10}$$

where the subscript b now denotes the radius of the star structure under consideration. The first double summation A appearing above takes into account all possible ℓ and m pairs confined to one or both of two branches which together define a <u>linear</u> chain of 2n segments; the second summation

B is confined to all possible ℓ,m pairs situated on one linear branch of n segments.

The formulation (10) greatly simplifies computation of $\overline{s_b^2}$, inasmuch as the procedure employed permits expression of the latter in terms of various linear components of the star structure. Thus, from Eq. (10) and the appropriate forms of Eq. (9) for the linear constituents of the branched molecule we may write

$$\overline{s_b^2} = (1/p^2)[4(p_2)(\overline{s_{2n}^2})^* - p(p-2)(\overline{s_n^2})^*] \tag{11}$$

where $(\overline{s_{2n}^2})^*$ is the mean square radius of a linear chain of 2n segments in the presence of p-2 other n-segment linear chains attached by one end at the mid-segment of the former, and $(\overline{s_n^2})^*$ is the analogous quantity for one linear branch of n segments, again, in the presence of the remaining p-1 chains.

The two constituent mean square radii appearing in Eq. (11) may be computed separately, by employing in each instance a suitable defining relationship based upon application of Eq. (9). The procedure is essentially equivalent to that previously employed[12,13] in the treatment of the isolated linear chain. In the present case, however, the additional contact conformations introduced by the presence of linear components of the star structure other than those directly considered must be taken into account. We find for $(\overline{s_{2n}^2})^*$ the expression

$$(\overline{s_{2n}^2})^* = 2nb^2/6$$
$$+ 1/(2n)^2 \sum_{\ell>m} \sum_i \sum_j \sum_r \sum_\alpha \left[(\overline{r_{\ell m}^2})_0 P^{*(\alpha)}(E_{ij}) - r^2 P^{*(\alpha)}(E_{ij}) \right] + \cdots \tag{12}$$

where $P^*(E_{ij})$ is the probability that in a particular random flight conformation of a star molecule in which elements ℓ and m situated somewhere along one or both of two branches are separated by a distance r, two particular segments i and j, located anywhere in the molecule, are in contact. The summations in (12) extend over all ℓm and ij pairs, over all separations r which segments ℓ and m can assume and over all contact combinations (α) which affect the separation r. The parameter $(\overline{r_{\ell m}^2})_0$ is the unperturbed mean square separation of elements ℓ and m under random flight conditions. For $(\overline{s_n^2})^*$ we may write

$$(\overline{s_n^2})^* = nb^2/6$$
$$+ 1/n^2 \sum_{\ell>m} \sum_i \sum_j \sum_r \sum_\alpha \left[(\overline{r_{\ell m}^2})_0 P^{*(\alpha)}(E_{ij}) - r^2 P^{*(\alpha)}(E_{ij}) \right] \tag{13}$$

Combination of Eqs. (12) and (13) in accordance with Eq. (11) yields upon completion of the summations, the final result, expressed as the ratio α_s^2 of mean square radius of the star molecule to its random flight value

$$\alpha_s^2 = \overline{s^2}/\overline{s_0^2} = 1 + [6/p^{1/2}(3p - 2)][(p - 1)C_1/2 - (p - 2)C_2 + (p - 1)(p - 2)C_3]z + O(z^2) + \cdots \quad (14)$$

where the coefficients C_i assume the values

$$C_1 = 2^{7/2}(67/315)$$
$$C_2 = C_1/2^{7/2}$$
$$C_3 = (2/45)(101\sqrt{2} - 138)$$

In Table IX, a few values of the numerical coefficients of z in Eq. (14) for various p are given.

Table IX

First Order Interaction Coefficients for Star Molecules of Equal Branch Lengths

p	a_1
1[a]	1.276
2[a]	1.276
3	1.298
4	1.342[b]
8	1.559
$\to \infty$	$\to 0.43p^{1/2}$

(a) For p = 1,2, the molecule is a linear chain.
(b) The lower value 1.12 reported by Fixman[13] appears to be in error.

Although the procedure is more cumbersome, it is a simple matter to extend the reasoning given here to the case of the irregular star molecule with branches of unequal length.

D. Conclusions

Our extension of the "exact" theoretical treatment of the dimensions of polymer chains with small excluded volumes has led to the conclusion that, for the general class of p-functional star molecules, α_S^2 is initially augmented by increasing degrees of branching at fixed total molecular weight.

IV. Second Virial Coefficient for Star Molecules in Poor Solvents — Edward F. Casassa

An obvious further step after the derivation of the radius of a star molecule near the theta point is to apply the perturbation treatment to the interaction of two molecules to obtain an expression for the second virial coefficient. The parameters involved--the number N of statistical segments in a molecule, each characterized by a root-mean-square length b_0 and a mutually excluded volume β per segment pair--are just those appearing in the conformational problem for the single molecule; and in fact the calculations to determine the initial effect of volume exclusion on the bimolecular interaction are somewhat simpler than those for the dimensions of the single molecule.

For any structure, irrespective of chain branching, the virial coefficient A_2 is given by[14,15,16]

$$A_2 = -\frac{N_0}{2VM^2}\int [F_2(1,2) - F_1(1)F_1(2)]d(1)d(2) - \int [F_2(1,2) - F_1(1)F_1(2)]$$

$$= \beta V \sum_{i_1 i_2} \left[1 - \beta \sum_{j_1 j_2} P(O_{j_1 j_2})_{i_1 i_2} + O(\beta^2)\right] \qquad (15)$$

where A_2M is the coefficient Γ_2 of Eq. (1). The indices i_1, i_2, j_1, j_2 indicate segment i of molecule 1, segment i of molecule 2, etc. The McMillan-Mayer[15] distribution functions $F_1(1)$, $F_1(2)$ for single molecules 1 and 2 and $F_2(1,2)$ for two molecules simultaneously are defined in the usual way. The macroscopic volume of the system is V and Avogadro's number N_0. The symbols d(1), d(2), refer to differential elements of the configuration space of the molecules. In a way analogous to that described for a single molecule in the preceding section, Eq. (15) represents the first two terms of a series development giving successive orders of correction to the unperturbed chain statistics. In general the coefficients involve probabilities for multiple contacts, both intramolecular and intermolecular,[16,17] between pairs of segments: $P(O_{j_1 j_2})_{i_1 i_2}$, for instance, designating the probability of a contact j_1—j_2 conditional upon the existence of an initial intermolecular contact i_1—i_2.

Introducing the random-flight quantities for the double contact probability, we write

$$P(O_{j_1 j_2})_{i_1 i_2} = [(2\pi b_0^2/3)(\nu_1 + \nu_2)]^{-3/2}$$

where $\nu_1 + \nu_2$ represents the number of chain segments in the closed loop formed by making the contacts i_1—i_2, j_1—j_2, between molecules 1 and 2. It is convenient to number the segments of each linear subchain outward

from the branch point. Thus a specific segment identification requires two subscripts: $i_{1\mu}$ for example to denote segment i on the μ-th branch of molecule 1. There are two forms for ν_1 and ν_2 depending on the locations of the contacts.

$$\nu_1 = |i_{1\mu} - j_{1\lambda}|, \qquad \nu_2 = |i_{2\mu} - j_{2\lambda}|; \qquad \text{for } \mu = \lambda$$

$$\nu_1 = i_{1\mu} + j_{1\lambda}, \qquad \nu_2 = i_{2\mu} + j_{2\lambda}; \qquad \text{for } \mu \neq \lambda$$

To simplify the calculation we consider only the case of the regular star molecule with p identical arms of N/p segments. In taking account of the multiplicity of summations, it is useful first to consider i_1 and i_2 as fixed. Then, the double summation over j_1 and j_2 is to be performed once when $\mu = \lambda$ for both molecules, p-1 times when $\mu \neq \lambda$ for either molecule, and $(p-1)^2$ times when $\mu \neq \lambda$ for both molecules. The final double sum is taken p^2 times and divided by two to compensate for double counting of configurations. Since the random-flight model of the polymer corresponds to reality (even at the theta point) only for $n \gg 1$, it is permissible to replace the sums by integrals. The final result may be written

$$\frac{2A_2M^2}{N_0\beta n^2} = 1 - C_p z + O(z^2) \tag{16}$$

$$C_p = [32/15\ p^{1/2}][7 - 4\sqrt{2}$$

$$+ (p-1)(17\sqrt{2} - 9\sqrt{3} - 8) + (p-1)^2(9\sqrt{3} - 6\sqrt{2} - 7)]$$

where $z = (3/2\pi b_o^2)^{3/2}N^{1/2}\beta$ is the variable used earlier. From the calculated values of the coefficient C_p given in Table X it can be seen that in the vicinity of the theta point, at least, the effect of branching at a given molecular weight is to decrease the virial coefficient. The result is in accord with immediate physical intuition: increasing branching at fixed mass requires a more compact molecule; and thus the intermolecular interactions which produce deviations from van't Hoff's law because of less weight statistically. The result for linear chains has been known for a long time.[14] The only branched model which has been considered before is the cruciform molecule (p = 4) for which Stockmayer and Fixman[8] found $C_p = 4.00$. Since they did not give their derivation, we cannot trace the source of the slight discrepancy but suspect an arithmetical oversight in their calculation.

Table X

Coefficient of Linear Term in Eq. (16)

p	C_p	p	C_p
1	2.865	6	5.340
2	2.865	8	7.219
3	3.279	10	9.296
4	3.873	$p \to \infty$	$0.2201\ p^{3/2}$

V. Relationship of Chain Dimensions to Second Virial Coefficients — T. A. Orofino and J. W. Mickey

A. Introduction

In a previous section we have outlined the development and evaluation of the coefficients in the "exact" series developments for the mean square radii $\overline{s^2}$ of linear or branched molecules. Analogous expressions for the second virial coefficients Γ_2 of these structures, in terms of the same excluded volume parameter z, may also be derived.[14,18] As has been suggested earlier,[12] combination of the two series expressions for a given polymer through elimination of the parameter z provides a direct relationship between observable intra and intermolecular parameters. The dilute solution data for weakly interacting systems presented in Sections I and II of this report are pertinent to an analysis of this kind, the usefulness of which we shall explore in this final section of our report.

B. Theory

Combination of the series expressions for $\overline{s^2}$ and Γ_2 applicable to either linear or branched polymers yields the expression

$$\Gamma_2 = (4\pi^{3/2}N_0/D)[(\overline{s_o^2})^{3/2}/M][(\alpha_s^2 - 1) + d_1(\alpha_s^2 - 1)^2 + \cdots] \qquad (17)$$

where $\overline{s_o^2}$ represents the θ-solvent mean square radius of the polymer, M is polymer molecular weight, N_0 is Avogadro's number, and α_s is the intramolecular expansion factor defined through the relationship

$$\alpha_s^2 = \overline{s^2}/\overline{s_o^2}$$

The numerical value of the constant D derives from the corresponding value of the coefficient a_1 in the series for $\overline{s^2}$ (see Eq. (7)); for linear chains D is 1.276; for uniform trifunctional star molecules, 0.891. The coefficient d_1 depends upon the coefficients of higher terms in the series for $\overline{s^2}$ and Γ_2, the values of which are not presently available. Eq. (17) may also be expressed in the alternate form

$$\Gamma_2 = (4\pi^{3/2}N/a_1)[(\overline{s_o^2})_\ell^{3/2}/M][(\alpha_s^2 - 1) + d_1(\alpha^2 - 1)^2 + \cdots] \qquad (17A)$$

where $\overline{s_{o\ell}^2}$ now refers to the mean square radius of a linear polymer of the same molecular weight as the branched (or linear) polymer to which this equation may be applied.

Finally, one may derive an expression analogous to Eqs. (17) or (17A) applicable only to linear polymers in which the expansion factor α_s^2 is replaced by α_R^2, the corresponding ratio of mean square end-to-end distances $\overline{r^2}/\overline{r_0^2}$. The relationship follows by combination of the series expression for Γ_2 with the development for $\overline{r^2}$ analogous to Eq. (17). The result is

$$\Gamma_2 = 3N(\pi/6)^{3/2}[(\overline{r_0^2})_\ell^{3/2}/M][(\alpha_R^2 - 1) + c_1(\alpha_R^2 - 1) + \cdots] \qquad (18)$$

where, again, c_1 and higher coefficients depend upon the coefficients of higher terms in the parent series. Owing to the availability of the coefficient of the second contact term in the series for $\overline{r^2}$, c_1 can be computed.[13] Its value is -0.982.

Unlike the constituent series developments in the excluded volume parameter z or β, limited in application to very weakly interacting polymer-solvent systems, the Eqs. (17), (17A), and (12) appear to afford a useful basis for the correlation of dilute solution data.

C. Application to Experimental Data

In Figs. 11 and 12 are shown plots of Γ_2 versus $\alpha^2 - 1$ for the two linear polymer-solvent pairs polystyrene-cyclohexane and polystyrene-diethylmalonate (see Section I). The parameter α^2 employed here is alternatively computed from either the familiar operational definition involving the intrinsic viscosity $[\eta]$ and its θ-solvent value $[\eta]_\theta$

$$[\eta]/[\eta]_\theta = \alpha^3 \qquad (19A)$$

or, as more recently suggested by Yamakawa and Kurata,[31] the correspondence

$$[\eta]/[\eta]_\theta = \alpha^{2.43} \qquad (19B)$$

In all cases, variations in α^2 (and Γ_2) arise from variations in temperature of the systems at fixed polymer molecular weight (4.06×10^5).

The open circles in Fig. 11 denote light scattering Γ_2 values, the lined circles osmotic pressure values α^2 in each instance having been obtained through relationship (19A). The full and half-shaded circles represent the same, respective data interpreted in accordance with Eq. (19B).

Both sets of circles in Fig. 12 denote light scattering data, the open set derived from (19A), the shaded set from (19B).

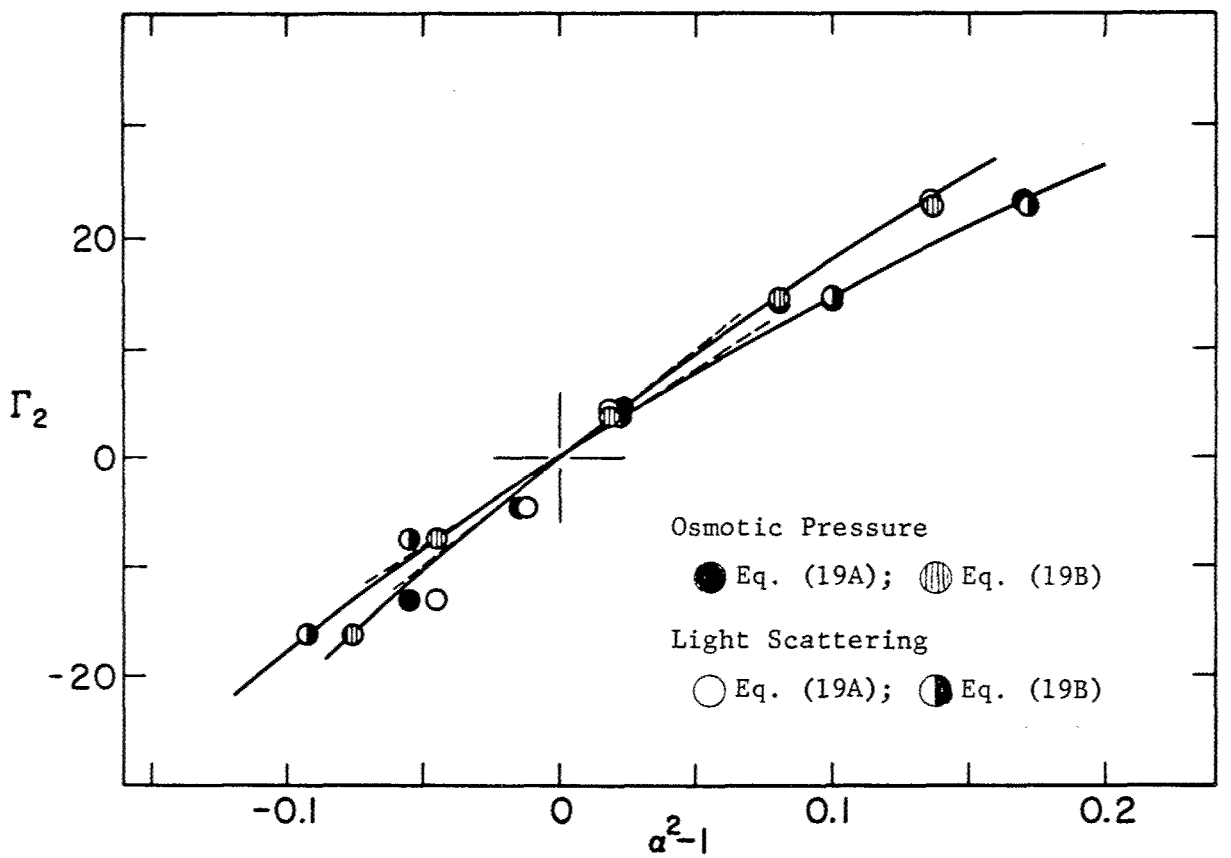

Figure 11 Plots of Γ_2 Versus $\alpha^2 - 1$ for the System Linear Polystyrene-Cyclohexane (See text for explanation of construction.)

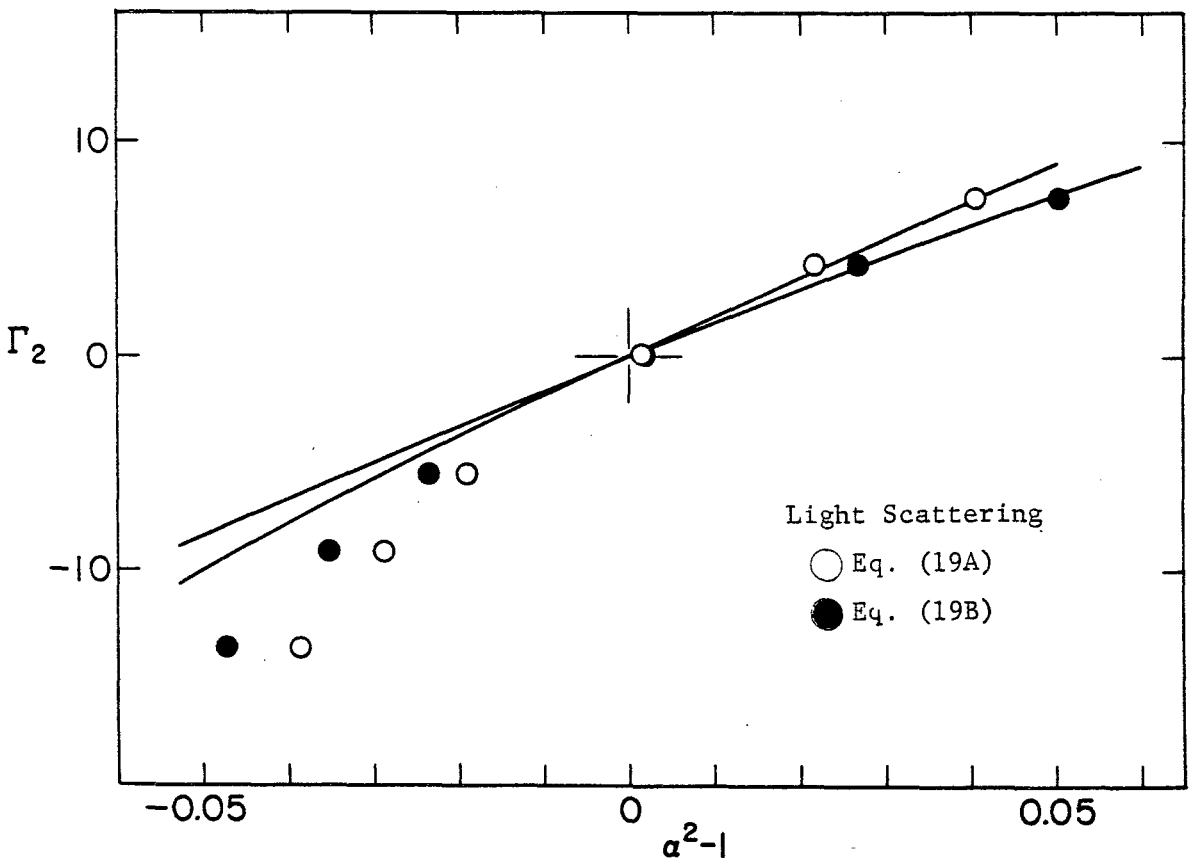

Figure 12 Plots of Γ_2 Versus $\alpha^2 - 1$ for the System Linear Polystyrene-Diethylmalonate (See text.)

The curves drawn in Figs. 11 and 12 represent the best fits of Eq. (18) to these data on the assumption that the definitions (19A) and (19B) successively provide adequate estimates of α_R^2 appearing therein. The dashed lines represent the limiting tangents at the points $\Gamma_2 = \alpha^2 - 1 = 0$ and were derived analytically through the curve fitting procedure.

In Table XI are listed values of the molecular weight independent quantity (for linear chains) $(\overline{r_o^2}/M)$, derived from the limiting tangent slopes of Figs. 11 and 12 in accordance with the relationship (18). Also listed are values of $\overline{r_o^2}/M$ derived from the same data in accordance with Eq. (17A), on the assumption that α^2 defined by Eq. (19) also provides an adequate estimate of α_S^2 appearing in (17A). In the computations based on the latter relationship we cannot quantitatively assess the curvature predicted by theory inasmuch as the numerical value of d_1 is not presently known.

Inspection of Figs. 11 and 12 reveals that for Γ_2 values greater than zero, theory and experimental data on linear polymer-solvent systems, as here interpreted, can be quantitatively reconciled. In support of this contention, we note first that the values of $\overline{r_o^2}/M$ deduced for the cyclohexane system are in reasonable agreement with the ratio found experimentally,[2,18] $0.50 \pm 0.05 \times 10^{-16}$. Also, the decrease in $\overline{r_o^2}/M$ associated with the diethylmalonate system is in agreement with a similar trend shown in our previous analyses of these systems (see Table III, Section I). Finally, we note that both qualitatively (in regard to sign) and quantitatively the curvature in the plot of Γ_2 versus $\alpha^2 - 1$ predicted by theory is borne out by our data.

The disparity between theory and experiment for Γ_2 values less than zero, evident in the plots of Figs. 11 and 12, may in part be attributable to inadequacy of the general series equations (17) and (18) for temperatures much below θ. The improved agreement of theory and osmotic pressure data for the cyclohexane system (Fig. 11) in this range, however, strongly suggests that much of the disagreement shown by the light scattering data points may arise from inaccuracies in the corresponding Γ_2 values obtained below θ (the trend is in the direction with which slight phase separation of the polymer-solvent mixture would be attendant). We should point out, however, that plots of the kind presented here are very sensitive to slight errors in the experimental data. The disparity noted, even if wholly attributable to inaccuracies in data in the range $T < \theta$, does not constitute a serious condemnation of the experimental results.

In Fig. 13 is shown a plot of Γ_2 versus $\alpha^2 - 1$, the latter computed with the aid of Eq. (19A), derived from cyclohexane data on a trifunctional star sample (Section II). The slope of the tangent line here was interpreted in accordance with Eq. (17) (or Eq. (17A)), utilizing the a_1 value derived for this system in Section III. The value of $\overline{r_o^2}/M$ for the linear polystyrene molecule of the same molecular weight as the star sample obtained from these data is also listed in Table XI.

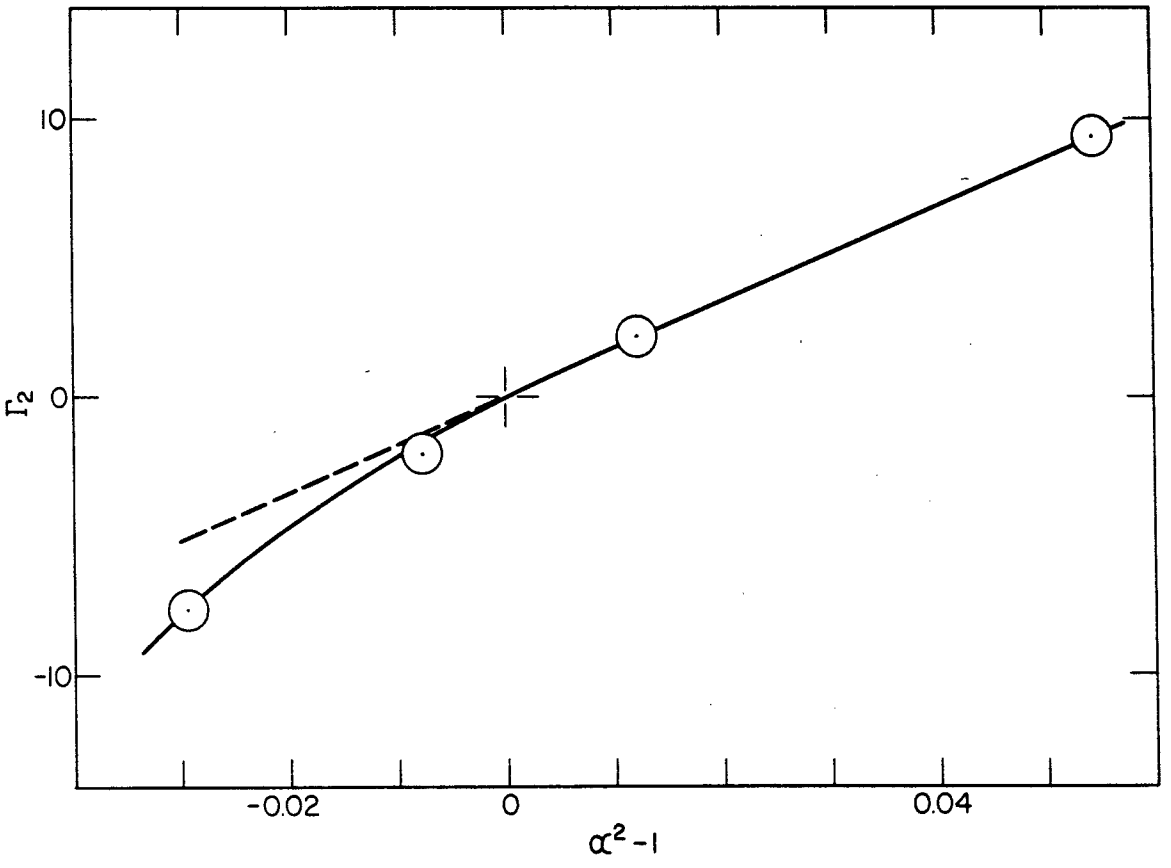

Figure 13 Plot of Γ_2 Versus $\alpha^2 - 1$ for Star Sample 8-III$_2$ in Cyclohexane

Table XI

Coil Dimensions of Polystyrene in θ-Solvent Media

$10^{16}(\overline{r_0^2}/M)$

	linear polystyrene $M = 4.06\times 10^5$				star polystyrene $M = 3.48\times 10^5$
Solvent	from (18), (19A)	from (17), (19A)	from (18), (19B)	from (17), (19B)	from (17), (19A)
Cyclohexane	0.59	0.57	0.52	0.51	0.56*
Diethylmalonate	0.57	0.55	0.51	0.50	

*For consistency, this value should be compared with the entry in the second column for the linear polymer, as has been done in Table III, Section II.

D. Conclusions

The combined intra and intermolecular series relationships utilized here in the analysis of pertinent dilute solution data perhaps represent the most useful aspect of the "exact" excluded volume developments. It is of particular interest to note that through this procedure, applied to sufficiently accurate and extensive data, a measure of coil dimensions may be obtained for polymer molecules whose overall sizes are too small to permit direction evaluation of the latter from the light scattering envelope.

VI. Effect of Heterogeneity in Molecular Weight on the Second Virial Coefficient of Linear Polymers in Good Solvents — Edward F. Casassa

A. Introduction

Since ordinary synthetic high polymers are heterogeneous in chain length to some degree, even after the most exacting fractionation procedures, interpretation of measurements of thermodynamic and hydrodynamic properties that depend on molecular weight is hampered by the difficulty that the effects of heterogeneity are not well understood even though, as is far from always the case, the nature of the weight distribution may be known precisely.

Because an exact treatment of the statistical thermodynamics of polymers in good solvents appears almost hopelessly difficult, a number of theories based on approximate molecular models have been developed[4,17,19-26] for the molecular weight dependence of the second virial coefficient. For none of these treatments, however, has it so far proved feasible to carry the generalization for a distribution of molecular weights to the point of numerical computations: at most, in some cases, results for a mixture of two solute species are obtained without great difficulty.[21] Hence, experimental tests of the theories are somewhat ambiguous in that the idealized homogeneous systems dealt with theoretically may not be well enough approximated in practice. The problem of heterogeneity also arises directly in comparisons of virial coefficients obtained by the two most important experimental techniques, osmometry and light scattering; for the two measurements are not exactly equivalent, yielding, as they do, different averages over any distribution of species present.[27-30]

In view of these questions, we have deemed it of interest to investigate the effect of polydispersity on the virial coefficient by utilizing very simple assumptions that make it possible to obtain results in analytical form. We can make no claim for the adequacy of the most important of our simplifications (except a perhaps naive one of some physical plausibility) and in any case do not pretend to have alleviated the need for realizing developments based on the more sophisticated models.

Conveniently, the problem may be described under two heads. First, we require a means of expressing the thermodynamic interaction of two linear chain molecules unlike in chain length, though otherwise identical. A complete theory of the second virial coefficient would of course provide this as a general result; but for the immediate purpose, we pursue the more limited aim of expressing this interaction as a function of parameters, which may be purely empirical, determined by the interactions in the common solvent, between pairs of like molecules of the two species. In other words, we seek a basis for some way of relating given virial coefficients for homogeneous systems to obtain coefficients for interaction of unlike species. At this stage results can be applied to the idealized case of two perfectly sharp polymer fractions. Finally, if it is possible to sum (or integrate) over a molecular weight distribution, virial coefficients can be computed for polydisperse systems. Although molecular weight

distributions produced in polymerization reactions or by fractionation procedures sometimes assume fairly uncomplicated forms, or can be expressed in approximate ways, the double integrations of expressions for bimolecular interactions over the distribution appear quite impossible analytically for any of the earlier statistical thermodynamic theories cited above except in poor solvents as the virial coefficient approaches zero. But in this limit, rigorous theory can be applied[31] just as easily.

B. Interaction of Polymer Chains of Different Length

We assume at the outset that the second virial coefficient A_2 in a solution of a homogeneous polymer of degree of polymerization $\underline{n}$ is given by

$$A_2 = B_0 n^{-a} \tag{20}$$

where B_0 and $\underline{a}$ are constants characteristic of the polymer-solvent pair at a particular temperature, but independent of the molecular weight of the polymer. This expression has little theoretical basis for molecular weights of ordinary magnitude* but does in fact conform, well within the limits of experimental error, to virtually all reliable light scattering and osmotic pressure data for polymer fractions in good solvents over wide ranges of molecular weight. Theoretical expressions of unrelated functional form might of course fit the experimental results equally well. Thus we can best regard Eq. (20) merely as a representation of experimental fact without seeking any other justification. The relation is useful because it contributes to making the ensuing mathematical operations extremely simple; and while the analytical forms that result may be of slight interest, the validity of conclusions, in quantitative numerical terms, will be no less, for this assumption at least, than if we were to make a purely numerical analysis based on experimental results directly, so long as we can avoid difficulties with mathematical convergence.

In order to proceed toward the treatment of a molecular weight distribution by expressing the virial coefficient for interaction of unlike polymer molecules in terms of B_0 and $\underline{a}$, we make the speculative assumption that the form of averaging appropriate for hard spheres of different sizes is applicable. For hard spheres of radii r_i and r_j and respective molar masses M_i and M_j, the interaction coefficient is given by[33]

$$B_{ij} = \frac{2\pi N_0}{M_i M_j} \int_0^\infty [1 - e^{-u(r)/kT}] r^2 dr$$

where the potential energy of interaction $u(r)$ is infinite for $0 \leq r \leq r_i + r_j$ and zero elsewhere. The integration then gives simply

$$B_{ij} = \frac{2\pi N_0}{3M_i M_j} (r_i + r_j)^3 \tag{21}$$

*Some of the theoretical models indicate that at high molecular weights, A_2 may become asymptotically proportional to $n^{1/2}/\alpha^3$, α being the factor by which the chain molecule is expanded beyond random flight dimensions by the intramolecular volume exclusion effect in good solvents. If, in this limit, α depends on a power of n, the form of Eq. 1 is obtained.[16,24,32]

and thus the virial coefficient B_{ii} for a homogeneous system of spheres is

$$B_{ii} = \frac{16\pi N_0}{3M_iM_j} r_i^3$$

expressed in the units of volume/(mass)^2 customarily used in studies of macromolecular substances. It follows by combination of these last two relations that

$$(B_{ij}M_iM_j)^{1/3} = \frac{1}{2}\left[(B_{ii}M_i^2)^{1/3} + (B_{jj}M_j^2)^{1/3}\right] \tag{22}$$

Applying this relation to polymers by equating B_{ii} to $B_0 n_i^{-a}$ and noting that M_i is proportional to n_i, we obtain the equation

$$(B_{ij}n_in_j)^{1/3} = \frac{B_0^{1/3}}{2}\left[n_i^{(2-a)/3} + n_j^{(2-a)/3}\right] \tag{23}$$

which can then be substituted in the general expressions for the virial coefficients for heterogeneous systems: for the osmotic pressure,[27]

$$A_2^{(\mathrm{II})} = \sum_i \sum_j B_{ij}w_iw_j \tag{24}$$

and for Rayleigh scattering,[28, 29]

$$A_2^{(R)} = \sum_i \sum_j B_{ij}M_iw_iM_jw_j \Big/ \left(\sum_i M_iw_i\right)^2$$

$$= \sum_i \sum_j B_{ij}n_iw_in_jw_j / \langle n\rangle^2 \tag{25}$$

where w_i, w_j are weight fractions of species in the solute (hence $\Sigma w_i = 1$) and $\langle n\rangle$ is $\Sigma n_i w_i$, the weight average degree of polymerization.

C. Mixtures of Two Polymer Species

Before undertaking the summations in Eqs. (24) and (25) we can use the results so far advanced to discuss the behavior of a ternary solution containing two homogeneous fractions of the same polymer. From Eq. (24) it is evident that $A_2^{(\mathrm{II})}$ for such a system, as a function of either of the weight fractions $\underline{w}$ determining the composition, is described by a parabola. Similarly $A_2^{(R)}$ is a more complicated quotient of quadratic expressions in $\underline{w}$; and thus $A_2^{(R)}$ and $A_2^{(\mathrm{II})}$ are alike only for $\underline{w}$ equal to zero and to unity (and at one other point for some values of the three B_{ij}).

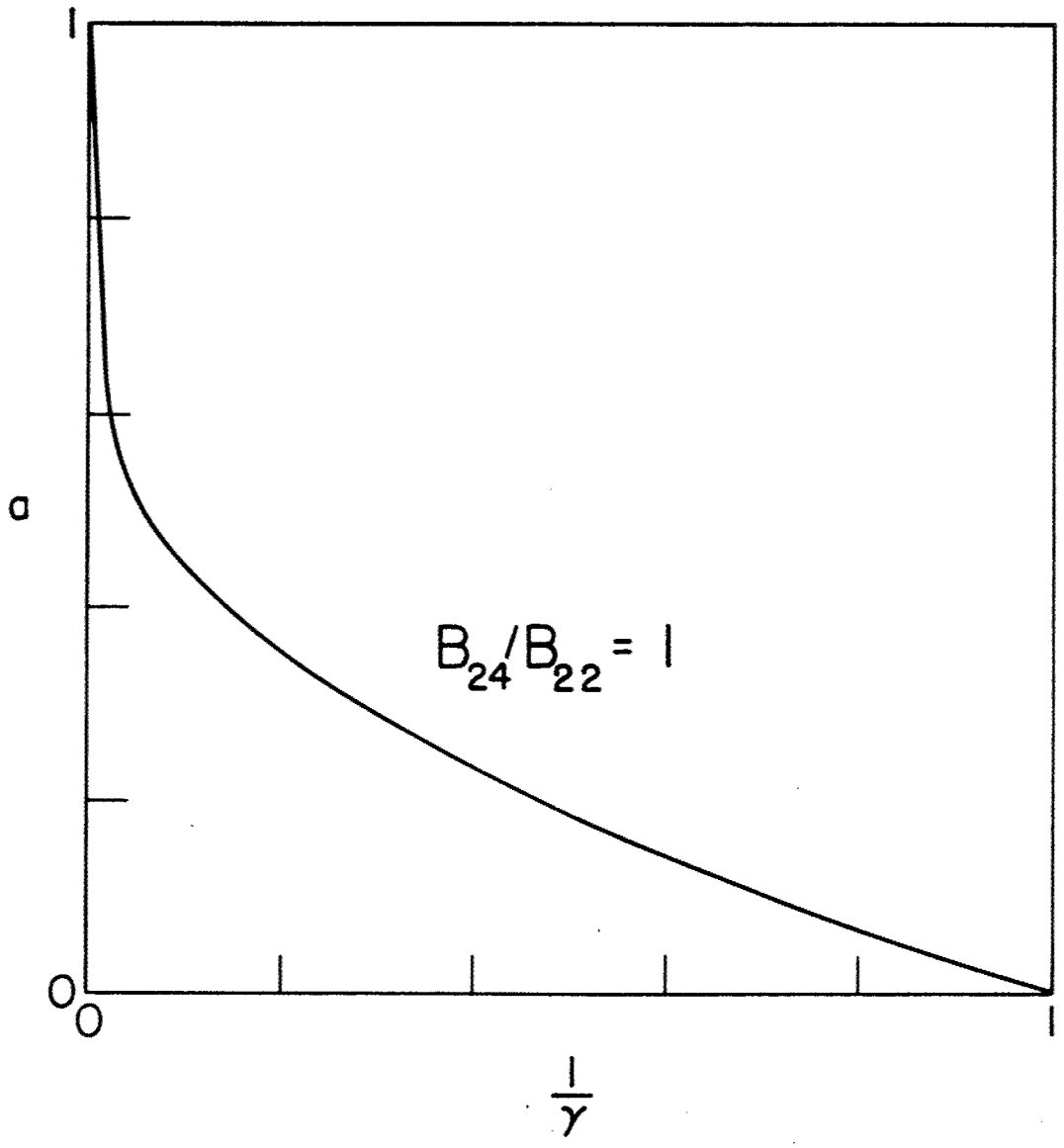

Figure 14 System of Two Polymer Fractions in One Solvent: Plot of Eq. (26) for $B_{24}/B_{22} = 1$. In the area bounded by the curve and the coordinate axes, $B_{24}/B_{22} > 1$; and in the field to the right $B_{24}/B_{22} < 1$.

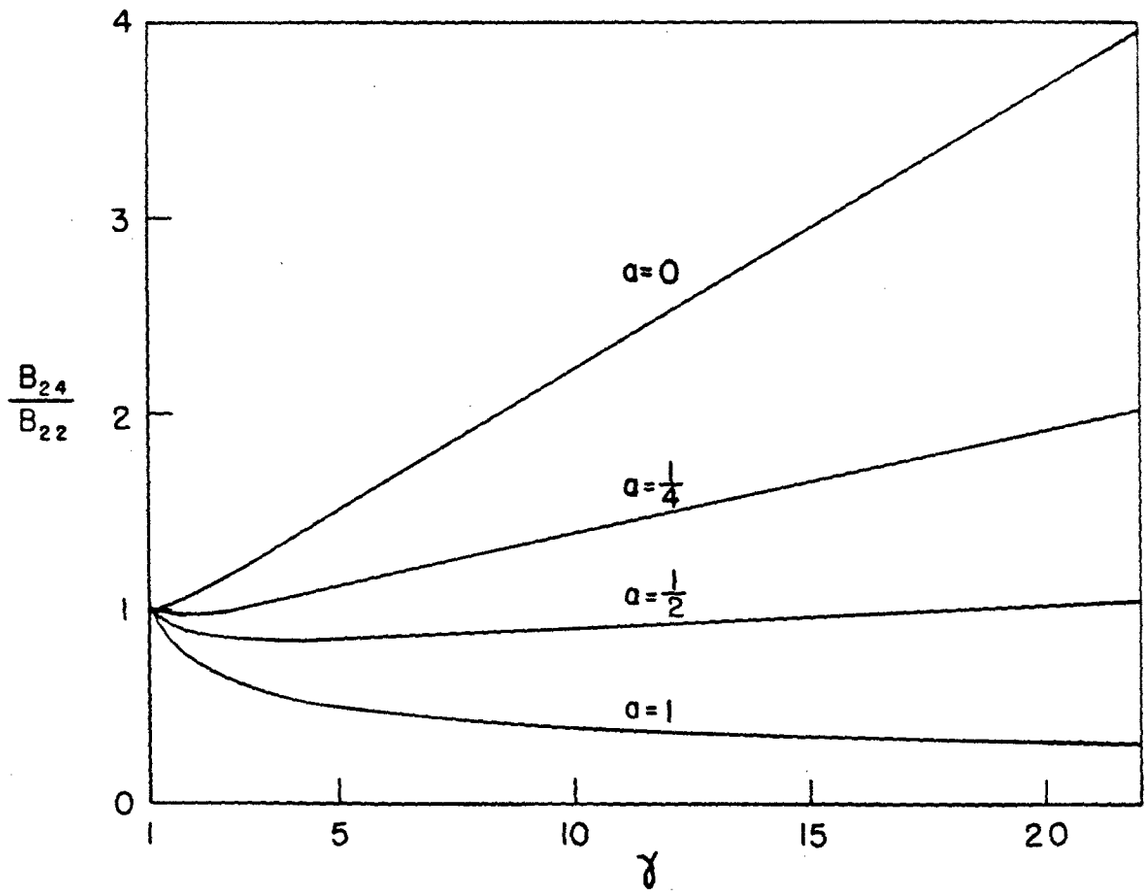

Figure 15 B_{24}/B_{22} from Eq. (26) as a Function of γ at Constant a

As one result of the statistical theory of Flory and Krigbaum,[20,21] in which the interaction of two chains of different length is considered explicitly, it is predicted that under certain conditions--certain magnitudes of the thermodynamic parameters characterizing interactions between two chain segments, and of the molecular weights of the two species--the values of both $A_2^{(II)}$ and $A_2^{(R)}$ pass through a maximum with variation of $\underline{w}$. It is very easy to show from the general equations (24) and (25) that the necessary and sufficient condition for the appearance of a maximum is simply that the cross-coefficient B_{ij} with $i \neq j$ be the largest of the three parameters.[30] If we designate the higher molecular weight component as 4 and the lower as 2, we thus require that $B_{24} > B_{22}$ since all theories agree with experiment in having $B_{22} > B_{44}$. The appearance of a minimum A_2 requires that $B_{24} < B_{44}$, but neither theory nor experiment so far indicate this as a possibility.

In the scheme developed here, Eq. (4) gives

$$\frac{B_{24}}{B_{22}} = \frac{1}{8\gamma}\left[1 + \gamma^{(2-a)/3}\right]^3 \tag{26}$$

where γ is the molecular weight ratio n_4/n_2. For $0 < a < 1$, B_{24}/B_{22} initially decreases from unity as γ increases and then increases, approaching $\gamma^{1-a}/8$ asymptotically. When $\underline{a}$ is zero, the ratio is never less than unity; and for $a = 1$, it decreases monotonically to approach the limit 1/8. As $\underline{a}$ becomes smaller, the critical γ for $B_{24} > B_{22}$ decreases. These points are illustrated in Figs. 14 and 15. Empirically, 1/4 is a typical value of $\underline{a}$ for systems in very good solvents. Roughly, the magnitude of $\underline{a}$ seems to parallel the solvent power and is seldom found to be much larger than this.[6,34,35]

From Eq. (4) we also get

$$\frac{B_{24}}{B_{44}} = \frac{1}{8\gamma^{1-a}}\left[1 + \gamma^{(2-a)/3}\right]^3 \tag{27}$$

As this ratio is always greater than unity over the meaningful range of $\underline{a}$, no minimum in A_2 is allowed.

Experimentally, the maximum in A_2 has been found as expected in some systems and not in others; but the possible comparisons with Eq. (26) are at the moment very limited, only few sufficiently reliable results having been published. The best work is probably that of Krigbaum and Flory[6] whose experimental results for two systems (polyisobutene-cyclohexane and polystyrene-toluene) are given in Table XII. In the last column, values of B_{24}/B_{22} as required by the Flory-Krigbaum[21] theory are also listed. These were calculated entirely from the theory* and the thermodynamic constants obtained independently of the A_2 measurements by interpretation of intrinsic viscosity data according to the method of Flory and Fox.[11]

*Equations (43) to (45) below were used in the calculations together with an approximate closed form given by Orofino and Flory[21] for the function F(X) in Eq. (43).

Table XII

Second Virial Coefficients in Solutions of Mixtures of Two Polymer Fractions

System and Method	$M_2 \times 10^{-3}$	γ	a	Experimental[a] $B_{22} \times 10^4$	$B_{44} \times 10^4$	B_{24}/B_{22}	B_{24}/B_{22} (Flory-Krigbaum theory)	B_{24}/B_{22} Eq. (26)
Polystyrene-toluene (II[b], 30°C)[6]	0.614	9.80	0.22[d] (0.22)[6]	4.98	3.26	1.28	1.08	1.48
Polyisobutene-cyclohexane (II, 30°)[6]	0.814	8.85	0.16 (0.14)[6]	7.26	5.38	1.14	1.10	1.56
PMMA[c]-butanone (R[b], 25°)[32]	1.26	21.0	0.33 (0.24)[32]	2.93	1.08	0.58	1.14	1.68
PMMA-butanone (R, 25°?)[37]	3.8	8.32	0.21	2.13	1.29	1.34	1.18	1.41
PMMA-acetone (II, 25°)[e,38]	0.86	12.2	0.24 (0.22)[f,34]	3.10	1.42	0.99	1.08	1.27
PMMA-acetone (R, 25°)[e,38]	0.92	12.8	0.085 (0.22)[f,35]	1.92	1.45	1.04[g]	1.08	2.20

[a]Most of the listed coefficients are least-squares parameters for Eqs. (24) and (25). [b]II denotes osmotic pressure; R, light scattering. [c]Poly-(methyl methacrylate). [d]Values of a were calculated from A_2 for the two fractions in question: more extensive measurements give the figures in parentheses. The former were used in determining B_{24}/B_{22} from Eq. (26). [e]The Same fractions were used in osmotic and light scattering measurements. [f]From measurements at 30°C. [g]Another analysis[30] of the same data gives $B_{24}/B_{22} < 1$.

Another procedure of forcing B_{22} and B_{44} to fit the experimental data and retaining the theory only in combining these coefficients to obtain B_{24} leads to physically meaningless results in some cases unless a constant appearing in the theory is altered. These modifications are discussed elsewhere,[30,36] but here only the original treatment as described by Krigbaum and Flory[6] is considered. For the first two systems in Table XI, the Flory-Krigbaum theory correctly predicts a maximum A_2, but it gives values of B_{24}/B_{22} apparently somewhat too low while the present treatment seems to exaggerate the magnitude of the ratio. Studies of systems of mixed fractions of poly-(methyl methacrylate) in good solvents have given contradictory results, as indicated in the tabulation. In one study of a poly-(methyl methacrylate)-butanone system, the experimental data indicated the occurrence of a maximum in A_2 to be impossible;[32] but in another similar investigation[37] a maximum was found, although there may be some question as to the magnitude of experimental error. Finally, measurements on ternary solutions of poly-(methyl methacrylate) in acetone have given equivocal results.[30,38] In all these last three cases both the Flory-Krigbaum theory and our treatment demand that $B_{24} > B_{22}$, our theory always giving by far the larger B_{24}/B_{22} ratio.

We digress briefly at this point from the main course of the argument to observe that Eq. (20) can be regarded as a generalization of the hard sphere relation. For matter of uniform density the radius is proportional to the cube root of the mass so that B_{ii} is proportional to M^{-1}. Thus $\underline{a}$ is unity, and, according to Eqs. (26) and (27) B_{24} for hard spheres is always intermediate between B_{22} and B_{44}. If a polymer molecule is regarded as an impenetrable sphere of size determined by a random-flight dimension (e.g., the radius of gyration) proportional to $n^{1/2}$, the virial coefficient varies with $n^{-1/2}$ and, depending on γ, B_{24} may be either larger than B_{22} or intermediate between B_{22} and B_{44}. For a real polymer chain, the excluded volume effect causes the radius of gyration to increase more rapidly than $n^{1/2}$ and $\underline{a}$ should be less than 1/2, as is actually found to be the case. Equation 1 and the more specific hard sphere relation agree in giving a virial coefficient that becomes infinite as $\underline{n}$ approaches zero. On the other hand, all the statistical theories, both approximate[4,17,19-26] and rigorous,[14,16] assume the form of a constant multiplied by a series $1 + O(n^{1/2})$ in integral powers of $n^{1/2}$. This discrepancy is trivial, however, in regard to molecular weight inasmuch as we can require $n \gg 1$ to be a condition for physical significance.* This assumption appears to be implicit in all the statistical derivations.

D. The Virial Coefficient for Heterogeneous Polymers

In calculating the virial coefficient for systems with a distribution of molecular weights, we adopt the familiar distribution

*The double integrals following (e.g., Eqs. (29), (30)) with Eq. (20) and the form of molecular weight distribution we adopt, remain convergent even though we integrate over the entire range $0 \leq n \leq \infty$. The fractional contribution to the integrals from the range $0 \leq n \leq n_o$ is of the order of $(n_o/\langle n \rangle)^{2-a+\delta}$ where $\delta > 0$.

function first applied to polymers by Schulz:[39]

$$f(n) = y^{Z+1} \frac{n^Z}{\Gamma(Z+1)} e^{-yn} \tag{28}$$

$$y = (Z+1)/\langle n \rangle$$

where $f(n)dn$ is the weight fraction of the solute with n within the differential increment dn, and $\Gamma(x)$ denotes the gamma function. The value of Z increases with decreasing heterogeneity: the limit of infinite sharpness is characterized by $Z = \infty$ while $Z = 1$ corresponds to the "most probable" distribution obtained in the polyester type of condensation and also in free-radical polymerizations carried to low degrees of conversion in the presence of a chain transfer agent.[2]

We substitute Eq. (28) into the integral expressions corresponding to the sums of Eqs. (24) and (25)

$$A_2^{(II)} = \int_0^\infty \int_0^\infty B(m,n) f(m) f(n) dm dn \tag{29}$$

$$A_2^{(R)} = \langle n \rangle^{-2} \int_0^\infty \int_0^\infty B(m,n) m f(m) n f(n) dm dn \tag{30}$$

and let $B(m,n)$ be given by

$$B(m,n)mn = \frac{B_0}{8}\left[m^{(2-a)/3} + n^{(2-a)/3}\right]^3 \tag{31}$$

in accordance with Eq. (23). The definite integrals resulting reduce in every case to various combinations of the single standard form

$$\int_0^\infty u^{t-1} e^{-ku} du = \Gamma(t)/k^t$$

In the case of the osmotic pressure, we obtain

$$\begin{aligned} A_2^{(II)} &= \frac{B_0 y^{2(Z+1)}}{8[\Gamma(Z+1)]^2} \int\int m^{Z-1} n^{Z-1} \left[m^{(2-a)/3} + n^{(2-a)/3}\right]^3 e^{-y(m+n)} dm dn \\ &= \frac{B_0 y^{2(Z+1)}}{4[\Gamma(Z+1)]^2} \\ &\times \int\int \left[m^{Z+1-a} n^{Z-1} + 3m^{(3Z+1-2a)/3} n^{(3Z-1-a)/3}\right] e^{-y(m+n)} dm dn \\ &= B_0 y^a \varphi^{(II)}/4[\Gamma(Z+1)]^2 \end{aligned} \tag{32}$$

where

$$\varphi^{(II)} = \Gamma(Z + 2 - a)\Gamma(Z) + 3\Gamma[3Z + 4 - 2a)/3]\Gamma[(3Z + 2 - a)/3] \quad (33)$$

Since the number average degree of polymerization n_N is given by

$$n_N^{-1} = \int\left(\frac{f(n)}{n}\right) dn = y/Z$$

the ratio of $A_2^{(II)}$ to the virial coefficient B_{NN} of the homogeneous polymer with degree of polymerization n_N is

$$A_2^{(II)}/B_{NN} = Z^a\varphi^{(II)}/4[\Gamma(Z + 1)]^2 \quad (34)$$

For light scattering, the analogous relations are

$$A_2^{(R)} = B_0 y^a \varphi^{(R)}/4[\Gamma(Z + 2)]^2$$

$$\phi^{(R)} = \Gamma(Z + 3 - a)\Gamma(Z + 1) + 3\Gamma[(3Z + 7 - 2a)/3]\Gamma[(3Z + 5 - a)/3] \quad (35)$$

and

$$A_2^{(R)}/B_{WW} = (Z + 1)^a\varphi^{(R)}/4[\Gamma(Z + 2)]^2 \quad (36)$$

where B_{WW} refers to a homogeneous polymer with $n = \langle n \rangle$. The ratio of the two virial coefficients for one polymer is obviously

$$A_2^{(II)}/A_2^{(R)} = (Z + 1)^2\varphi^{(II)}/\phi^{(R)} \quad (37)$$

Finally the ratio of Eq. (34) to Eq. (36)

$$A_2^{(II)}B_{WW}/B_{NN}A_2^{(R)} = [Z/(Z + 1)]^a A_2^{(II)}/A_2^{(R)} \quad (38)$$

if of interest since it represents the comparison obtained by superimposing osmotic and scattering data plotted against n_N and $\langle n \rangle$ respectively.

The expressions just derived for heterogeneous polymers have the property that for any given distribution, characterized by Z, the form of

the relation between the virial coefficient and average molecular weight is still that of Eq. (20) for a single species: thus double logarithmic plots of $A_2^{(II)}$ versus n for a sharp fraction and of $A_2^{(II)}$ and $A_2^{(R)}$ versus n_N or $\langle n \rangle$ are all predicted to be straight lines of the same slope, -a. The ratios defined by Eqs. (34) and (36-38) for a = 1/4 are shown as functions of Z in Fig. 16. All are seen to increase from unity with increasing heterogeneity. As Z approaches zero, $\varphi^{(II)}$ becomes infinite--because of the divergence of the integral $\Gamma(0)$--and all the ratios become infinite except $A_2^{(R)}/B_{WW}$ which attains its maximum value of 1.13. The most pronounced effect is on $A_2^{(II)}/A_2^{(R)}$ for the same polymer; in comparison, divergences between virial coefficients for heterogeneous samples and for sharp fractions of molecular weight corresponding to the appropriate average are less marked. Numerical values of the ratios for Z = 1 and a = 1/4 are listed in the second column of Table XIII. These figures indicate that comparison of virial coefficients from osmotic pressure and light scattering measurements on the same normally heterogeneous polymer sample may reveal a significant effect due to polydispersity; but since the experimental error in determination of $A_2^{(II)}$ is perhaps five percent at best, one could scarcely expect on the basis of this theory to discover an experimentally significant difference in comparing $A_2^{(II)}$ as a function of n_N with $A_2^{(R)}$ as a function of $\langle n \rangle$ obtained by independent measurements on different series of polymers. In view of these results it appears that by reasonably good fractionation one can hope to eliminate the effects of heterogeneity for all practical purposes to the extent that a solution of a single polymer fraction can be considered as a simple binary system.

E. Mixtures of Heterogeneous Polymers

The unexplained disagreements between experiment and theory for mixtures of two fractions of the same polymer prompt a question as to whether the expected maximum in A_2 could have been vitiated if the individual fractions were in fact rather heterogeneous. For poly-(methyl methacrylate) in particular it has been recognized that good fractionation is difficult to attain.[35,40-42] To investigate this problem we again use the Schulz distribution assuming that polymers 2 and 4 each exhibit a distribution in molecular weight characterized by Z_2 and Z_4 in the distribution functions $f_2(n)$, $f_4(n)$ given by Eq. (28). Thus we describe the composite distribution by

$$\phi(n) = f_2(n)w_2 + f_4(n)w_4$$

where, as above, $w_2 + w_4 = 1$ and

$$\int \phi(n)dn = 1$$

as is required.

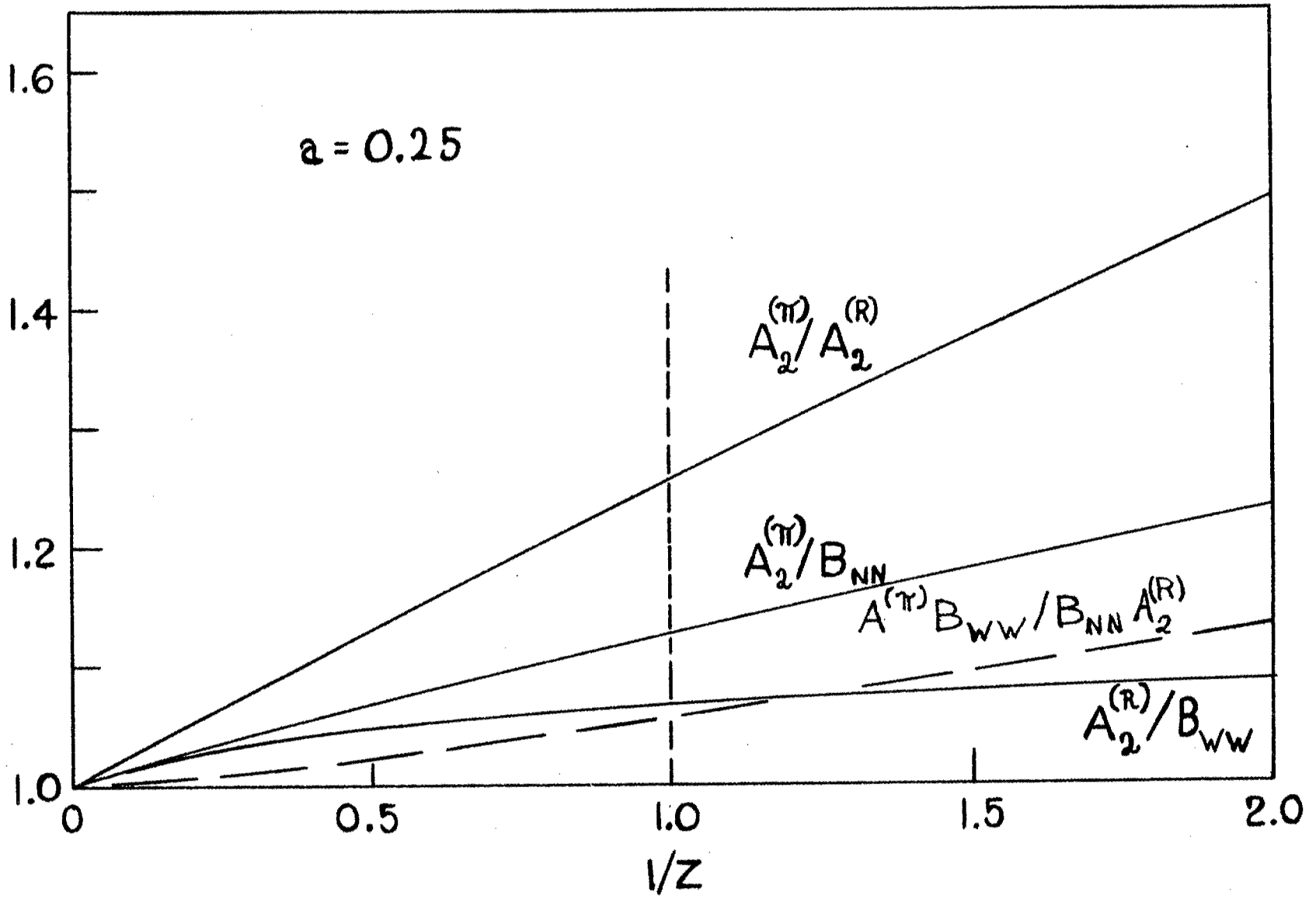

Figure 16 Effect of Polymer Heterogeneity on the Second Virial Coefficient. The ordinate represents the ratios given by Eqs. (34) and (36-38) with $\underline{a} = 1/4$.

Table XIII

Calculated Effect of Polymer Heterogeneity on Virial Coefficients for the Most Probable Distribution (Z = 1)

B_{ij} from:	Eq. (23)	Eqs. (20), (47)		Eqs. (20), (48)	
	a = 1/4	a = 1/3	a = 1/4	a = 1/4 ν = 0	a = 1/4 ν = 1
$A_2^{(II)}/A_2^{(R)}$	1.255	1.190	1.138	1.143	1.455
$A_2^{(II)}/B_{NN}$	1.127	0.885	0.909	0.919	1.608
$A_2^{(R)}/B_{WW}$	1.068	0.937	0.950	0.956	1.315
$A_2^{(II)}B_{WW}/A_2^{(R)}B_{NN}$	1.055	0.945	0.957	0.961	1.223

The virial coefficient for the osmotic pressure is thus

$$A_2^{(II)} = \int\int B(m,n)\phi(m)\phi(n)\,dmdn = \langle B_{22}^{(II)}\rangle w_2^2 + 2\langle B_{24}^{(II)}\rangle w_2 w_4 + \langle B_{44}^{(II)}\rangle w_4^2 \qquad (39)$$

where

$$\langle B_{ij}^{(II)}\rangle = \int\int B(m,n) f_i(m) f_j(n)\,dmdn$$

As before, we assume Eq. (3i) for $B(m,n)$. The coefficients $B_{22}^{(II)}$ and $B_{44}^{(II)}$ are then given directly by Eqs. (29) and (32). The remaining one $B_{24}^{(II)}$ is readily derived in similar fashion; but the general result for $Z_2 \neq Z_4$ and $y_2 \neq y_4$ is more cumbersome:

$$\langle B_{24}^{(II)}\rangle = \frac{B_0\langle n_2\rangle^{-a}}{8\xi}\frac{(Z_2+1)(Z_4+1)}{\Gamma(Z_2+1)\Gamma(Z_4+1)}\left\{\frac{\Gamma(Z_2+2-a)\Gamma(Z_4)}{(Z_2+1)^{2-a}}\right.$$
$$+\frac{3\Gamma[(3Z_2+4-2a)/3]\Gamma[(3Z_4+2-a)/3]\xi^{(2-a)/3}}{[(Z_2+1)^{2/3}(Z_4+1)^{1/3}]^{2-a}}$$
$$+\frac{3\Gamma[3Z_2+2-a)/3]\Gamma[(3Z_4+4-2a)/3]\xi^{2(2-a)/3}}{[(Z_2+1)^{1/3}(Z_4+1)^{2/3}]^{2-a}}$$
$$\left.+\frac{\Gamma(Z_2)\Gamma(Z_4+2-a)\xi^{2-a}}{(Z_4+1)^{2-a}}\right\}$$

where $\xi = \langle n_4\rangle/\langle n_2\rangle$, the ratio of the weight average molecular weights $\langle n_2\rangle$, $\langle n_4\rangle$, replaces γ used above in discussion of a binary solute. In the simpler case in which $Z_2 = Z_4 = Z$, this expression reduces to

$$\langle B_{24}^{(II)}\rangle/\langle B_{22}^{(II)}\rangle = (2\xi\varphi^{(II)})^{-1}\Big\{(1+\xi^{2-a})\Gamma(Z)\Gamma(Z+2-a) + 3(\xi^{(2-a)/3}+\xi^{2(2-a)/3})\Gamma[(3Z+2-a)/3]\Gamma[(3Z+4-2a)/3]\Big\} \quad (40)$$

where $\varphi^{(II)}$ is defined by Eq. (33).

For light scattering, the virial coefficient for the mixture of two polymers is given by

$$A_2^{(R)} n_w^2 = \langle B_{22}^{(R)}\rangle\langle n_2\rangle^2 w_2^2 + 2\langle B_{24}^{(R)}\rangle\langle n_2\rangle w_2\langle n_4\rangle w_4 + \langle B_{44}^{(R)}\rangle\langle n_4\rangle^2 2_4^2$$

Eq. (30) gives $\langle B_{22}^{(R)}\rangle\langle B_{44}^{(R)}\rangle$, and the other coefficient is

$$\langle B_{24}^{(R)}\rangle = (\langle n_2\rangle\langle n_4\rangle)^{-1}\int\int B(m,n)mf_2(m)nf_4(n)\,dmdn$$

$$= \frac{B/8\xi\langle n_2\rangle^a}{\Gamma(Z_2+1)\Gamma(Z_4+1)}\Bigg\{\frac{\Gamma(Z_2+3-a)\Gamma(Z_4+1)}{(Z_2+1)^{2-a}} + \frac{3\Gamma[3Z_2+7-2a)/3]\Gamma[(3Z_4+5-a)/3]\xi^{(2-a)/3}}{[(Z_2+1)^{2/3}(Z_4+1)^{1/3}]^{2-a}} + \frac{3\Gamma[(3Z_2+5-a)/3]\Gamma[(3Z_4+7-2a)/3]\xi^{2(2-a)/3}}{[(Z_2+1)^{1/3}(Z_4+1)^{2/3}]^{2-a}} + \frac{\Gamma(Z_2+1)\Gamma(Z_4+3-a)\xi^{2-a}}{(Z_4+1)^{2-a}} \quad (41)$$

When $Z_2 = Z_4$, this becomes

$$\langle B_{24}^{(R)}\rangle/\langle B_{22}^{(R)}\rangle = (2\xi^{(R)})^{-1}\Big\{(1+\xi^{2-a})\Gamma(Z+3-a)\Gamma(Z+1) + 3(\xi^{(2-a)/3}+\xi^{2(2-a)/3})\Gamma[(3Z+5-a)/3\Gamma[(3Z+7-2a)/3]\Big\} \quad (42)$$

with $\varphi^{(R)}$ given by Eq. (35).

It is apparent from Eqs. (40) and (42) that the ratios $\langle B_{24}^{(II)}\rangle/\langle B_{22}^{(II)}\rangle$ and $\langle B_{24}^{(R)}\rangle/\langle B_{22}^{(R)}\rangle$ both increase as Z decreases, with the effect somewhat more marked in the case of the osmotic pressure. These relations are shown in Fig. 17 for a = 1/4. When Z is unity, the apparent B_{24}/B_{22} for the osmotic pressure is increased by factors of 1.02, 1.07, 1.16 and 1.20 respectively for ξ equal to 2, 5, 10, and 20: the corresponding figures for light scattering are 1.01, 1.03, 1.09, and 1.11. It

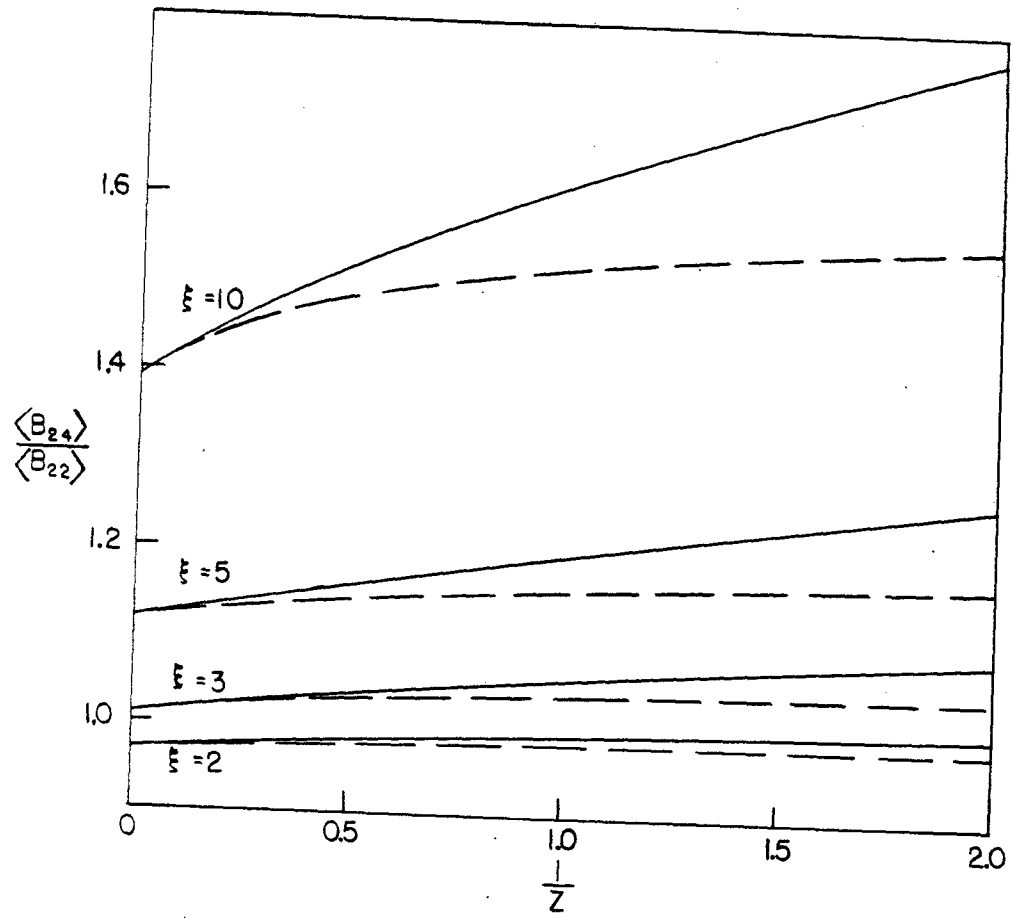

Figure 17 $\langle B_{24}\rangle/\langle B_{22}\rangle$ for Mixtures of Two Polymers of the Same Heterogeneity ($Z_2 = Z_4$) with $\underline{a} = 1/4$: the osmotic pressure Relation (solid curves) given by Eq. (40); the light scattering result (dashed curves) by Eq. (42).

is predicted then, that the effect that leads to a maximum in A_2 as a function of composition for a binary solute is enhanced rather than suppressed by an equal degree of heterogeneity in the two components. As heterogeneity increases in this way, the critical molecular weight ratio ξ for appearance of the maximum decreases; thus at fixed $\langle n_2 \rangle$ and $\langle n_4 \rangle$ a heterogeneous system may give a maximum A_2 for particular values of $\langle n_2 \rangle$ and $\langle n_4 \rangle$ for which a strictly two-component solute would not.

The situation is different if we consider the possibility that Z_2 is not the same as Z_4. An increase in the heterogeneity of polymer 4 relative to that of polymer 2 increases the ratio $\langle B_{24}^{(II)} \rangle / \langle B_{22}^{(II)} \rangle$ at a fixed value of the number average molecular weight ratio,

$$\epsilon \equiv \xi [Z_4(Z_2 + 1)/Z_2(Z_4 + 1)]$$

while a decrease has the opposite effect. In particular, therefore, $\langle B_{24}^{(II)} \rangle / \langle B_{22}^{(II)} \rangle$ is greater when $Z_4 < Z_2$ than the value given by Eq. (40) for the same ϵ and $Z = Z_2$, and does not decrease to unity when ϵ is unity. Conversely, when Z_4 is infinite, $\langle B_{24}^{(II)} \rangle / \langle B_{22}^{(II)} \rangle$ at finite Z_2 is smaller than the B_{24}/B_{22} ratio for homogeneous polymers and again does not become unity for $\epsilon = 1$. (When one Z is infinite, $\langle B_{24} \rangle$ is easily gotten from the integrals given above, in Eqs. (39) and (41), by using a delta function to describe the distribution of the homogeneous component.) The same qualitative relations hold with regard to $\langle B_{24}^{(R)} \rangle / \langle B_{22}^{(R)} \rangle$, the comparisons being made at a given value of ξ. Consequently a maximum A_2 predicted for a mixture of two homogeneous fractions at a particular value of γ would not appear in a real system if in fact fractionation were inadequate and Z_2 happened to be sufficiently less than Z_4. Calculations for the case $Z_2 = 1$, $Z_4 = \infty$, $a = 1/4$, $\epsilon = 10$ (i.e., $\xi = 5$), give $\langle B_{24}^{(II)} \rangle / \langle B_{22}^{(II)} \rangle = 1.22$ and $\langle B_{24}^{(R)} \rangle / \langle B_{22}^{(R)} \rangle = 1.04$ as compared to B_{24}/B_{22} equal to 1.13 and 1.41 for mixed homogeneous fractions with γ of 5 and 10 respectively.

The generalization of this development for a mixture of two heterogeneous polymers to more complex molecular weight distributions is at once obvious. The assumption of the Schulz distribution is therefore scarcely restrictive since almost any distribution could be described reasonably well as a combination of several heterogeneous polymers each characterized by an appropriate value of Z and $\langle n \rangle$.

F. Other Forms for B_{ij}

In choosing the rigid sphere relation for combining second virial coefficients of homogeneous systems to obtain the interaction coefficient B_{ij} for unlike components, we have made perhaps the simplest possible assumption suggested by a physical model. Aside from this tenuous justification, the treatment is arbitrary and acceptable only to the degree to which it may be found to agree with experiments or with

developments of greater rigor. Unfortunately the exact statistical treatment of polymer solutions has been worked out only for systems near the theta point, the limit of vanishing A_2, where Eq. (20) is not valid.*

Among the approximate theories, that of Flory and Krigbaum[20,21] includes the calculation of B_{ij} for molecules of dissimilar size. In their model, the polymer molecule is represented as a spherically symmetrical cloud of chain segments with a gaussian density distribution normalized so that the radius of gyration agrees with that of the real polymer chain. The interaction (interpenetration) of two such spheres is then treated according to standard statistical mechanical techniques to obtain B_{ij}. The result may be written in the form

$$B_{ij} = \frac{N_0 \beta n_i n_j}{2M_i M_j} F(X_{ij}) \tag{43}$$

$$\left(\frac{X_{ij}}{n_i n_j}\right)^{2/3} = \frac{2(X_{ii}/n_i^2)^{2/3}(X_{jj}/n_j^2)^{2/3}}{(X_{ii}/n_i^2)^{2/3} + (X_{jj}/n_i^2)^{2/3}} \tag{44}$$

$$X_{ii} = (\beta n_i^{1/2}/\alpha_i^3)(9/2\pi b_0^2)^{3/2} \tag{45}$$

where n_i is now the number of segments or steps of root-mean-square length b_o in the equivalent unperturbed chain representing a polymer molecule of weight M_i, and α_i is the linear factor by which the radius of the chain in a good solvent, is expanded by intramolecular interactions. The function $F(X)$ expressing the molecular weight dependence of A_2 cannot be written exactly in closed form; however it is unity for $X = 0$ and decreases monotonically to approach zero as X becomes infinite. In terms of parameters of the assumed chain model, the molecular radius of gyration is given by

$$\langle R_i^2 \rangle = n_i b_0^2 \alpha_i^2 / 6$$

Putting this into Eq. (45) and thence into Eq. (44), we obtain an effective radius for interaction of two unlike molecules defined by

$$\langle R_{ij}^2 \rangle \equiv \left(\frac{n_i n_j}{X_{ij}}\right)^{2/3} \frac{3\beta^{2/3}}{4\pi} = \frac{1}{2}\left(\langle R_i^2 \rangle + \langle R_j^2 \rangle\right)$$

which may be compared with the simple mean

$$r_{ij} = (r_i + r_j)/2$$

*The exact and the approximate statistical theories agree in form in having $\partial \log A_2 / \partial \log n$ proportional to $n^{1/2}$ in the neighborhood of the theta point.

of the radii r_i, r_j, of hard spheres implied by Eq. (21).

As a consequence of the form of the Flory-Krigbaum result, it is not possible to express B_{ij} directly as a function of B_{ii}, B_{jj}, and molecular weights, as in Eq. (22) except in the limit as $\beta n^{1/2}$ becomes very large[4,24] and even then only in approximation. The limiting relation is

$$F(X) \sim 4(\ln X)^{3/2}/3\pi^{1/2}X$$

but over a finite range of X for sufficiently large X this is equivalent to F(X) proportional to 1/X. In that case we can write

$$(B_{ij}n_in_j)^{2/3} = \frac{1}{2}\left[(B_{ii}n_i^2)^{2/3} + (B_{jj}n_j^2)^{2/3}\right] \qquad (46)$$

which is analogous to Eq. (22) for hard spheres except for the exponents 2/3 in place of 1/3. If the definition of X Eq. (45), is accepted literally though, the limiting form of F(X) is not realized in a physically attainable range of the variable, at least not for uncharged macromolecules. Since the Flory-Krigbaum theory and our theory are in accord qualitatively to the extent of predicting $B_{24} > B_{22}$ for two fractions under some conditions, it would be of interest to make a quantitative comparison of results for more complicated molecular weight distributions. Unfortunately, however, it does not seem possible to carry out analytically the integrations required after combining the Schulz distribution function with even the fairly simple form for B_{ij} given by combining Eqs. (20) and (46).

In addition to the schemes already discussed one might choose to obtain B_{ij} in various arbitrary ways from values of B_{ii} and B_{jj}. Use of the geometric mean

$$B_{ij} = (B_{ii}B_{jj})^{1/2} \qquad (47)$$

for example, has been proposed.[43] Another completely arbitrary but tractable from is given by

$$B_{ij}(n_in_j)^{\nu} = \frac{1}{2}(B_{ii}n_i^{2\nu} + B_{jj}n_j^{2\nu}) \qquad (48)$$

which for $\nu = 0$ reduces to the ordinary arithmetic mean. With B_{ii} and B_{jj} positive, B_{ij} is always intermediate in value for both the geometric and arithmetic averages, the latter being the greater of the two. These rules, therefore, would never allow the appearance of a maximum in the composition dependence of A_2 for mixtures of two polymers; hence they are untenable in view of experience. When ν is not zero, Eq. (48) does, under some conditions, yield a maximum.

In combination with the B_{ii} of Eq. (20) and the Schulz distribution, Eqs. (47) and (48) both lead to simple expressions in terms of gamma functions for $A_2^{(II)}$ and $A_2^{(R)}$ for heterogeneous polymers.

Explicitly, the geometric mean gives

$$A_2^{(\Pi)} = B_0 y^a \left[\frac{\Gamma(Z + 1 - a/2)}{\Gamma(Z + 1)}\right]^2$$

$$A_2^{(R)} = B_0 y^a \left[\frac{\Gamma(Z + 2 - a/2)}{\Gamma(Z + 2)}\right]^2$$

while Eqs. (29) leads to

$$A_2^{(\Pi)} = B_0 y^a \frac{\Gamma(Z + 1 + \nu - a)\Gamma(Z + 1 - \nu)}{[\Gamma(Z + 1)]^2}$$

$$A_2^{(R)} = B_0 y^a \frac{\Gamma(Z + 2 + \nu - a)\Gamma(Z + 2 - \nu)}{[\Gamma(Z + 2)]^2}$$

It will be noted that these last expressions diverge for some values of Z and ν.

For comparison with the theory based on hard sphere interactions, some numerical values calculated by these averaging procedures are listed in Table XIII for Z unity. For both light scattering and osmotic pressure, the effect of heterogeneity as determined by Eq. (48) vanishes for ν approximately 0.5 in the sense that then $A_2^{(\Pi)}/B_{NN}$ and $A_2^{(R)}/B_{WW}$ become unity.

VII. Light Scattering Photometer — G. C. Berry

A. Introduction

The light scattering apparatus, described at length in ASD Technical Report 61-22, has now been calibrated to give absolute Rayleigh ratios, and is being used to study some polystyrene solutions. Modifications of the instrument are not major, and taken separately, they add little improvement in the performance of the instrument. In aggregate, however, the effect of the modifications is to increase markedly the stability and reproducibility of the instrument response. The alterations will be described in two parts, optical and electrical, followed by a description of the calibration procedure. An example of the calculations required to go from the original data to the desired parameters is also given.

B. Optical Alterations

1. Neutral filters. Repeated determination of the transmission factors for the neutral glass filters used to attenuate the incident beam revealed variations of the order two to four per cent between different sets of measurements. The variations in the transmission factors determined for a single set of measurements would normally be an order magnitude below this value. While the cause of this behavior is not completely clear, it may in part be due to the combined effect of a slight nonuniformity in the transmission of the filters and small variations in the position of the beam in passing through the filters. The optical design is such that the beam is stationary at the sample cell, but will move elsewhere along the optical train if, as is the case, the position of the arc in the mercury lamp fluctuates. In order to circumvent this difficulty, we have ceased routine use of the filters to attenuate the incident beam, using instead an electrical attenuation described below. The light incident on the monitor tube is still attenuated by neutral filters, but the filter combination is held constant for any given set of measurements, so transmission factors need not be known. This procedure also reduces the effect of movements in the mercury arc over the time required for a single set of measurements since the optical lever arm determining any motion is shorter.

2. Monitor optics. The instability in the mercury arc position has required a further change in the optical arrangement of the monitoring system. The lens L_5 is now placed near the beam splitter prism and has a focal length (245 mm) such that an image of the field stop S_1 is focused on a diffuser placed immediately before the monitor photomultiplier tube. This arrangement provides the monitor tube with a light source that is nearly the optical equivalent of that for the detector tubes, and thus reduces the effects of lamp fluctuations on the measured null balance.

3. Beam splitter prism. The fraction of the total incident beam that is reflected by the beam splitter prism to the monitor tube is strongly dependent on the temperature of the prism. The fraction of the

intensity reflected was found to suffer a variation of approximately five per cent per degree Centigrade, an effect apparently due to the difference in temperature coefficients of refractive index for glass and optical cement. The fact that the refractive indices are nearly identical magnifies the effect of temperature on the Fresnel reflection. A new beam splitter is being constructed with a different cement to reduce this effect. In the meantime, satisfactory performance is obtained by thermostating the housing of the beam splitter.

4. Color filters. The final change is in the use of the color filters. Transmission spectra of the two green filter combinations, Corning glasses 3489, 5120 and Corning glasses 3484, 4303, 5120, show that the former, or less dense filter, will not completely isolate the Hg 5461 A line from the HG 5780 A line present in the spectrum of the ME/D high pressure mercury source. The latter, more dense, filter eliminates this difficulty, but also reduces the available intensity of the 5461 A line by a factor of three.

C. Electrical Alterations

1. Lamp power supply. A DC power supply as shown in Fig. 18 was constructed for use with the ME/D mercury lamps in the hope that the lamp would exhibit more stability on DC operation than on AC. Any effect appears to be marginal at best. The average lifetime of the lamps may be better with the DC operation than with AC, but this is not certain since the lamp has been cooled with an air blower from the time D_c operation was initiated. At any rate, it can be stated that the average lifetime of a ME/D lamp operated on a DC supply and air cooled exceeds that of a lamp operated on an AC supply. Excessive cooling can, however, cause the lamp to cease operating.

2. Null-balance bridge. The elimination of the neutral filters to adjust the light intensity incident on the sample cell has required some modifications in the bridge circuit. The revised circuit is shown schematically in Fig. 19, which is to be compared with Fig. 13 in ASD Report 61-22. The alterations increase the electrical symmetry of the bridge and make the phase balance adjustments easier. The cathode follower tube is eliminated since the transformer has a high enough impedance to be connected directly across the bridge. The resistor R_D is a 100 Kohm voltage divider, while R_M is a 100 Kohm helipot. The null conditions remain those cited in the previous report; namely the resistance ratio R_1/R_2 at null balance gives the current ratio I_D/I_M as required, independent of the capacitor settings required to achieve balance.

3. Photomultiplier tube. The detector photomultiplier, Dumont K1780, has been replaced by a Dumont K2201 tube. These tubes differ only in the nature of the dynode surfaces, Ag-Mg in the former and Cu-Be in the latter. The former tube exhibits a time dependent non-linearity of response shown schematically in Fig. 20.

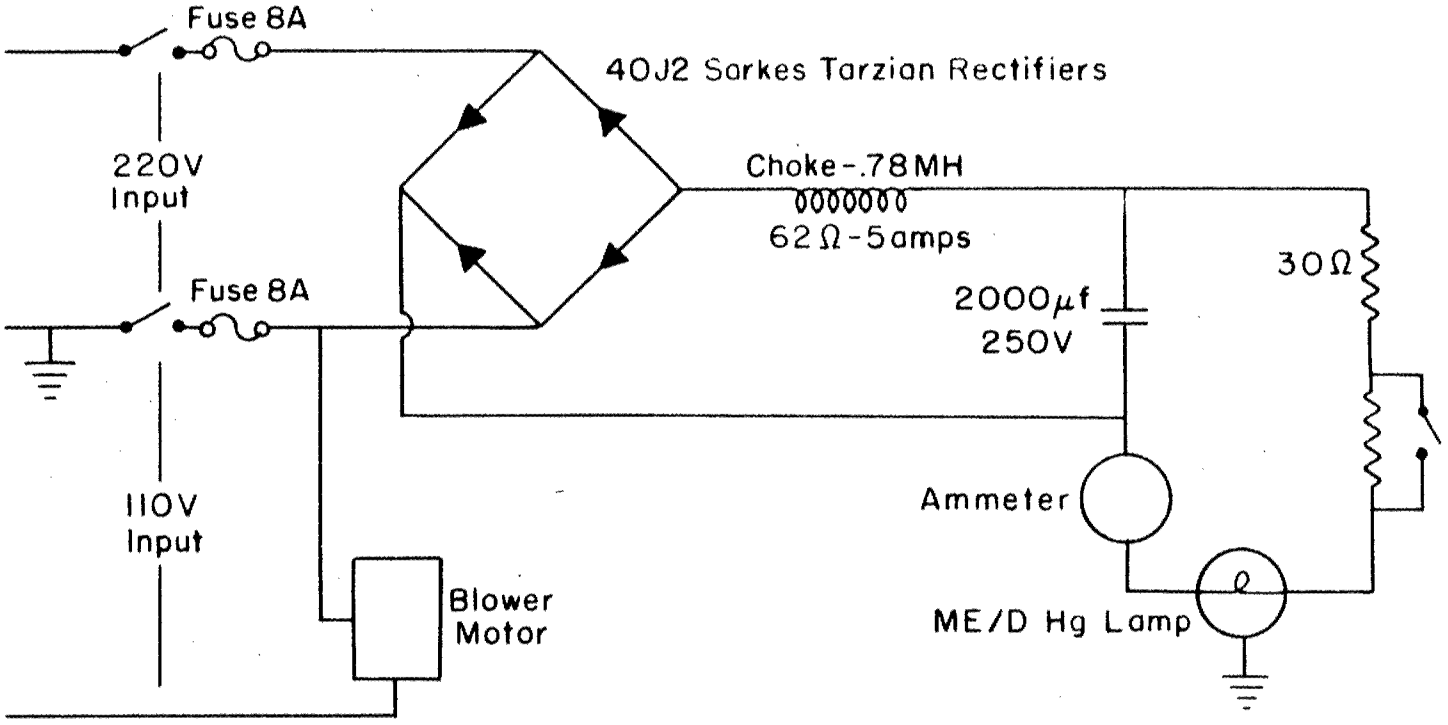

Figure 18 Lamp Power Supply

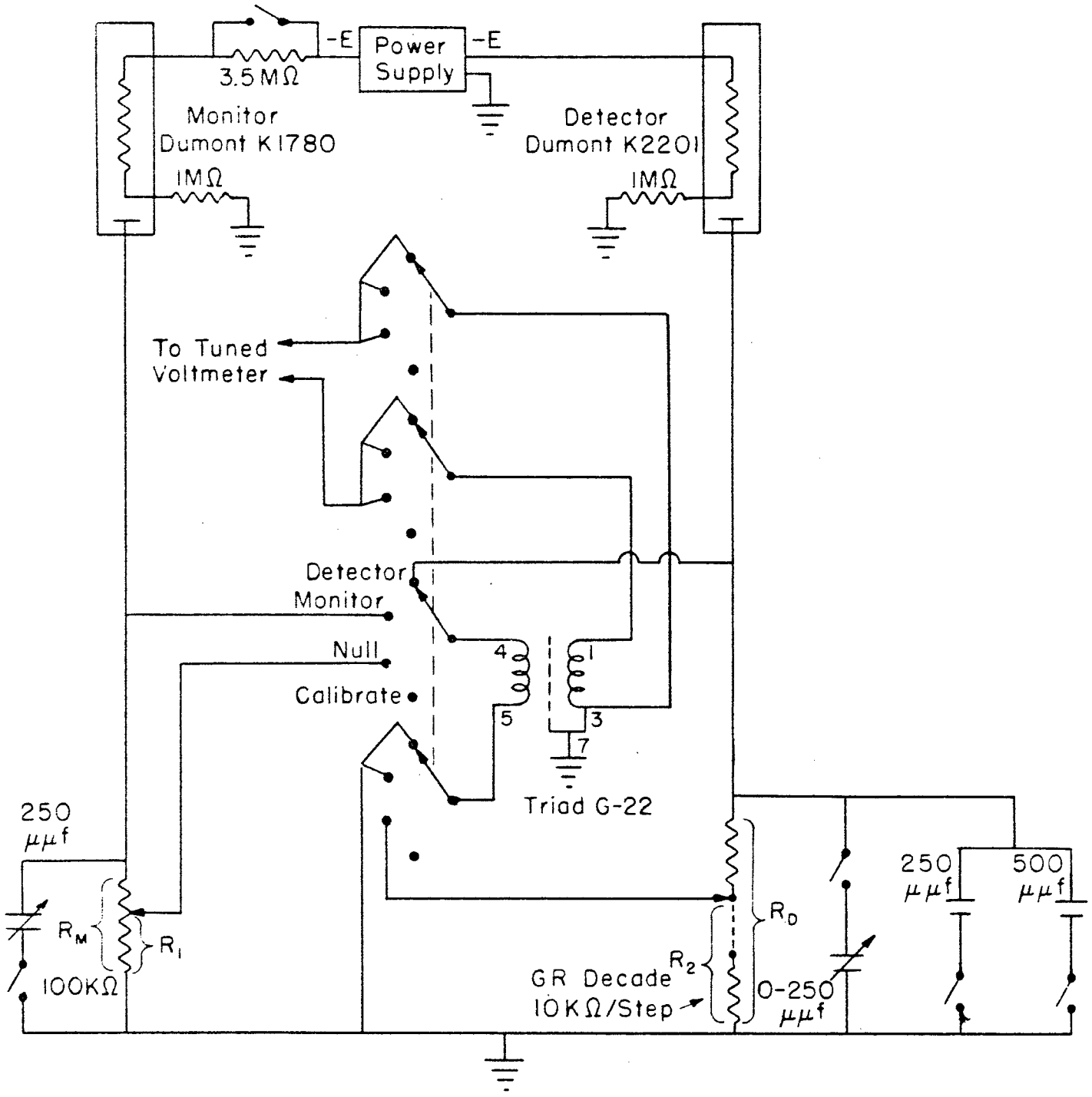

Figure 19 Null-Balance Bridge

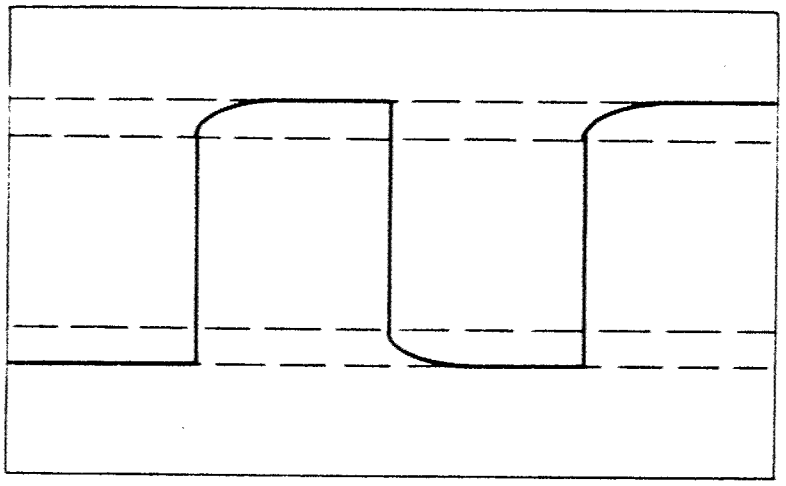

Figure 20 Non-linear Response of K1780 Photomultiplier Tube

The variation is approximately 2 to 4% in the intensity range of ordinary interest. The K2201 tube gives a response linear to within experimental error over the same intensity range. This difference in behavior is not entirely understood, but is apparently due to presence in both tubes of traces of free cesium from the cathode surface. The Cs interacts with the dynode surfaces but is not held tightly in the K1780 tube as the tube current increases, and its accumulation in the space above the dynodes causes the tube gain to change. The Cu-Be surface, however, does bind the Cs tightly throughout the range of current of interest.

D. Instrument Calibration

1. Scattering cells. Three hand-blown solution cells in the form of Erlenmeyer flasks have been constructed. Repeated cracking of glass cells cemented to brass bases with an epoxy resin led to the construction of a cell in which a glass base plate is attached to the cell at two points by fusing to short sections of glass rod. The cells are fitted with a standard glass joint. The dimensions of the optically important portions of these cells must be held to rather close tolerances if undesirable reflections are to be avoided. Properly constructed cells deflect reflection from incident and scattered light downward out of the field of view of the detector optical system.

2. Cell symmetry. The cells have been tested for symmetry by measuring the yellow-green fluorescence from an aqueous florescein solution irradiated with blue light. Since any scattered or stray light is blue, it is easily eliminated by placing a yellow filter in front of the detector. The goniometer was adjusted so the measured intensity was as nearly symmetrical, about 90°, as possible. Volume corrections to account for the change in scattering volume with angle θ were determined by normalizing all intensities to 90°. The empirical factors closely approximated the ideal cosecant θ relation, deviations being of the order of 1% over the range 18° to 135°. The ratio of the observed volume correction to sin θ may be defined as a cell symmetry factor for angle θ.

3. Stray light. The absence of any serious stray light contributions in the above cells has been demonstrated by the measurement of the angular dependence of the scattering from benzene. The scattering, normalized to 90°, was within 1 per cent of the expected value between 45° and 135° and deviated by only 5 per cent at 22°.

4. Primary standard. The calibration of the instrument response in terms of the absolute Rayleigh ratio has been obtained in two ways: (1) Measurement of the excess scattering at 90° and the excess turbidity for a Rayleigh scattering system; (2) Measurement of the excess scattering at 90° for a system of known scattering power. An aqueous silica solution, "Ludox," is used in the former procedure, and a standard polystyrene solution in the latter. The absolute calibration constant for the instrument is, of course, independent of the particular cell used to determine the constant. There is, in principle then, a distinction between a cell calibration constant and the instrument calibration constant. The former including any optical effects peculiar to a cell, for example. In practice, however, the instrument response to the scattered intensity from a given solution is identical for all of the cells considered here, so no further distinction will be made between the two constants.

The use of Ludox (Dupont Ludox HS) is complicated by the presence of particles large enough to cause dissymmetry of the scattering. The dissymmetry of the solutions depends on the ionic strength, the pH, the method of clarification, the concentration of solids in the solutions and on the history of the Ludox concentrate used to prepare the solution. It was found that best results were obtained by the following procedure:

(1) Centrifuge the Ludox concentrate for 40 minutes at 20,000 g prior to use.

(2) Dilute 1 to 2 parts of the supernatant from the centrifugation with 100 parts of distilled water previously adjusted to 0.1 molar in NaCl and pH = 9.8 with NaOH.

(3) Pass the solution repeatedly (10 to 12 times) through millipore filters of pore size down to 0.30 micron.

Solutions prepared under these conditions will have a dissymmetry ratio (intensity at 45°/intensity at 135°) in the range 1.05 to 1.10. Further reduction of the dissymmetry has not been consistently attained.

Ideally the dissymmetry should be unity if the direct relation between the excess intensity scattered through 90° (solution scattering less solvent scattering) and the excess turbudity τ given by

$$\tau = n^2 k T_{xs}(90) \tag{49}$$

is to be valid. Here, $T_{xs}(90)$ is the instrument response corresponding to the scattering at $90°^{xs}$ relative to the intensity of the incident beam,

n is the refractive index of the solution, and k is the calibration constant. Since Ludox is presumably a suspension of spheres, the effect of dissymmetry ratios greater than unity may be estimated,[44] at least in the limit of infinite dilution, by assuming that the dissymmetry arises from a uniform suspension of spheres of dimensions large enough to account for the observed dissymmetry. The calculated dimension may then be used to estimate the error to be expected in using Eq. (49) to determine k. It turns out that the error is less than 1 per cent for dissymmetry ratios up to 1.4. No correction is applied here, since the estimated error is small and the assumption of a uniform suspension of spheres is probably unjustified.

The turbidity was measured from 3400 A to 6000 A with a Cary recording spectrophotometer using a transmission cell 10 cm long. If the solution is a Rayleigh scattering system showing no absorption, then one has

$$\frac{\lambda^4 \tau}{(ndn/dc)^2} = \text{constant} \qquad (50)$$

where n and dn/dc are the refractive index and refractive increment of the solution, respectively. Thus the measured value of the ratio of turbidities for 4358 A and 5961 A light should be a constant at all Ludox concentrations. In fact, this ratio was constant to within ± 0.6%, varying from 2.55 to 2.59, in agreement with the value 2.57 calculated for this ratio by taking the dispersion in n as identical to that of water, and using the dispersion in dn/dc reported by Goring.[45]

The experimentally observed ratios of $\tau\alpha/T_{xo}(90)$ are tabulated as a function of τ in Table XIV. The factor α, to be described in detail below, is introduced to account for attenuation effects and becomes unity for $\tau = 0$.

Table XIV

Calibration of Photometer with Ludox

τ_{5461} cm^{-1}	τ_{4360} cm^{-1}	$\left[\frac{\tau\alpha}{T_{xs}(90)}\right]_{5461}$, cm^{-1}	$\left[\frac{\tau\alpha}{T_{xs}(90)}\right]_{4360}$, cm^{-1}
0.0246	0.0635	0.01248	0.0489
0.01445	0.03725	0.01332	0.0528
0.01229	0.03150	0.01309	0.0515
0.00866	0.02215	0.01320	0.0533
0.00616	0.01570	0.01358	0.0549
0.00439	0.01118	0.01355	0.0549

Analysis of these data yields $[\tau\alpha/T_{xs}(90)]_{\tau=0}$ equal to 0.0563 and 0.01385 for the blue and green light respectively. Division by n^2 to obtain the calibration constant, k, yields the values 0.0308 cm^{-1} and 0.0077_7 cm^{-1} for blue and green light respectively. Inspection of Table I shows that apparent values of k determined for $\tau > 0$ are in error, even though the values of τ are low.

The 90° intensity from a polystyrene-butanone solution of "known" scattering power has also been determined. Carefully purified butanone, shown to have negligible absorbance for 4360 A and 5461 A light, was used here. The 90° intensity for the polystyrene used has been compared to that for the Cornell polystyrene on several occasions, so the value of τ is a known factor times the turbidity reported for the Cornell polystyrene.[46] The constant of calibration, k, is calculated by the relation

$$k = \frac{\alpha\tau}{n^2 T_{xs}(90)} \qquad (51)$$

where α is not equal to unity, since we do not extrapolate to $\tau = 0$. The calibration factors determined in this way are $k = 0.0309$ cm^{-1} and $k = 0.0079$ cm^{-1} for the blue and green light respectively. These are seen to be in reasonable agreement with the values obtained above.

Attempts to use two different low molecular weight (negligible dissymmetry) polystyrenes in either toluene or butanone in the same manner as Ludox proved to be unsuccessful. These solutions should behave as Rayleigh scattering systems, but in fact, the constant indicated by Eq. (50) was found to be strongly dependent on λ. This effect is probably due to very slight absorption by the polymer, sufficient to make the measurement of τ by transmission considerably in error, yet having negligible effect on the measurement of $T_{xs}(90)$.

5. Working standards. Several schemes employing working standards (standards affording convenient reference intensities, stable though not known absolutely) have been examined. These are conveniently classed into two groups, as follows:

Group I:	0° Standards	1	Transmission through a neutral filter
		2	Diffuse transmission through an opal plate located in the cell position
		3	Diffuse transmission through an opal plate located outside the cell position
Group II:	90° Standards	4	90° scatter from a polystyrene solution
		5	90° scatter from a slightly turbid glass.

Method 3 was first employed. It, as well as the other methods of Group I, have proved to be unreliable for reasons probably related to the long optical lever arms employed and the instability of the mercury arc position. The detector optics are such that movement of the beam will result in a shift of the image on the photocathode surface and hence in a change of signal. Thus, changes may be observed in the 0° transmission response even though the intensity of scattered light is stable. Method 2 proved to be the most reliable of the working standards of Group I.

Method 4 offers the advantage that effects due to fluctuations in the arc position affect response from the scattering solution and the working standard in the same way. The response is, however, temperature sensitive and the scattering from the solution is subject to change over a long period. These latter difficulties are avoided by using a slightly turbid glass, method 5, as the working standard. Repetitive measurements on a polystyrene solution made over a period of time showed that the turbid glass provides a very reproducible working standard.

All of the working standards listed above except methods 1 and 3 require a correction for the turbidity of the solution being studied. The correction is made automatically in using working standards 1 or 3. In practice, the instrument response, $G(\theta)_R$, to the scattering at some arbitrary angle, θ_R, is determined periodically during the measurement of the response, $G(\theta)$, over the scattering envelope from $\theta = 18°$ to $\theta = 135°$ for a solution under study. The response at θ_R is usually found to remain constant to almost within experimental error, in contrast to the reading at 0° which may vary over 5% even though the scattered intensity is constant for any given angle. After measurement of the scattering envelope is completed, the response to the 90° scattering from the turbid glass, G (glass), is related to $G(\theta_R)$ by the ratio $G(\theta_R)/G(\text{glass})$. Thus, for each angle, the ratio

$$T(\theta) = \frac{G(\theta)}{G(\theta_R)} \left[\frac{G(\theta_R)}{G(\text{glass})} \right]$$

is computed, where the $G(\theta_R)$ in brackets refers to the final response measured at θ_R, and is not necessarily equal to the $G(\theta_R)$ outside of the brackets. The response $T(\theta)$ requires a correction by a factor $(1/\alpha)$ to account for the attenuation of the light by the solution in the measurement of $G(\theta_R)/G(\text{glass})$. We require, in effect, the transmission factor for the cell filled with solution. This may be obtained by determining the response at 0° with the cell in place, G(0), and with the cell removed, $G_R(0)$, for solutions of different turbidity. Thus, $\ln [G(0)/G_R(0)]$ plotted against $T_{xs}(90)$ will result in a straight line whose slope, a, may be used to compute the attenuation factor α_λ for light of wavelength λ by the relation

$$\alpha_\lambda = \exp\{-a[kT_{xs}(90)]_\lambda\} \qquad (52)$$

where k is the calibration constant obtained above.

The value of a has been found to be identical for solutions in water, butanone and decalin for both blue and green light, as expected. It is important to realize that the attenuation factor, α, corrects for attenuation due to either absorption or scattering by the solute; it does not correct for absorption by the solvent. Thus, it is important to use solvents that do not absorb light in the wavelength of interest. Butanone, or decalin, for example, will absorb strongly for λ = 4360 A unless carefully purified. For this reason all solvents used here were examined spectrophotometrically.

It should be noted that the correction factor α may be ignored if only parameters determined in the limit for $\tau = 0$ are of interest, since $\alpha = 1$ in this limit.

E. Sample Calculation

Some data on the scattering of a polystyrene (McCormick S -108)* in butanone a solution are given here in order to illustrate the numerical calculations necessary to go from the measured data of resistances on a null-balance bridge to the desired parameters. Table XV gives the resistance measurements for some of the angles measured for one of the four concentrations studied. The reference angle, θ_R, is 90° for these data. The response $G(\theta)$ is computed as $(R_M/R_D)_\theta$

Table XV

Light Scattering Data

θ	$R_M \times 10^{-2}$ ohm	$R_D \times 10^{-4}$ ohm	$G(\theta)/G(\theta_R)$	$T(\theta)$
90	762	10	1.000	0.2605
105	836	10	1.094	0.2850
120	540	5	1.417	0.3692
135	783	5	2.055	0.5354
90	762	10	---	----
glass	585	2	---	----

$$G(\theta_R)/G(\text{glass}) = 0.2605$$

Similar values of $T(\theta)$ for other angles and concentrations, including the solvent, allow extrapolation of $T_{xs}(\theta)$ against $\sin^2 \theta/2$ to $\theta = 0$ for each of the concentrations. The results of these extrapolations are given in Table XVI.

*A narrow molecular weight distribution anionic polystyrene kindly supplied by Dr. H. S. McCormick. It is used here since other investigators have reported values for its $\langle M \rangle_w$.

Table XVI

Extrapolation of Scattering Data

C_r	$T_{xs}(90)$	α	$\left(\frac{\alpha C_r V}{T_{xs}}\right)^{1/2}_{\theta=0}$	$\left(\frac{C_r V}{T_{xs}}\right)^{1/2}_{\theta=0}$
0.308	0.160	0.987	1.328	1.337
0.533	0.255	0.980	1.375	1.390
0.710	0.324	0.975	1.409	1.429
1.000	0.414	0.961	1.467	1.993

The value of α is computed from Eq. (52) with a = 10.32 and the k for 5461 A. The concentrations are expressed as reduced variables, by taking the concentration (0.00651 gm/cc) of the most concentrated solution as a base. The factor V is equal to $(1 + \cos^2\theta)/\sin\theta$ divided by the cell symmetry factor for each angle θ.

Extrapolation of the data in the last two columns against C_r to $C_r = 0$ yields the common intercept 1.265, showing that parameters measured in the limit of $\tau = 0$ are independent of the correction factor α. The slope of the two lines, however, differs by 13%. Thus, values of A_2 computed without introduction of the factor α would be 13% too high for these data. The molecular weight is computed from the relation

$$\langle M \rangle_w = \left(\frac{k}{H(dn/dc)^2}\right)_\lambda \left(\frac{\alpha CV}{T_{xs}}\right)^{-1}_{\substack{c=0 \\ \theta=0}} \qquad (53)$$

where H is a numerical constant for a given λ. ($H_{4360} = 15.2 \times 10^{-5}$ and $H_{5461} = 6.18 \times 10^{-5}$). Note that the factor n^2 usually found in the numerator of Eq. (53) is exactly cancelled by a factor n^2 in the denominator, which is required as a refraction correction. These data-- dn/dc = 0.220, $k = 0.0077_7$ --give $\langle M \rangle_w = 2.53 \times 10^5$. The polystyrene studied here has also been examined in toluene solution with 4361 A light--dn/dc = 0.112, k = 0.0308--to obtain $\langle M \rangle_w = 2.59 \times 10^5$. The agreement is regarded as satisfactory and indicates that the refraction correction employed is correct. Values of $\langle M \rangle_w$ obtained for this polystyrene by others are given in Table XVII.

Table XVII

Molecular Weight of a Polystyrene Sample

$\langle M \rangle_w \times 10^{-4}$	Source	Method
2.53	This study (in butanone)	
2.59	This study (in toluene)	
2.51	Orofino	Light Scatter‡
2.30	Bywater[47]	Light Scatter
2.67	McCormick[48]	Sedimentation

‡Instrument calibration based on osmotic pressure measurements and $\langle M \rangle_w / \langle M \rangle_n$ ratios determined by fractionation analysis.

F. Future Work

Studies are presently centered on the system polystyrene: decalin over the temperature range 19.2°C to ca. 100°C. This system has been chosen because of the low, but easily accessible, theta temperature near 15°C (a temperature analogous to the Boyle temperature of a real gas) and the high boiling point of the solvent decalin. The thermodynamic properties of this system change rapidly with temperature; so that a good-solvent condition is approached for the higher temperatures. Linear polymers of narrow molecular weight distribution over the molecular weight range ca. 50,000 to 8,000,000 will be studied. In addition a lesser number of branched polymers will be examined and their behavior compared to that of linear molecules.

These studies will include measurement of the virial coefficient, the dimension, and the intrinsic viscosity for fractions and mixtures of fractions.

LIST OF REFERENCES

1. T. A. Orofino, Abstracts, 140th Meeting of the American Chemical Society, Chicago, September, 1961.

2. P. J. Flory, Principles of Polymer Chemistry (Cornell University Press, Ithaca, New York, 1953).

3. W. R. Krigbaum, J. Am. Chem. Soc. 76, 3758 (1954).

4. T. A. Orofino and P. J. Flory, J. Chem. Phys. 26, 1067 (1957).

5. T. A. Orofino and F. Wenger, Abstracts, 141st Meeting of the American Chemical Society, Washington D.C., March, 1962.

6. W. R. Krigbaum and P. J. Flory, J. Am. Chem. Soc. 75, 1775 (1953).

7. B. H. Zimm and W. H. Stockmayer, J. Chem. Phys. 17, 1301 (1949).

8. W. H. Stockmayer and M. Fixman, Ann. N. Y. Acad. Sci. 57, 334 (1953).

9. T. A. Orofino, Polymer 2, 305 (1961).

10. B. H. Zimm and R. W. Kilb, J. Polymer Sci. 37, 19 (1959).

11. P. J. Flory and T. G Fox, J. Am. Chem. Soc. 73, 1904 (1951).

12. B. H. Zimm, W. H. Stockmayer and M. Fixman, J. Chem. Phys. 21, 1716 (1953).

13. M. Fixman, J. Chem. Phys. 23, 1656 (1955).

14. B. H. Zimm, J. Chem. Phys. 14, 164 (1946).

15. W. G. McMillan and J. E. Mayer, J. Chem. Phys. 13, 276 (1945).

16. A. C. Albrecht, J. Chem. Phys. 27, 1002 (1957).

17. E. F. Casassa, J. Chem. Phys. 31, 800 (1959).

18. W. R. Krigbaum and D. K. Carpenter, J. Phys. Chem. 59, 1166 (1955).

19. P. J. Flory, J. Chem. Phys. 13, 453 (1945).

20. P. J. Flory, J. Chem. Phys. 17, 1347 (1949).

21. P. J. Flory and W. R. Krigbaum, J. Chem. Phys. 18, 1086 (1950).

22. A. Isihara and R. Koyama, J. Chem. Phys. 25, 712 (1956).

23. R. Koyama, J. Chem. Phys. 27, 234 (1957).

24. E. F. Casassa and H. Markovitz, J. Chem. Phys. 29, 493 (1958).

25. O. B. Ptitsyn and Yu. E. Eizner, Vysokomol. Soed. 1, 1200 (1959).

26. W. R. Krigbaum, D. K. Carpenter, M. Kaneko, and A. Roig, J. Chem. Phys. 33, 921 (1960).

27. G. Scatchard, J. Am. Chem. Soc. 68, 2315 (1946).

28. J. G. Kirkwood and R. J. Goldberg, J. Chem. Phys. 18, 54 (1950).

29. W. H. Stockmayer, J. Chem. Phys. 18, 58 (1950).

30. E. F. Casassa, Polymer 1, 169 (1960).

31. H. Yamakawa and M. Kurata, J. Chem. Phys. 32, 1852 (1960).

32. E. F. Casassa and W. H. Stockmayer, Polymer 3, 53 (1962).

33. J. O. Hirschfelder, C. F. Curtiss, and R. B. Bird, Molecular Theory of Gases and Liquids (John Wiley & Sons, Inc., New York, 1954) Chapter 3.

34. T. G Fox, J. B. Kinsinger, H. F. Mason, and E. M. Schuele, Polymer 3, 71 (1962).

35. E. Cohn-Ginsberg, T. G Fox, and H. F. Mason, Polymer 3, 97 (1962).

36. W. H. Stockmayer, J. Polymer Sci. 15, 595 (1955).

37. V. V. Varadaiah and V. S. Rao, J. Polymer Sci. 50, 31 (1961).

38. Chien, J.-Y. Shih, L.-H., and Yu, S.-C., J. Polymer Sci. 29, 117 (1958).

39. G. V. Schulz, Z. phys. Chem. B43, 25 (1939).

40. J. Bischoff and V. Desreux, Bull. Soc. Chim. Belg. 61, 10 (1952).

41. G. Meyerhoff and G. V. Schulz, Makromol. Chem. 7, 297 (1952).

42. J. Bischoff and V. Desreux, J. Polymer Sci. 10, 437 (1957).

43. J. J. Blum and M. F. Morales, J. Chem. Phys. 18, 153 (1950).

44. H. C. van de Hulst, Light Scattering by Small Particles (John Wiley & Sons, Inc., New York, 1957).

45. D. A. I. Goring, Canad. J. Chem. 31, 1078 (1953).

46. C. I. Carr and B. H. Zimm, J. Chem. Phys. 18, 1616 (1950).

47. J. M. Cowie, D. J. Worsfold and S. Bywater, Trans. Farad. Soc. 57, 705 (1961).

48. H. W. McCormick, private communication.

PART II - MOLECULAR MOBILITY AND MECHANICAL BEHAVIOR OF MACROMOLECULES

I. Structural Factors Affecting Flow in Macromolecular Systems — V. R. Allen and T. G Fox

A. Introduction

Two flow laws of broad applicability have been established[1,2] for fractions of linear amorphous flexible macromolecular substances in bulk or in concentrated solution:

$$\eta = AZ^{3.4} \qquad Z > Z_c \tag{54}$$

$$\eta = BZ^{a} \qquad Z < Z_c \tag{55}$$

$$\ln \frac{\eta_T}{\eta_{T_g}} = \frac{40(T - T_g)}{52 + T - T_g} \qquad 100° \geq (T - T_g) \geq 0 \tag{56}$$

Here η is the limiting Newtonian viscosity coefficient observed at low shear rate, Z is the number of chain atoms in the macromolecule, T is the absolute temperature, and A, B, a, Z_c, and the glass temperature, T_g, are parameters characteristic of the macromolecular system. For polymer fractions it is further established for bulk polymers that

$$T_g = T_{g,\infty} - \frac{K}{Z}$$

where $T_{g,\infty}$ is the glass temperature for a polymer fraction of infinite chain length; further, for polymer-diluent mixtures containing weight fractions w_1 of the polymers it is found that

$$\frac{1}{T_g} \cong \frac{w_1}{T_g(p)} + \frac{w_2}{T_g(d)}$$

where $T_g(p)$ and $T_g(d)$ represent the glass temperatures of the polymer and diluent, respectively.

According to current concepts, the strong isothermal dependence of the viscosity on chain length in Eq. (54) arises from the long range restrictions on the flow of individual chain segments communicated through the intramolecular primary valence bonds and intermolecular chain entanglements. Thus Bueche[3] suggests that Eq. (54) represents the former law

expected for chains sufficiently long ($Z > Z_c$) that they are entangled into infinite networks, whereas Eq. (55) with a = 1 is the expected behavior for chains so short ($Z < Z_c$) that the influence of interchain entanglement on flow is negligible. Here Z_c is identified as the average number of chain atoms between chain entanglement points. The strong dependence of η on $(T - T_g)$ in Eq. (56) is believed to reflect the dependence of local resistance to flow on the density of packing of neighboring polymer chain segments or diluent molecules (or on free volume) in the liquid.

Although the above concepts are useful in providing a molecular interpretation of the viscoelastic behavior of polymeric systems, it is clear that more exact experimental data relating the viscosity to the various details of molecular chain structure and more precise theoretical concepts are needed. In the present work we are concerned with determining the effects of molecular weight heterogeneity and of the type and amount of added diluent on the viscosity and on its temperature coefficient. The result of the first study should provide decisive evidence concerning the molecular-weight average that determines the melt viscosity of heterogeneous systems. Viscosity data[4] on mixtures of polystyrene fractions or of polyisobutylene fractions indicated that

$$\eta = AZ_w^{3.4} \qquad Z_w > Z_c; \qquad Z_n > Z_o$$

$$\eta = BZ_w^{a} \qquad Z_w > Z_c; \qquad Z_n > Z_o$$

$$\frac{\partial \log \eta}{d(1/T)} = F(T) \cdot f(Z_n) \qquad \text{(for any } Z_n\text{)}$$

$$T_g = T_{g,\infty} - K/Z_n$$

i.e. for such heterogeneous systems the viscosity-temperature coefficient is uniquely a function of the number-average chain length, Z_n, whereas the isothermal viscosity for systems with $Z_n > Z_o$ is uniquely a function of the weight-average chain length, Z_w. No adequate specification of the molecular weight dependence of η was found for heterogeneous polymers with Z_n below a limiting value designated by Z_o.

Recently Bueche[5] has suggested that another "average" may be the controlling one for heterogeneous systems having a very broad chain length distribution. Employing the aforementioned approximate theoretical treatment[3] he predicts for heterogeneous systems having components of $Z \gg Z_c$:

$$\eta \sim Z_t^{3.5} \qquad Z > Z_c$$

where $Z_t = Z_w$ for $Z_z/Z_w < 1.8$

and $Z_t \rightarrow Z_z$ for $Z_z/Z_w > 1.8$

Data which are pertinent to the second study were reported recently[6] in an investigation of the molecular weight-concentration-temperature relationships for fractions of linear polyvinyl acetate in a thermodynamically good solvent, diethyl phthalate, and in a thermodynamically borderline solvent, cetyl alcohol. The data were represented to a satisfactory approximation by the equations

$$\log \eta = a \log (Z/Z_c) + b \log \phi + \frac{k}{T^4} \exp(m\phi) + \text{const.}$$

$$\alpha = 3.4 \qquad (Z > Z_c)$$

$$\alpha = (1 - 0.6\phi)^{-1} \qquad (Z < Z_c)$$

$$Z_c = 690/\phi$$

where b, k, and m are empirical constants. The observed inverse dependence of Z_c on the polymer concentration (as volume fraction ϕ) and its independence of the thermodynamic solvent power of the added diluent favor the concept[3] of simple rope-like entanglements.

Here we report the results of studies of the viscosities of linear fractions, and mixtures of fractions, of polystyrene of narrow chain-length distribution prepared by anionic techniques. Also, some preliminary viscosity data are reported for concentrated solutions of fractions in dibenzyl ether, a good solvent.

B. Experimental

The fractionation, characterization, preparation of samples, and measurement of η involve standard procedures which were described in detail in the previous report[7] and are not repeated here. However, it is necessary to describe several procedures that are specific to this phase of the investigation.

1. Preparation of mixtures and concentrated solutions. The mixtures used in this study were prepared by simple techniques. Weighed samples of two linear fractions were dissolved together with 0.5 per cent by weight of an antioxidant, phenyl-b-naphthylamine, in benzene. The solvent was removed either by evaporation, to form films, or by freeze-drying. The latter method was followed when the molecular weight of one of the components was large ($M > 2 \times 10^6$).

The different average molecular weights were calculated according to well-known expressions (listed in the appendix) from the molecular weights and weight fractions of the respective components. The dilute-solution intrinsic viscosity, $[\eta]$, was determined (first, in benzene, and later in cyclohexane at the theta temperature) on the mixture both before and after the measurement of η. This provided a measure of the agreement

between the calculated and observed viscosity average molecular weight, M_v, of the mixture and information on the extent of degradation during the high-temperature measurement of η.

The concentrated solutions of the linear fractions of polystyrene in dibenzyl ether were not prepared in the way proposed in the previous report[7] since it was eventually found that this method (evaporation of the solvent chloroform from the ternary solution) resulted in preferential evaporation of the dibenzyl ether from the surface and, thus, in an inhomogeneous sample.

A more satisfactory procedure was obtained by cosolution in the viscometer cell of the polymer and ether (slight excess) in 10-15 cc benzene followed by freeze-drying and then evaporation of residual solvent at 80°C under vacuum for two hours. The last traces of benzene were removed by heating the solution in the viscometer apparatus to 218°C and flashing with vacuum. The final concentration was calculated from the difference in weight between the cell plus polymer initially, and the total weight after evaporation of benzene.

2. Characterization of high molecular weight fractions and mixtures. In order to prepare mixtures with large values of M_z/M_w and of M_w/M_n, and also having $M_n > M_o$, it was necessary to have M very large for one of the components. It has been reported[8] that the effect of shear in dilute solution viscometry must be considered, especially in "good" solvents, when $M > 2\text{-}3 \times 10^6$. Thus, for the high molecular weight fractions, we measured $[\eta]$ in both benzene (a "good" solvent) and in cyclohexane (a "theta" solvent) at 34.5°C using two viscometers which differed in length and radius of the capillary (shear rates at the capillary walls were ca. 2.6×10^3 and 1.3×10^3 sec^{-1}). Although we did observe a severe dependence on shear rate for one sample in benzene, there was no observable effect on the (lower) value of $[\eta]_\theta$ from the two viscometers. Thus, we used the observed $[\eta]_\theta$ for the calculation of M_v.

3. Molecular weight determination. Molecular weights designated as M_θ were computed from the relation of Flory and Krigbaum[9]

$$[\eta]_\theta = 8.2 \times 10^{-4} M_\theta^{0.5} \qquad (57)$$

where $[\eta]_\theta$ is the intrinsic viscosity for polystyrene in cyclohexane at the θ-temperature of 34.5°C. The value of $[\eta]_\theta$ in cyclohexane was measured directly on three mixtures, A, B, and F. For the others, the viscosities were measured in benzene at 34°C. The molecular weights were calculated from the equation of Ewart and Tingey.[10]

$$[\eta]^{30°C}_{\text{Benzene}} = 9.72 \times 10^{-3} M_v^{0.74}. \qquad (58)$$

Table XVIII

Viscosity-Molecular Weight Data on Fractions of Anionic Polystyrene

Designation Polymer	Fraction	$M_\theta \times 10^{-3}$ (a)	η_{218} poises	$[\eta]_\theta^a$ dl/gm
D-6	BA	215	63,000	0.382
D-5	BA	190	43,200	.358
D-4	CA	155	20,100	.327
D-3	BA	145	14,600	.308
D-4	(unfract.)	128	11,900	.299
D-1	(unfract.)	74.3	1,460	.232
11	BA	72.1	1,920	.228
D-1	BA	69.5	1,390	.223
D-1	CA	65.5	1,330	.218
11	CA	59.5	685	.208
11	CA	59.5	620	.208
12	CB	45.2	220	.183
7	AA	36.2	204	.165
7	AA	36.2	185	.165
9	BB	25.0	70	.138
8	CB	19.0	44.5	.122
8	CB	19.0	42.5	.122
8	AA	17.3	41.1	.117
8	EB	14.9	22.0	.108

(a) Calculated from $[\eta]$ in benzene and Eqs. (57) and (58).

Table XIX

Viscosity-Temperature Data on Fractions of Anionic Polystyrene

Designation Polymer	Fraction	$\log \frac{\eta_{203}}{\eta_{218}}$	$\log \frac{\eta_{193}}{\eta_{218}}$	$\log \frac{\eta_{180}}{\eta_{218}}$	$\log \frac{\eta_{156}}{\eta_{218}}$
D-4	CA	0.34			
D-3	BA	0.35			
D-1	BA		0.69		
11	CA				2.30
7	AA		0.76	1.09	2.25
Reference 3		0.37	0.69	1.17	2.38

Table XX

Composition and Dilute Solution Viscosities of the Mixtures

Mixture	Composition: Polymer Fraction	Composition: Weight Percent	Composition: Mol. Wt. ($\times 10^{-3}$)	Intrinsic viscosity (dl/g)[a]: Calc'd.	Intrinsic viscosity (dl/g)[a]: Observed before η_{218}	Intrinsic viscosity (dl/g)[a]: Observed after η_{218}
A	24-FA	13.0	7,600	0.593	0.603	0.492[b]
	D-4-B	87.0	175			
B	24-FA	8.1	7,600	.348	.350	.320
	12-BB	91.9	51.5			
C	5-1-1	5.0	1,900	.910	.927	.867
	D-4-B	95.0	175			
D	5-1-2	10.0	1,760	.666	.610	.560
	12-BB	90.0	51.5			
E	5-1-1	3.9	1,900	.712	.730	.693
	D-3-C	96.1	125			
F	14-AA	33.0	510	.315	.310	.324
	12-BB	67.0	51.5			
G	14-BA	41.0	440	.673	.714	.658
	8-BB	59.0	20			
H	D-6-C	50.0	220	.461	.475	.456
	8-BA	50.0	10.6			

(a) The viscosities of the components and mixtures thereof were measured in cyclohexane at 34.5°C (theta) for A, B, and F and in benzene at 33-35°C for the others. Calculated values were obtained from the data on the individual fractions and Eq. (62).

(b) Measured on a 50 percent solution of the sample in dibenzyl ether.

Table XXI

Comparisons of the Calculated and Observed Viscosities of Mixtures

Mixture	$[\eta]_{obs}/[\eta]_{calc'd}$ (before det'n. of η_{218})	Effect of η_{218} det'n. $[\eta]_{obs\ before}/[\eta]_{obs\ after}$
A	1.01	1.22[a]
B	1.005	1.09
C	1.02	1.07
D	0.925	1.09
E	1.025	1.05
F	0.985	0.96
G	1.04	1.08
H	1.03	1.04

(a) The intrinsic viscosity of this mixture was measured on a 50 percent solution in dibenzyl ether.

C. Results and Discussion

The viscosity-temperature-molecular weight data obtained on fractions of linear polystyrene prepared by anionic techniques (including those previously reported[7]) are listed in Tables XVIII and XIX. There is shown in Fig. 21 a plot of log η_{218} vs. log M_θ together with the $\eta_{218} - M$ data reported by Fox and Flory[4] for "free radical" polystyrene. The viscosity-temperature-molecular weight relations for these two types of polystyrenes are evidently the same, within experimental error, over the range of variables studied.

In order to determine which, if any, molecular weight average uniquely defines the viscosity of a mixture, we wished to prepare from the available fractions mixtures exhibiting the maximum ratios possible for M_Z/M_W and/or M_W/M_V. Expressions for these maxima are given in the Appendix in terms of the relative molecular weights and weight fractions of the components. Further, it was necessary to make mixtures with sufficiently low viscosities at the highest temperature of measurement that a bubble-free melt could be obtained in the bottom of the viscometer cell in a reasonable length of time and without excessive degradation.

The composition of the mixtures and the dilute solution viscosity data are given in Table XX. Mixtures F to H were purposely made comparable to mixtures studied previously by Fox and Flory;[4] mixtures C and E have a high ratio M_Z/M_W; and mixtures A, B, and D have a large value for M_W/M_V.

It is apparent from Table XXI that with one exception the observed solution viscosities agree within a few percent with those calculated from the viscosities and weight fractions of the components according to Eqs. (57) and (58) and Eq. (A-4) in the Appendix. The last column in Table XXI shows the effect of degradation during the heating period. The decrease in the intrinsic viscosity of 4-9 percent observed after the melt viscosity measurement (Table XXII) is slightly greater than that ($\leq$ 6 percent) observed earlier for fractions. In one case (F) there was observed a small increase in the solution viscosity after the melt viscosity measurement. The large apparent decrease in the molecular weight of sample A is surprising, since in this case the melt viscosity measurement was made in dibenzyl ether and entailed a relatively short period of heating at 218°C. The intrinsic viscosity measurement in this instance, made on the polymer-diluent mixture, may be in error because of uncertainty in the polymer concentration in the sample employed in the latter measurement.

In Table XXII are listed the M_Z, M_W, and M_n values calculated from the values of $[\eta]$ observed for the components, with Eqs. (57) and (56) and the relations given in the Appendix. In columns 5 and 6 are the values of M_V calculated both for a thermodynamically "good" solvent ($\underline{a} = 0.8$) and for a "poor" one ($\underline{a} = 0.5$). In the last two columns are presented the observed viscosity at 218°C and M_η, the molecular weight of the fraction having the same viscosity as that observed for the mixture, calculated from the relation[4]

$$\log \eta_{218} = 3.4 \log M_\eta - 13.40 \qquad (M > M_c)$$

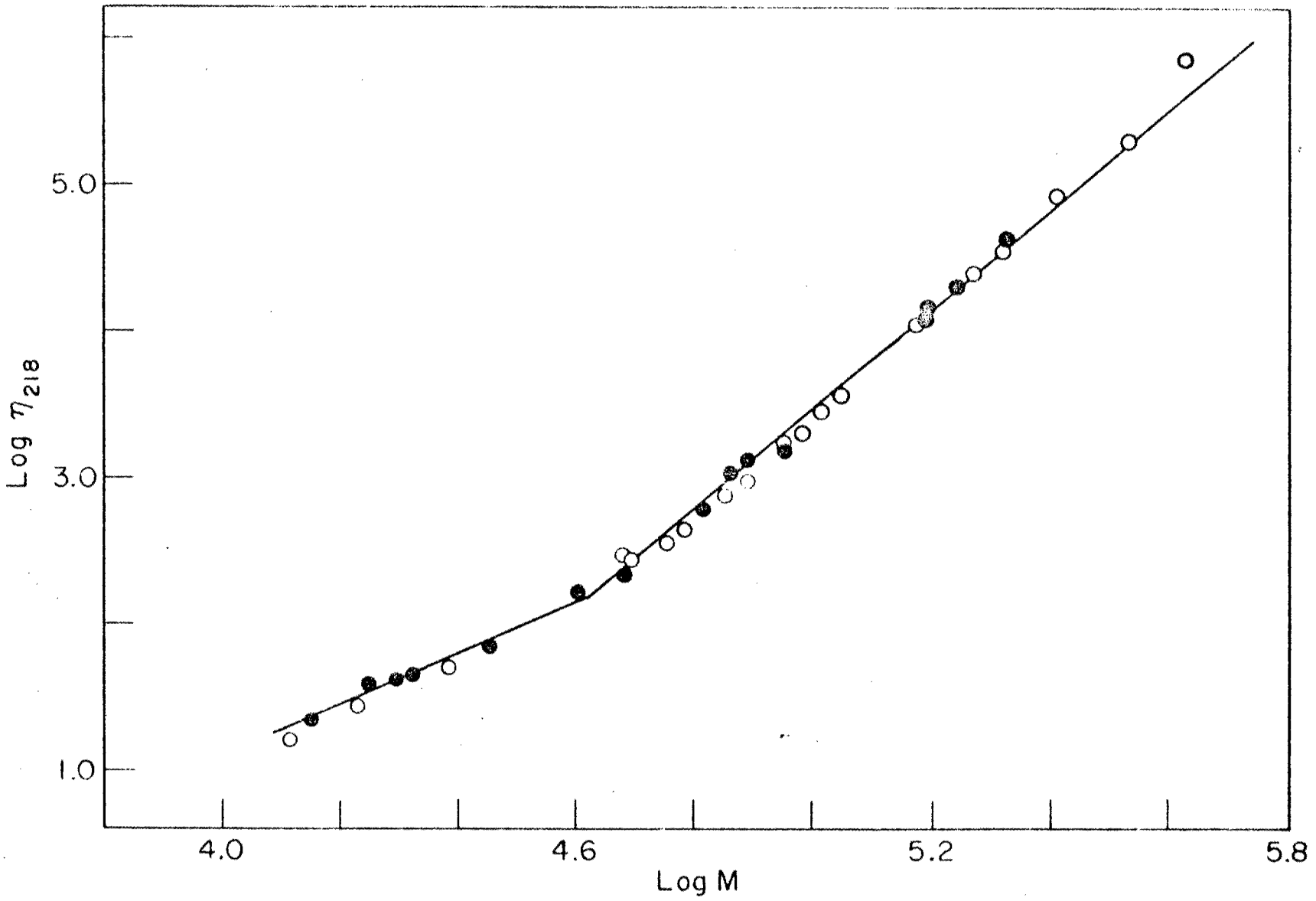

Figure 21 Viscosity-Molecular Weight Relations for Fractions of Anionic ● and Free-Radical O Polystyrene

Table XXII

Calculated Molecular Weight Averages and Melt Viscosities of Mixtures of Fractions of Anionic Polystyrene

Mixture	$M_z \times 10^{-3}$	$M_w \times 10^{-3}$	$M_n \times 10^{-3}$	$M_v \times 10^{-3}$ calc'd[a]		$M_\eta \times 10^{-3}$[b]	$\eta_{218} \times 10^{-3}$
	Calculated[a]			a = 0.8	a = 0.5	obs.	obs. (poises)
A	6,650	1,140	194	830	520	415	600[c]
B	6,500	660	56	400	180	173	31.3
C	770	261	184	246	218	208	51.0
D	1,390	223	57	168	114	130	10.6
E	800	194	128	175	155	147	15.4
F	440	204	50	182	147	178	30.0
G	415	192	34	168	126	174	27.0
H	210	116	21	102	82	98	3.9

(a) Expressions are given in the Appendix

(b) Molecular weight of the fraction having the observed η_{218}.

(c) Measured as a 50 percent solution in dibenzyl ether (cf. Table XXIV).

represented by the line of higher slope in Fig. 21. The value of M_η in Table XXII corresponds generally to the calculated value of M_v for $a = 0.5$ (i.e., $M_\theta = [w_1 M_1^{1/2} + w_2 M_2^{1/2}]^2$). However, in this comparison no consideration has been given to the effect of thermal degradation in lowering the various average molecular weights effective at the time of the viscosity measurement.

The molecular weights M_w^*, M_v^* shown in Table XXIII denote values corrected in the following approximate manner for degradation. For each mixture, a viscosity average molecular weight was computed from the observed intrinsic viscosity in either benzene or cyclohexane of the degraded sample, i.e. after the melt viscosity measurement was made. The other molecular weight averages were then obtained by multiplying the original calculated values (Table XXII) by the observed ratio of the degraded to the original expected value of M_v. The observed bulk viscosities of the mixtures are plotted in Fig. 22 versus the corrected molecular weight averages. Included for comparison are the viscosity-molecular weight relations for fractions, cf. Fig. 21.

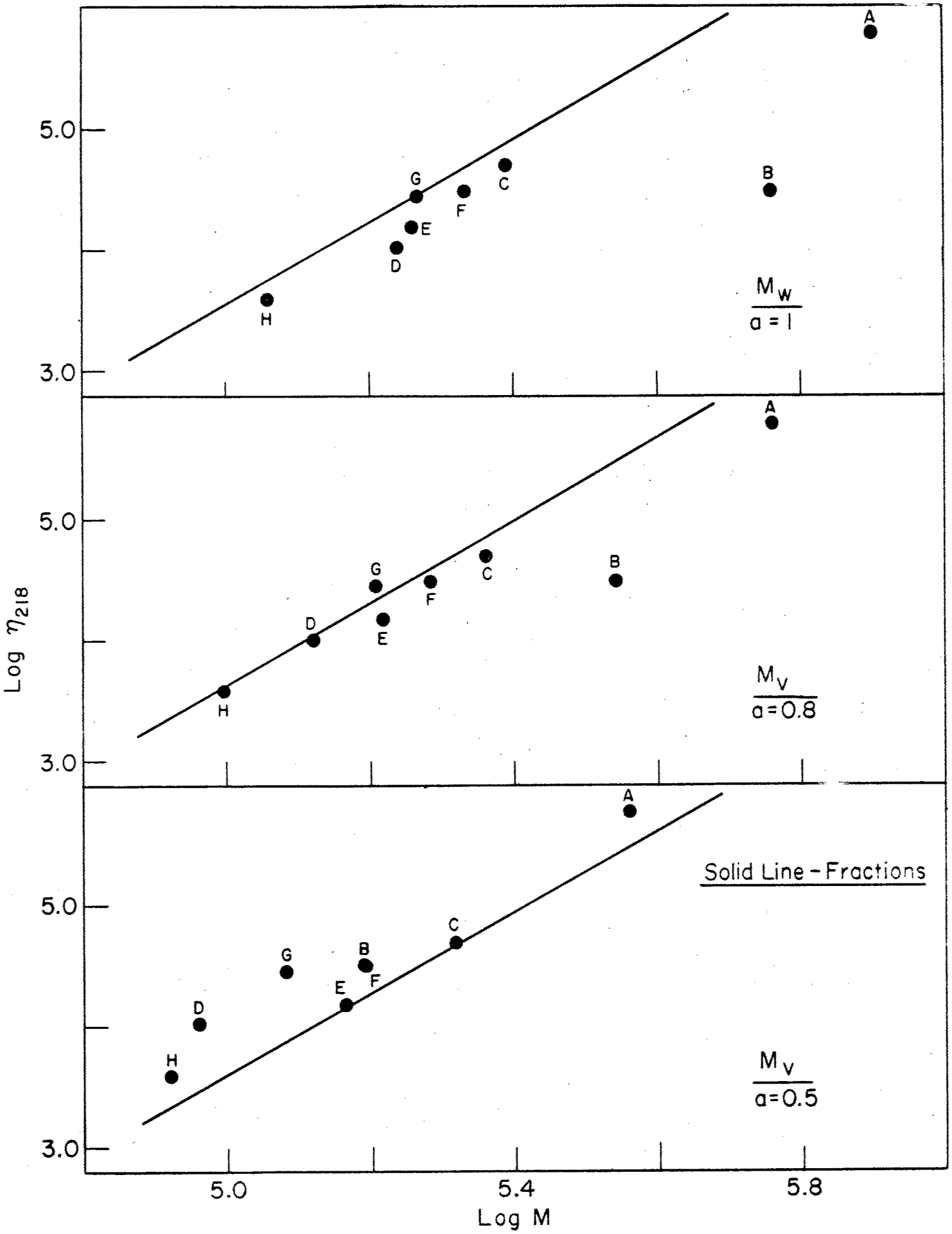

Figure 22 η_{218} – M Data of the Mixtures for the Different Average Molecular Weights

Table XXIII

Comparisons of the Molecular Weight Averages Corrected for Degradation

Mixture	Calc'd[(a)] molecular weights $\times 10^{-3}$ M_w^*	M_v^* (a=0.8)	M_v^* (a=0.5)	M_w^*/M_η	M_v/M_η^* (a=0.8)	M_v/M_η^* (a=0.5)
A	790	575	360	1.9	1.39	0.87
B	575	345	156	3.3	2.00	0.91
C	245	230	204	1.18	1.11	0.98
D	175	132	90	1.35	1.02	0.69
E	183	165	146	1.25	1.12	1.00
F	216	193	156	1.21	1.09	0.88
G	184	161	121	1.06	0.93	0.70
H	115	101	82	1.17	1.03	0.84

(a) M^* is the calculated molecular weight corrected for degradation and errors in preparation; i.e. $M^* = M[M_v$ after η_{218}/M_v calc'd].

Comparison of the values of M_η with the various computed molecular weight averages, corrected as described, suggests the following conclusions:

1. $M_z^*/M_\eta > 1$ in all cases
2. $M_w^*/M_\eta > 1$ in most cases
   [$M_w^*/M_\eta \sim 1$ for the least heterogeneous mixtures (F, G, and H)]
3. $M_v^*/M_\eta > 1$ for a = 0.8, often
   [$M_v^*/M_\eta \sim 1$ for a = 0.8 for the least heterogeneous mixtures (F, G, and H)]
4. $M_v^*/M_\eta \sim 1$ for a = 0.5 in most cases
   [$M_v^*/M_\eta < 1$ for a = 0.5 for the least heterogeneous mixtures (F, G, and H)]

Thus for the most heterogenous mixtures, the isothermal viscosity is related to an average molecular weight lower than either M_z or M_w; it appears that η is more closely related to M_v for a = 0.5 [i.e., to $M_\theta = (w_1 M_1^{1/2} + w_2 M_2^{1/2})^2$] than to any other average considered. For the less heterogeneous mixtures, η seems to be related to an average higher than M_θ, and possibly to either M_w or M_v for a = 0.8.

These new data, then, do not support Bueche's suggestion that η is related to higher average molecular weights (approaching M_z) for broad distributions. Rather they suggest a new finding that the opposite trend is observed, i.e., η is related to a lower average chain length. Additional experiments on new heterogeneous mixtures under conditions such that degradation is eliminated or at least reduced with the various molecular weight averages measured carefully both before and after the melt viscosity measurement are planned in an attempt to determine more clearly which, if any, of the various average molecular weights uniquely determine the melt viscosity of a heterogeneous polymer.

There is presented in Table XXIV and shown in Fig. 23 the preliminary results of the study of the viscosity-molecular weight-concentration relation for polystyrene in dibenzyl ether. From these results it appears that this system obeys the general form of the relations found for concentrated solutions of polyvinyl acetate. It is significant that the slope 3.4 was found for the solutions above M_c. Also, the product of $M_c\phi_2$ was found to be a constant for the two concentrations studied.

Table XXIV

Preliminary Viscosity-Molecular Weight-Concentration Data for Polystyrene Fractions in Dibenzyl Ether

Fraction	Mol. Wt. $\times 10^{-3}$	Measured				Calculated[b] η_{218}	
		ϕ_2	η_{218}[a]	ϕ_2	η_{218}[a]	$\phi_2 = 0.75$	$\phi_2 = 0.50$
14-B	417	---	---	0.490	656	---	725
D-5-B	195	0.850	2,640	.470	23	935	32
D-3-B	141	.760	255	.450	7.5	230	12.6
D-1-A	66	.865	76	.495	1.57	23	1.6
11-CA	60	.743	12.6	---	---	13.5	---
12-BH	50	---	---	.486	0.93	---	1.12
7-AA	38	.800	7.5	.497	0.65	4.6	0.66
9-BH	25	.753	2.6	.497	0.37	2.6	0.38
8-DH	16.6	.772	1.46	.475	0.161	1.17	0.21
8-EH	12.6	.775	0.73	.483	0.097	1.07	0.11

(a) Poises.

(b) From unpublished data of Fox and Schultz with $\partial \log \eta_{218}/\partial\phi_2 = 4.5$.

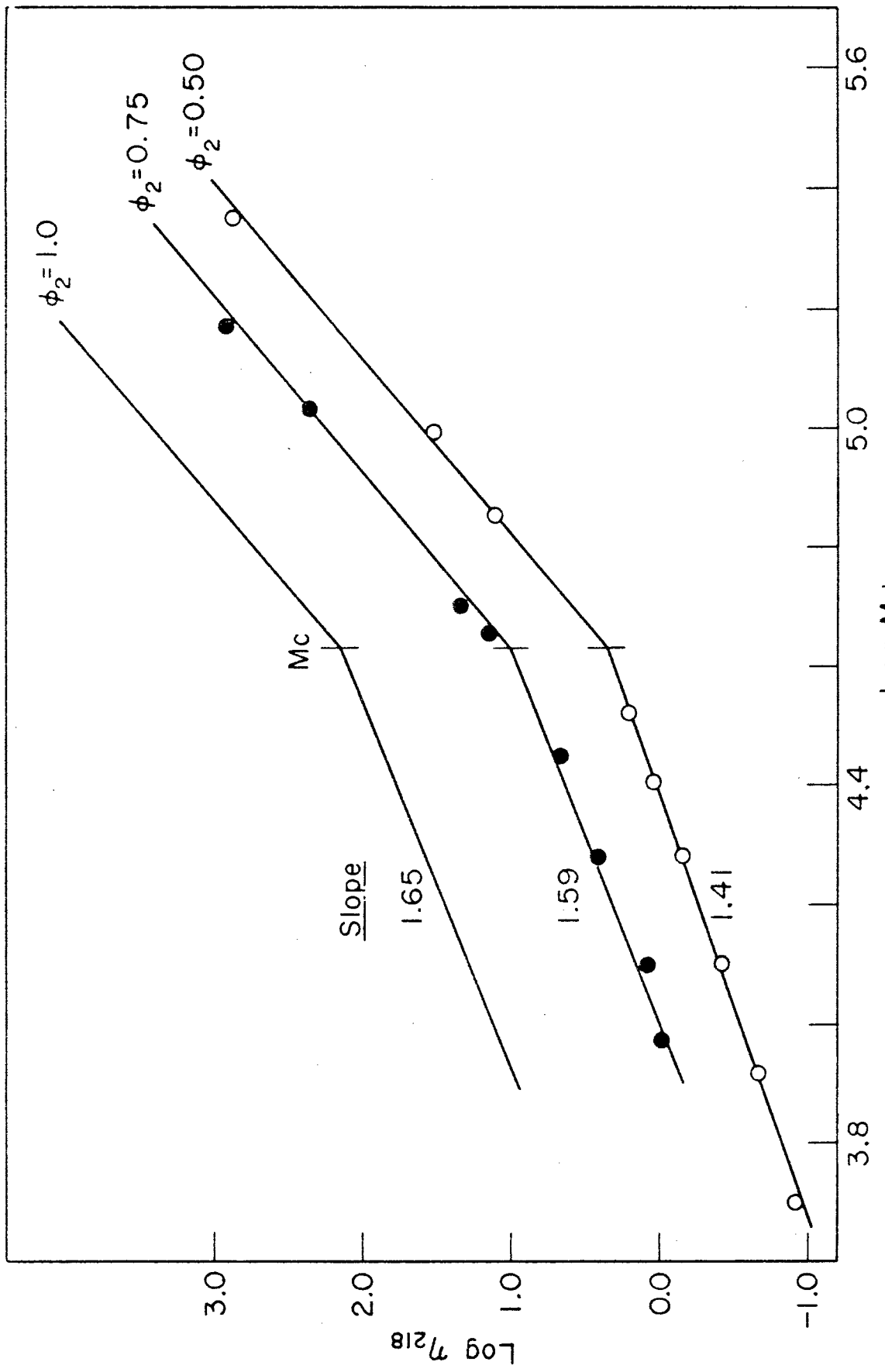

Figure 23 Viscosity-Molecular Weight-Concentration Relations for Fractions of Polystyrene in Dibenzyl Ether

II. Emulsion Polymerization of Vinyl Acetate in the Presence of Protein-Detergent Solubilizing Agents* — V. R. Allen and T. G Fox

A. Introduction

An attempt to obtain stereoregular polyvinyl acetate* (PVAc) by the method of Breuer and Strauss--who suggested[11] that the emulsion polymerization of olefinic monomers solubilized by protein-detergent complexes[12] is stereospecific--was reported[13] to have yielded intriguing but irreproducible and inconclusive evidence for the production of a crystalline product. More recently we have determined[14] that the observed crystallinity is due to impurities trapped in the insoluble product during the coagulation of the latex.

Since much interest was expressed in our previous report of crystallinity, we feel it appropriate to give here a further account of the observations which led us to identify the crystalline material as an impurity.

Thus we report: (1) a brief review of the evidence for crystallinity and of the characterization of the "crystalline" material, (2) the observations related to the nature of the graft polymerization of vinyl acetate with protein, and (3) the current status of the investigation of the abnormal properties of the graft copolymer.

B. Experimental

The polymerizations were normally carried out at 30°C according to standard emulsion techniques and recipes (100 ml H_2O and 100 ml monomer, 1.6 g of sodium dodecyl sulfate (SDS), and 0.3 g of potassium persulfate). The protein, 3.5 g of crystalline bovine serum albumin (BSA), was dissolved with the detergent and initiator.

The latex was coagulated in a concentrated salt solution; the product washed with water and dried in vacuo at 50°C for 12-18 hours. The dried polymer was separated into the acetone-soluble and -insoluble phases. These samples were studied by thermal and solvent annealing, infrared analysis, x-ray diffraction, and hydrolysis with subsequent reacetylation. The details of the procedures followed in these tests were described previously.[7]

C. Results and Discussion

1. Characterization of the crystalline component. X-ray diffraction data for some of the early products are presented in Table XXV. It was estimated that the sample VT-2, showing up to 22 lines in the

*This work was pursued in hope of obtaining polymers for use in a study of the effect of stereochemical structure on the melt viscosity and molecular mobility.

Table XXV

Bragg d-Spacings of "Crystalline" Poly-(vinyl acetate) Samples

Dimethyl formamide extracted VT-2		Original crumb VT-2		Acetone insoluble component											
				VT-134		VT-23		VT-21		VT-20		VT-16		VT-17	
7.2	s	7.2	s	7.1	s	4.7	f					4.7	f	4.7	f
4.3	f	4.4	f			4.4	m			4.4	f	4.3	f	4.3	vf
4.0	f	3.95	m			3.95	f			3.95	s				
3.5	s	3.50	m	3.5	s	3.57	vf			3.57	f	3.6	vf		
3.35	s(spots)			3.3	m			3.40	f						
3.02	s	3.03	f												
2.85	m	2.82	m					2.90	f						
2.55	vf	2.52	vf	2.55	vf			2.50	vf						
2.36	vf	2.36	f					2.30	vf						
2.10	vf			2.10	vf										
2.00	vf	2.00	vf	2.00	vf										
1.90	vf	1.91	vf												
1.80	vf														
1.75	vf	1.75	vf												
1.67	vf														
1.54	vf														
1.49	vf														
1.38	vf														

s - strong m - medium f - faint vf - very faint

diffraction pattern, was 30-50 percent crystalline in character. The other "highly" crystalline sample, VT-134, exhibits a very similar x-ray diffraction pattern. It is clear from the data in Table XXV that the other five "slightly" crystalline samples had neither the same crystalline structure nor the same extent of crystallinity. Further, when other properties of these samples are compared (in Table XXVI) with an amorphous product and a conventional PVAc (prepared without BSA), it is apparent that the two, VT-2 and VT-134, were indeed quite different from the others.

More than one hundred polymerizations* were carried out in an attempt to reproduce the properties of these two samples. They involved systematic variations in the polymerization conditions and in the post-polymerization treatment. Study of the crystalline character of the emulsion ingredients, separately and as mixtures, the results shown in Table XXVII. From a comparison of these data with those in Table XXV, it appears that the "slightly crystalline" samples contain residual detergent (and protein). Indeed, it was observed that latices coagulated in ca. 10 percent salt solution were amorphous and those coagulated in a saturated (ca. 30 percent) solution often exhibited this low degree of crystalline character.

Although these extensive studies failed to yield the crystalline product obtained earlier, they indicated the possibility that the observed crystallinity in VT-2 and VT-134, in spite of its large amount (estimated >30%), might be due to an impurity. Although almost all of the product had been used up in the initial determination of properties, enough remained for infrared absorption determinations. These measurements revealed considerable absorption in the 9-10.5μ range in the spectra of both the acidic and alkaline hydrolysis products of VT-2, suggesting the presence of silicate. Even though the SiO_2 in the alkaline hydrolysis product could conceivably have come from the glass reaction bottles, its presence in the other case was quite surprising. Semi-quantitative analysis by emission spectroscopy then revealed that the two more interesting samples, VT-2 and VT-134, contained ca. 10 percent of both the aluminate and silicate ions, and the others up to 1 percent of each, as shown in Table XXVIII.

In checking the possibilities of inadvertent introduction of such a large amount of an inorganic material into the system either before or after the polymerization it was found that the sodium chloride solution used for coagulation was very probably the source. Indeed, as shown in Table XXIX, a sample of product coagulated in a bath containing commercial table-grade salt was found to have both the same diffraction pattern and properties as VT-2 and VT-134.

It is concluded that the intriguing crystalline character of the early polymerization products was due to an inorganic silico-aluminate, adsorbed from the coagulation bath in which a commercial salt had been used. Failure to reproduce this result followed since reagent-grade salt was used in subsequent trials.

---

*Including a parallel study by Dr. H. Schnecko not sponsored by this contract.

Table XXVI

Comparison of Properties of "Crystalline" and Amorphous Polymerization Products

Sample designation	Solubility in cold acetone (%)	Appearance of insoluble product		Relative rates of solution in media for		Hydrolyzed		Reacetylated	
		Crumb	Pressed film	Hydrolysis	Reacetylation	Solubility in H_2O	Crystallinity	Solubility in acetone	Crystallinity
Conventional polymer	100	(Transparent cast film)		1	1	Sol.	Strong	Sol.	Amorphous
VT-28 (Amorphous product)		Transparent	Transparent, uneven (strained)	2-3	1-2	Sol.	Strong	Sol.	Amorphous
VT-2	100	White	Opaque-tough	4	3	Insol.	Oriented by pressing	Insol.	Amorphous
VT-134	65	White	White-brittle (like parchment)	3-4	3	Insol.	Oriented by pressing	Sol.	Amorphous
VT-16	100	Yellow-green							
VT-17	100	Yellow-green							
VT-20	90	Same as VT-28		3-4	2-3	Insol.	Oriented by pressing	Insol.	Amorphous
VT-21	50	Same as VT-28		3-4	2-3	Insol.	Oriented by pressing	Sol.	Amorphous
VT-23	50	Same as VT-28		3-4	2-3	Insol.	Oriented by pressing	Insol.	Amorphous

Table XXVII

Bragg d-Spacings of the Emulsion Ingredients and Mixtures

Potassium persulfate	Na dodecyl sulfate	Bovine serum albumin	Protein, detergent,[a] and initiator	Protein, detergent[b] and conventional PVAc
		12.0 vf		
	8.4 vf			
		5.3 f	5.7 m	
4.9 f	5.0 f		5.0 m	5.0 m
	4.5 s			
	4.3 m		4.3 vf	4.3 m
3.7 m				3.5 s
3.2 s	3.2 f		3.4 f	3.3 m
	2.9 f			
			2.8 vf	2.8 vf
	2.0 vf		2.3 vf	

(a) Dissolved and aged in solution 48 hours at room temperature. Solvent evaporated and product preseed at 150°C with 20,000 psi.

(b) Coprecipitated from acetone and aqueous solutions. Dried in vacuo and annealed in 2-octanone at 80°C for 72 hours.

Table XXVIII

Concentration of Aluminum and Silicon in Polymerization Products

Product	Classification	Concentration[a] (%) Aluminum	Silicon
VC-1	Conventional[b]	1	3
VT-1	Insoluble-amorphous	0.3	0.3
VT-2	Insol.-crystalline	>3	10
PVA-2	Hydrolyzate of VT-2	3-10	10
VT-134-AI	Insol.-crystalline	10	10
VT-134-AS	Soluble-amorphous	0.1	<-1
VT-20	Insol. phase-slightly cryst.	1-3	<0.3
VT-23	Insol. phase-slightly cryst.	0.1	<-1
PVA-23	Hydrolysate of VT-23	1.0	1.0
VT-27	50 percent insol.-amorphous	0.1	0.1
VT-41	80 percent insol.-amorphous	0.1	0.1

(a) Semi-quantitative results of emission spectroscopy analysis.

(b) Control polymer prepared without protein.

Table XXIX

Properties of Polymerization Product Coagulated in Commercial Salt Solution

Bragg d-Spacings:			
A	Intensity	A	Intensity
7.2	s	2.8	f
4.4	f	2.4	vf
4.0	f	2.1	vf
3.5	s	2.0	vf
3.0	m	1.7	vf

Physical Properties:
Insoluble in cold acetone
White brittle pressed film
Insoluble in alkaline hydrolysis media after 48 hours at 80°C

2. Nature of the insoluble polymerization product. From studies of both the "crystalline" and amorphous products obtained in the early trials, it was established that there is produced both a soluble polyvinyl acetate, similar to that prepared in the absence of protein, and a portion insoluble in all non-hydrolytic solvents, consisting of PVAc with non-extractable protein. Further, abnormally slow rates of hydrolysis and subsequent reacetylation were observed for the insoluble product. Following the identification of the crystalline component as an impurity, we have reinvestigated the characteristics described above, employing amorphous samples free of the additional complication of the foreign crystalline matter.

From the combined results of this work and the parallel study conducted by Dr. Schnecko, it appears that the insoluble product is formed early in the polymerization. At ca. 30-40 percent conversion, all of the protein is found in the insoluble phase, and thereafter there is no increase in the amount of insoluble product. These and other observations suggest strongly that in fact the polymerization involves growth of PVAc branches grafted to the protein via free radical transfer to a limited number of highly active transfer sites on the protein substrate. In order to ascertain the macroscopic locus of polymerization, two latices were examined with an electron microscope. It was clearly evident that latex particles are present in a broad range of particle sizes, suggesting that the added protein does not change the nature of the emulsion.

The amount of soluble fraction, the nitrogen content and the conversion relations previously reported[3] have been confirmed by the

present study. The results, which are given in Figs. 24 and 25, clearly show the dependence of solubility and bound protein (nitrogen) on conversion and suggest that the PVAc-BSA graft is formed early and followed by the conventional polymerization yielding a soluble, protein-free polymer.

Reinvestigation of the previously reported abnormal rates of hydrolysis and subsequent reacetylation has revealed (1) that the apparent rate of hydrolysis is determined primarily by the rate of solution of the sample in the medium which, in itself, is directly related to the protein content, and (2) that the apparent rate of reacetylation is dependent on the extent of crystallization of the hydrolyzate. Further, there is indicated that this degree of crystallization (and solubility of the hydrolyzate in water) is related to the exact thermal history of the sample. Thus, it now appears that these interesting properties may be simply a result of the bound protein and its effect on the reaction rates and not an indication of a more stereoregular structure caused by the addition of protein to the emulsion.

3. Current status. Although, as mentioned above, the observed abnormal properties of the insoluble phase may be simply a result of the bound protein, we feel obliged to repeat these experiments again as a check of their validity and reproducibility. Consequently, we are currently engaged in the following systematic investigation. Under identical conditions, four polymers have been prepared, two with, and two without protein. One of each was terminated at low (Ca. 20 percent) conversion, and the other at ca. 50 percent. Solubility, protein content, and x-ray diffraction measurements correspond to results for the bulk of the samples prepared earlier during this investigation. Also, preliminary hydrolysis and reacetylation studies are consistent with the results previously obtained, i.e. apparent rates are lower for the protein-containing samples. We are currently engaged in checking possible techniques that may yield definitive results concerning the reason for the observed difference in rates.

D. Summary

The polymerization of an emulsion of vinyl acetate containing bovine serum albumin was found to yield a soluble phase, similar in all respects to that prepared without protein, and an insoluble phase containing non-extractable protein. The apparent rate of hydrolysis of the insoluble product is lower than that of the conventional polymer, but this may be due to the insolubility and/or protein content of this material.

The intriguing crystalline material obtained in the earliest work has been identified as an impurity, a silico aluminate, adsorbed by the polymer from the coagulating (NaCl) bath.

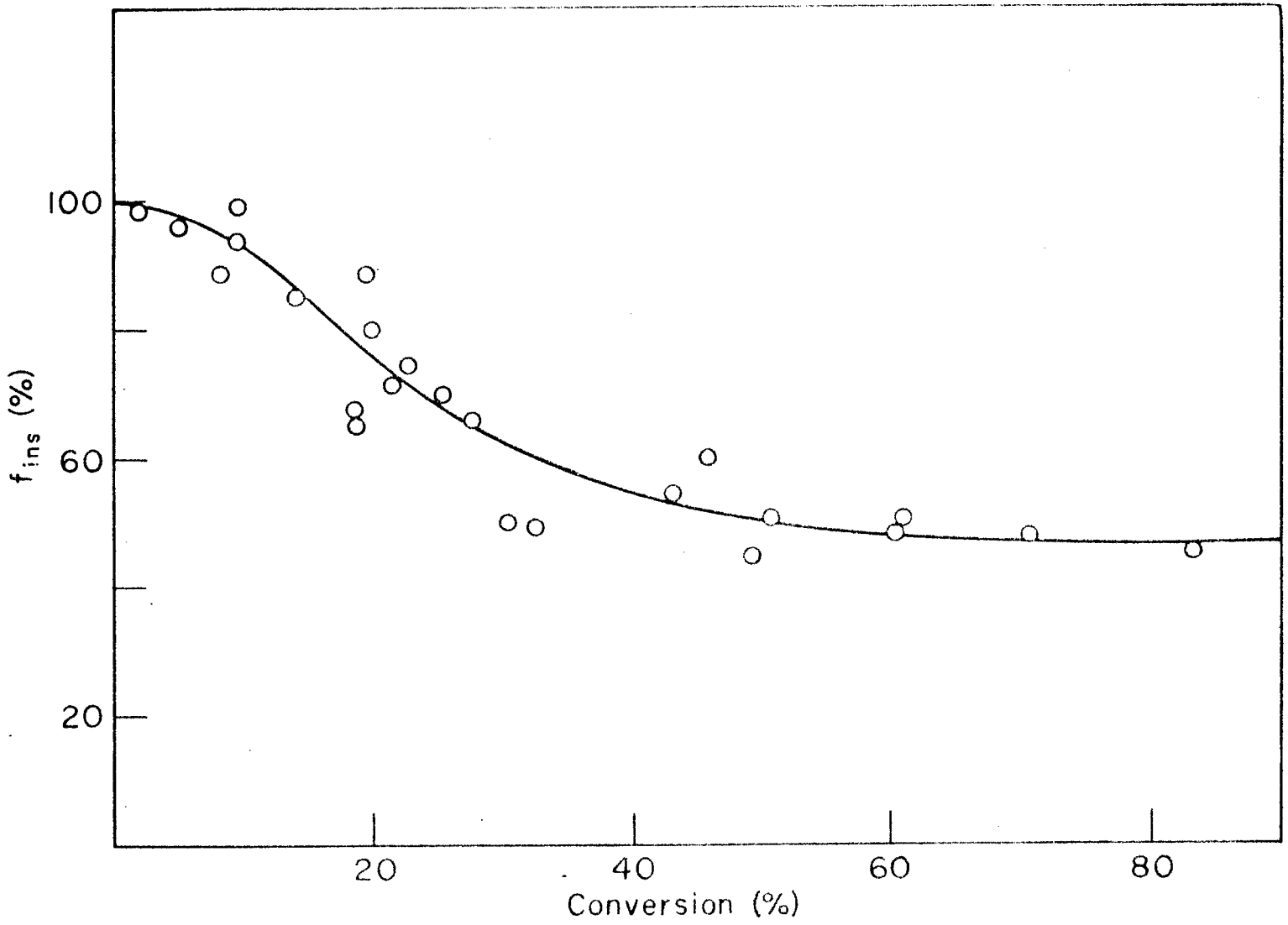

Figure 24 The Change in the Weight Fraction of Insoluble Material (f_{ins}) with Conversion

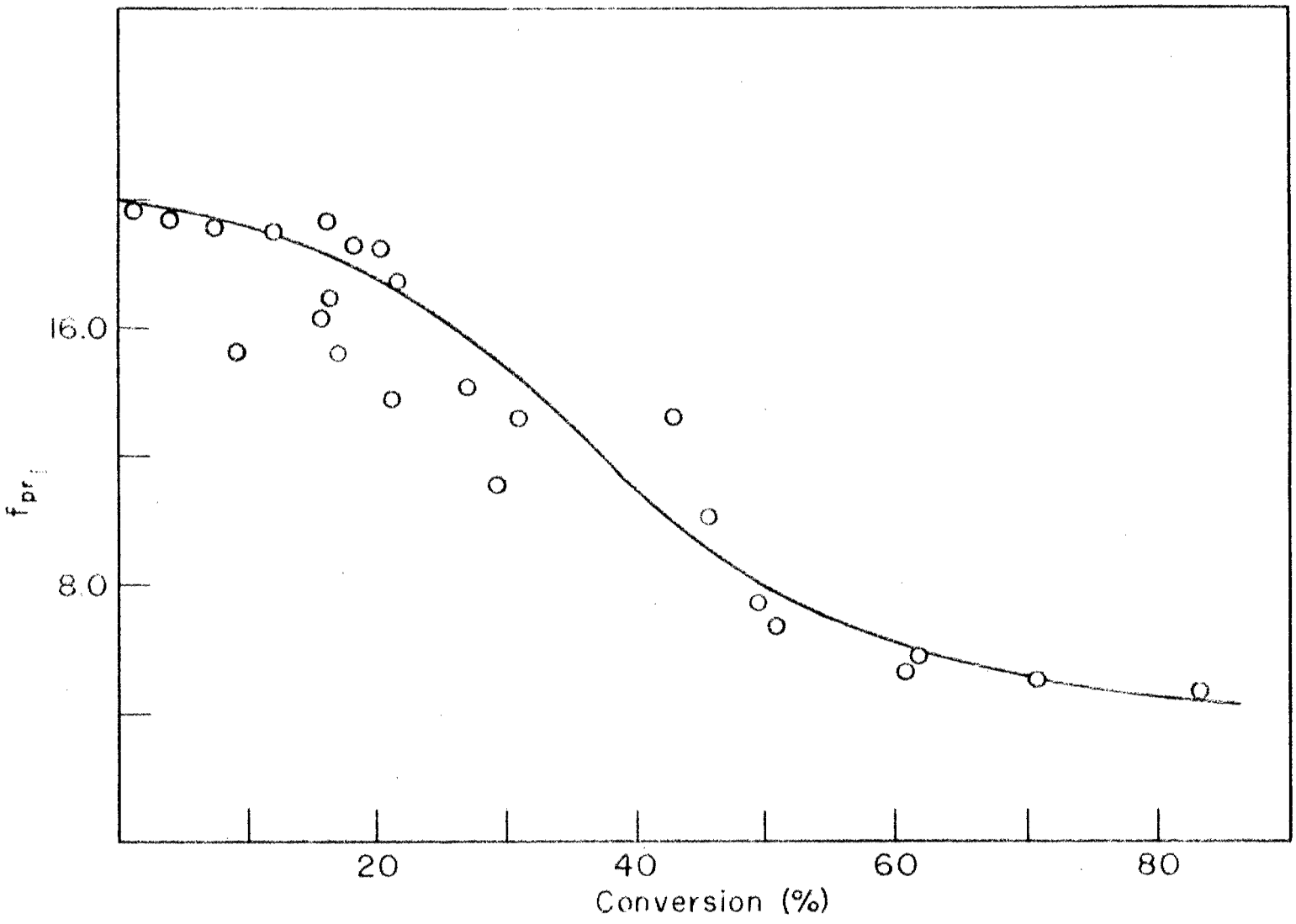

Figure 25 The Dependence of the Fraction of Bound Protein in the Insoluble Material (f_{pr_1}) on the Extent of Conversion

Appendix

Molecular Weight Averages in Heterogeneous Polymers

The various average molecular weights for heterogeneous polymers are defined by the equations

$$M_n = \frac{\sum_i N_i M_i}{\sum_i N_i} \qquad \text{number average } (M_n) \qquad (59)$$

$$M_w = \frac{\sum_i N_i M_i^2}{\sum_i N_i M_i} \qquad \text{weight average } (M_w) \qquad (60)$$

$$M_z = \frac{\sum_i N_i M_i^3}{\sum_i N_i M_i^2} \qquad \text{z-average } (M_z) \qquad (61)$$

$$[\eta]_{av} = \sum_i w_i [\eta]_i$$

$$M_v = \left[\frac{[\eta]_{av}}{K}\right]^{1/a} = \left[\sum_i w_i M_i^a\right]^{1/a} \qquad \text{viscosity average } (M_v) \qquad (62)$$

For a mixture of two homogeneous fractions consisting of weight fraction w_1 of molecular weight M_1 and $w_2 = 1 - w_1$ of molecular weight M_2,

$$M_n = \frac{M_2}{w_2}\left(\frac{r}{R} + 1\right)^{-1} \qquad (63)$$

$$M_w = w_2 M_2 (rR + 1) \qquad (64)$$

$$M_z = M_2\left(\frac{rR^2 + 1}{rR + 1}\right) \qquad (65)$$

$$M_z/M_w = (r + 1)\left(\frac{rR^2 + 1}{(rR + 1)^2}\right); \qquad M_w/M_n = \frac{(rR + 1)(r + r)}{(r + 1)^2 \cdot R} \qquad (66)$$

$$\text{where } r = \frac{w_1}{w_2}; \qquad R = \frac{M_1}{M_2} \qquad (67)$$

In the special case where $w_1 = w_2 = 0.5$ and $r = 1$

$$M_z = \frac{M_1^2 + M_2^2}{M_1 + M_2}; \quad M_w = (M_1 + M_2)/2; \quad M_n = \frac{2M_1M_2}{M_1 + M_2} \tag{68}$$

$$\frac{M_z}{M_w} = 2\,\frac{R^2 + 1}{(R + 1)^2}; \quad \frac{M_w}{M_n} = \frac{(R + 1)^2}{4R} \tag{69}$$

It can be shown that M_z/M_w for a mixture of two fractions is maximum where $r = 1/R$. Then

$$\frac{M_z}{M_w} = \frac{(R + 1)^2}{4R}$$

$$\frac{M_w}{M_n} = \frac{2(R^2 + 1)}{(R + 1)^2} \tag{70}$$

For a mixture of two fractions it can also be shown that M_w/M_v is a maximum when

$$r = [(R^a - 1) - a(R - 1)]/[aR^a(R - 1) - R(R^a - 1)]$$

with a the constant characteristic of the particular system.

LIST OF REFERENCES

1. T. G Fox, S. Gratch and S. Loshaek, Rheology, Theory and Applications Vol. I (F. R. Eirich, Ed., Academic Press, Inc., New York, 1956), Chapter 12.

2. J. D. Ferry, Viscoelastic Properties of Polymers (John Wiley & Sons, Inc., New York, 1961).

3. F. Bueche, J. Chem. Phys. 20, 1959 (1952); 25, 599 (1956).

4. T. G Fox and P. J. Flory, J. Am. Chem. Soc. 70, 2384 (1948); J. Polymer Sci. 14, 315 (1954).

5. F. Bueche, J. Polymer Sci. 43, 527 (1960).

6. H. Nakayasu and T. G Fox, Colloid Chem. Div. Abstracts, 137th Meeting of the American Chemical Society, Cleveland, April, 1960; Proc. 6th Joint Army, Navy, Air Force Conference on Elastomers, Boston, October, 1960, Vol. I, pp. 65-71.

7. ASD Technical Report 61-22, April 1961.

8. L. J. Sharman, R. H. Sones and L. H. Cragg, J. Appl. Phys. 24, 703 (1953).

9. W. R. Krigbaum and P. J. Flory, J. Polymer Sci. 11, 37 (1953).

10. R. H. Ewart and H. C. Tingey, Abstracts, 111th Meeting of the American Chemical Society, Atlantic City, April, 1947.

11. M. Breuer and U. P. Strauss, private communication, April, 1960.

12. M. Breuer and U. P. Strauss, J. Phys. Chem. 64, 223 (1960).

13. V. Allen, T. G Fox, S. S. Pollack and H Schnecko, SPE Transactions 2, 104 (1962).

PART III - ELASTICITY OF POLYMERIC NETWORKS

Specific Diluent Effects on the Elastic Properties of Polymeric Networks — C. A. J. Hoeve and M. O'Brien

A. Introduction

Possible specific diluent effects on the modulus of amorphous polyethylene networks were investigated further (see previous ASD Technical Report 61-22). Unfortunately, no equilibrium values were obtained for the force as function of elongation, as was apparent from hysteresis loops in the stress-strain curves. In an attempt to overcome these difficulties, measurements were performed in the swollen state only, for which hysteresis is known[1] to be smaller than in the dry state. Furthermore, the period of observation was increased from 15 minutes to several days. However, as a result of irreproducibility, described below, the margin of experimental error was not reduced. We decided, therefore, to perform measurements in the manner described previously. Since deviations from equilibrium values of the force must be approximately equal if the sample is diluted with different solvents, the chain dimensions may be obtained relative to those in a given diluent.

B. Experimental

Since polyethylene samples degraded slowly at 150°C, even in a flow of nitrogen (see previous report), the samples were loaded by suitable weights and immersed in a diluent contained in a glass vessel at room temperature. After several times degassing, the evacuated containers were sealed off and heated to 150°C. The distance between two pins, perforating the sample, was measured to within 0.1% with a cathetometer. Sample lengths became practically constant after about 48 hours, but unfortunately the values obtained were not reproducible. Sometimes measurements were extended to several weeks; however, no improvement resulted. After further extension of the sample, the length at a given weight was invariably larger than before. Apparently even with rigorous exclusion of air, slow degradation occurs of polyethylene networks at 150°C. Results obtained were not superior to the more simple stress-strain measurements performed originally. We decided, therefore, to perform these measurements in the manner described below. Samples were crosslinked by high-energy irradiation. Those marked A were irradiated by the electron beam of a van de Graaff accelerator with a dose of 40 megarep. Samples marked B and C were irradiated by γ-radiation from a Co^{60} source with doses of respectively 29.6 and 39.3 megarep.

C. Results and Discussion

Further experiments, together with the results given in the previous report, are given in Table XXX. It is observed that the values of R, defined as the ratio of the calculated force to that observed for the diluted sample, are appreciably different from unity. If these

Table XXX

Properties of Swollen Polyethylene Networks

Sample	Solvent	α	v_2'	R	P
A	DEHA	1.35	0.386	0.97	1.13
A	α-Cl.n.	1.275	0.218	0.86	1.01
A	n-hexad.	1.31	0.196	0.84	(1.00)
A	n-hexad.	1.35	0.221	0.87	
B	DEHA	1.24	0.348	1.67	0.97
B	α-Cl.n.	1.20	0.166	1.86	1.08
B	n-paraffin	1.178	0.219	1.57	0.91
B	n-hexad.	1.190	0.176	1.72	(1.00)
C	DEHA	1.203	0.393	1.34	1.12
C	α-Cl.n.	1.200	0.188	1.30	1.08
C	n-paraffin	1.225	0.262	1.19	0.99
C	n-hexad.	1.165	0.228	1.20	(1.00)

values were obtained at thermodynamic equilibrium, R would equal the ratio of the unperturbed mean-square end-to-end distance in the diluted state to that in bulk. However, the stress-strain results obtained in the bulk are particularly suspect; in diluted samples equilibrium is approached more readily. Since deviations from equilibrium may depend on mode and degree of crosslinking, the differences in ranges of R values for samples A, B, and C are understandable. In order to eliminate these effects, the best procedure is to calculate P, defined as the ratio of R for a given diluent to that for n-hexadecane. For any sample we have then that $P = \langle r_o^2 \rangle_{solvent} / \langle r_o^2 \rangle_{n\text{-hexadecane}}$. These values are given in the last column of Table XXX. As is observed, the values of P are close to unity, despite large variations in values of R. The average values of P for the solvents di-2-ethylhexyl azelate, α-chloronaphthalene, and n-paraffin are respectively 1.07, 1.03, and 0.95. We may therefore conclude that the unperturbed mean-square end-to-end distance of the polyethylene chain in these solvents is within ten per cent equal to that in n-hexadecane.

It is inconceivable that $\langle r_o^2 \rangle$ of polyethylene in bulk is appreciably different from that in n-paraffin and n-hexadecane in view of the similarity of the molecules. We may therefore conclude that within experimental error no specific solvent effects exist on the chain dimensions. This is the more remarkable, if the different nature of the solvents is considered. Apparently the distribution of trans and gauche states along the chain is unaltered by large environmental changes from an aliphatic solvent to a branched ester, or to a polar aromatic compound. Also whether the solvent is good (n-hexadecane), or bad (di-2-ethylhexyl azelate), has no effect on unperturbed chain dimensions. It is well known[2] that in such dilute solutions that the chains do not overlap, chain dimensions are perturbed by excluded volume

effects; therefore, in dilute solutions the chain will be much more expanded in the former than in the latter solvent.

In contrast, the unperturbed chain dimensions are determined mainly by intramolecular forces, intermolecular force, having no effect within experimental error, although our theoretical calculations[3] indicate the unperturbed chain dimensions of polyethylene to be sensitive to the distribution of conformations assumed along the chain. This result, heretofore implicitly assumed in rubber elasticity theory, is therefore a further justification of its basis.

LIST OF REFERENCES

1. A. Ciferri and P. J. Flory, J. Appl. Phys., 30, 1498 (1959).

2. P. J. Flory, Principles of Polymer Chemistry, Cornell University Press, Ithaca, N. Y., 1953, Chapter XIV.

3. C. A. J. Hoeve, J. Chem. Phys., 35, 1266 (1961).

DISTRIBUTION WITHIN AERONAUTICAL SYSTEMS DIVISION (ASD)

ASAPRL	Technical Documents Library Section
ASAPT	Technical Publications Branch
ASAPTT	Advanced Technology & Test Publications Section
ASEH	Office of Information Historical Division
ASNE	Engineering Evaluation Office
ASNY	Engineering Analysis Office
ASNV	B-70 Engineering Office
ASNG	GAM-87 Engineering Office
ASNL	C-141/Materials Handling Engineering Office
ASNR	Dyna-Soar Engineering Office
ASND	Directorate of Defense and Transport Systems Engineering
ASNN	Directorate of Aerospace Ground Equipment Engineering
ASNP	Directorate of Operational Support Engineering
ASNC	Directorate of Systems Dynamic Analysis
ASNS	Directorate of Strategic and Tactical Systems Engineering
ASNX	Directorate of Engineering Standards
ASO	DCS/Plans and Operations
ASRC	Directorate of Materials & Processes
ASRCE	Applications Laboratory
ASRCEM-1A	Information Processing Section
ASRCM	Metals & Ceramics Laboratory
ASRCN	Nonmetallic Materials Laboratory
ASRCNC	Plastics & Composites Branch
ASRCNE	Elastomers & Coatings Branch
ASRCNF	Fibrous Materials Branch
ASRCNL	Fuels & Lubricants Branch
ASRCNP	Polymer Branch
ASRCP	Physics Laboratory
ASRE	Deputy for Technology Evaluation Office
ASRM	Directorate of Aeromechanics
ASRMP	Propulsion Laboratory
ASRN	Directorate of Avionics
ASRNE	Electronic Technology Laboratory
ASRO	Deputy for Technology Research Management Office
ASROO	Deputy for Technology Technical Management Division
ASRS	Directorate of Advanced Systems Planning
AST	Deputy for Test and Support
ASZ	Deputy for Systems Management
MRO	Hq 6570th Aerospace Medical Research Laboratories

Aeronautical Systems Division, Dir/Materials and Processes, Nonmetallic Materials Lab, Wright-Patterson AFB, Ohio
Rpt No. ASD TR 61-22, Pt II. POLYMER STRUCTURES AND PROPERTIES. Final report, Oct 62, 103 pp. incl illus., tables, 64 refs.
Unclassified Report

Theoretical studies of the thermodynamical configurational properties of polymers in dilute solution are described. Experimental results are reported on the effects of chain branching in both good and poor solvents and on specific solvent effects on chain dimensions. Refinements have been made in the design of a light scattering photometer, and

(over)

calibration procedures have been critically evaluated. Melt viscosities of mixtures of polymer fractions appear to depend on the viscosity average molecular weight in a theta solvent rather than a higher molecular weight average. New characterization data have been obtained for the vinyl acetate polymer from emulsion polymerization in the presence of protein. Swelling studies of crosslinked polyethylene indicate no appreciable specific solvent effects for this polymer.

1. Dilute polymer solutions
2. Polymer properties
3. Polymer structure

I. AFSC Project 7342, Task 734203
II. Contract AF 33(616) -6968
III. Mellon Institute, Pittsburgh, Pa.
IV. T. A. Orofino et al
V. Not aval fr OTS
VI. In ASTIA collection

Aeronautical Systems Division, Dir/Materials and Processes, Nonmetallic Materials Lab, Wright-Patterson AFB, Ohio
Rpt No. ASD TR 61-22, Pt II. POLYMER STRUCTURES AND PROPERTIES. Final report, Oct 62, 103 pp. incl illus., tables, 64 refs.
Unclassified Report

Theoretical studies of the thermodynamical configurational properties of polymers in dilute solution are described. Experimental results are reported on the effects of chain branching in both good and poor solvents and on specific solvent effects on chain dimensions. Refinements have been made in the design of a light scattering photometer, and

(over)

calibration procedures have been critically evaluated. Melt viscosities of mixtures of polymer fractions appear to depend on the viscosity average molecular weight in a theta solvent rather than a higher molecular weight average. New characterization data have been obtained for the vinyl acetate polymer from emulsion polymerization in the presence of protein. Swelling studies of crosslinked polyethylene indicate no appreciable specific solvent effects for this polymer.

1. Dilute polymer solutions
2. Polymer properties
3. Polymer structure

I. AFSC Project 7342, Task 734203
II. Contract AF 33(616) -6968
III. Mellon Institute, Pittsburgh, Pa.
IV. T. A. Orofino et al
V. Not aval fr OTS
VI. In ASTIA collection

Aeronautical Systems Division, Dir/Materials and Processes, Nonmetallic Materials Lab, Wright-Patterson AFB, Ohio
Rpt No. ASD TR 61-22, Pt II. POLYMER STRUCTURES AND PROPERTIES. Final report, Oct 62, 103 pp. incl illus., tables, 64 refs.
Unclassified Report

Theoretical studies of the thermodynamical configurational properties of polymers in dilute solution are described. Experimental results are reported on the effects of chain branching in both good and poor solvents and on specific solvent effects on chain dimensions. Refinements have been made in the design of a light scattering photometer, and

(over)

calibration procedures have been critically evaluated. Melt viscosities of mixtures of polymer fractions appear to depend on the viscosity average molecular weight in a theta solvent rather than a higher molecular weight average. New characterization data have been obtained for the vinyl acetate polymer from emulsion polymerization in the presence of protein. Swelling studies of crosslinked polyethylene indicate no appreciable specific solvent effects for this polymer.

1. Dilute polymer solutions
2. Polymer properties
3. Polymer structure

I. AFSC Project 7342, Task 734203
II. Contract AF 33(616)-6968
III. Mellon Institute, Pittsburgh, Pa.
IV. T. A. Orofino et al
V. Not aval fr OTS
VI. In ASTIA collection

Aeronautical Systems Division, Dir/Materials and Processes, Nonmetallic Materials Lab, Wright-Patterson AFB, Ohio
Rpt No. ASD TR 61-22, Pt II. POLYMER STRUCTURES AND PROPERTIES. Final report, Oct 62, 103 pp. incl illus., tables, 64 refs.
Unclassified Report

Theoretical studies of the thermodynamical configurational properties of polymers in dilute solution are described. Experimental results are reported on the effects of chain branching in both good and poor solvents and on specific solvent effects on chain dimensions. Refinements have been made in the design of a light scattering photometer, and

(over)

calibration procedures have been critically evaluated. Melt viscosities of mixtures of polymer fractions appear to depend on the viscosity average molecular weight in a theta solvent rather than a higher molecular weight average. New characterization data have been obtained for the vinyl acetate polymer from emulsion polymerization in the presence of protein. Swelling studies of crosslinked polyethylene indicate no appreciable specific solvent effects for this polymer.

1. Dilute polymer solutions
2. Polymer properties
3. Polymer structure

I. AFSC Project 7342, Task 734203
II. Contract AF 33(616)-6968
III. Mellon Institute, Pittsburgh, Pa.
IV. T. A. Orofino et al
V. Not aval fr OTS
VI. In ASTIA collection

Aeronautical Systems Division, Dir/Materials and Processes, Nonmetallic Materials Lab, Wright-Patterson AFB, Ohio
Rpt No. ASD TR 61-22, Pt II. POLYMER STRUCTURES AND PROPERTIES. Final report, Oct 62, 103 pp. incl illus., tables, 64 refs.
Unclassified Report

Theoretical studies of the thermodynamical configurational properties of polymers in dilute solution are described. Experimental results are reported on the effects of chain branching in both good and poor solvents and on specific solvent effects on chain dimensions. Refinements have been made in the design of a light scattering photometer, and

(over)

calibration procedures have been critically evaluated. Melt viscosities of mixtures of polymer fractions appear to depend on the viscosity average molecular weight in a theta solvent rather than a higher molecular weight average. New characterization data have been obtained for the vinyl acetate polymer from emulsion polymerization in the presence of protein. Swelling studies of crosslinked polyethylene indicate no appreciable specific solvent effects for this polymer.

1. Dilute polymer solutions
2. Polymer properties
3. Polymer structure

I. AFSC Project 7342, Task 734203
II. Contract AF 33(616)-6968
III. Mellon Institute, Pittsburgh, Pa.
IV. T. A. Orofino et al
V. Not aval fr OTS
VI. In ASTIA collection

Aeronautical Systems Division, Dir/Materials and Processes, Nonmetallic Materials Lab, Wright-Patterson AFB, Ohio
Rpt No. ASD TR 61-22, Pt II. POLYMER STRUCTURES AND PROPERTIES. Final report, Oct 62, 103 pp. incl illus., tables, 64 refs.
Unclassified Report

Theoretical studies of the thermodynamical configurational properties of polymers in dilute solution are described. Experimental results are reported on the effects of chain branching in both good and poor solvents and on specific solvent effects on chain dimensions. Refinements have been made in the design of a light scattering photometer, and

(over)

calibration procedures have been critically evaluated. Melt viscosities of mixtures of polymer fractions appear to depend on the viscosity average molecular weight in a theta solvent rather than a higher molecular weight average. New characterization data have been obtained for the vinyl acetate polymer from emulsion polymerization in the presence of protein. Swelling studies of crosslinked polyethylene indicate no appreciable specific solvent effects for this polymer.

1. Dilute polymer solutions
2. Polymer properties
3. Polymer structure

I. AFSC Project 7342, Task 734203
II. Contract AF 33(616)-6968
III. Mellon Institute, Pittsburgh, Pa.
IV. T. A. Orofino et al
V. Not aval fr OTS
VI. In ASTIA collection

Aeronautical Systems Division, Dir/Materials and Processes, Nonmetallic Materials Lab, Wright-Patterson AFB, Ohio
Rpt No. ASD TR 61-22, Pt II. POLYMER STRUCTURES AND PROPERTIES. Final report, Oct 62, 103 pp. incl illus., tables, 64 refs.
Unclassified Report

Theoretical studies of the thermodynamical configurational properties of polymers in dilute solution are described. Experimental results are reported on the effects of chain branching in both good and poor solvents and on specific solvent effects on chain dimensions. Refinements have been made in the design of a light scattering photometer, and

(over)

calibration procedures have been critically evaluated. Melt viscosities of mixtures of polymer fractions appear to depend on the viscosity average molecular weight in a theta solvent rather than a higher molecular weight average. New characterization data have been obtained for the vinyl acetate polymer from emulsion polymerization in the presence of protein. Swelling studies of crosslinked polyethylene indicate no appreciable specific solvent effects for this polymer.

1. Dilute polymer solutions
2. Polymer properties
3. Polymer structure

I. AFSC Project 7342, Task 734203
II. Contract AF 33(616) -6968
III. Mellon Institute, Pittsburgh, Pa.
IV. T. A. Orofino et al
V. Not aval fr OTS
VI. In ASTIA collection

Aeronautical Systems Division, Dir/Materials and Processes, Nonmetallic Materials Lab, Wright-Patterson AFB, Ohio
Rpt No. ASD TR 61-22, Pt II. POLYMER STRUCTURES AND PROPERTIES. Final report, Oct 62, 103 pp. incl illus., tables, 64 refs.
Unclassified Report

Theoretical studies of the thermodynamical configurational properties of polymers in dilute solution are described. Experimental results are reported on the effects of chain branching in both good and poor solvents and on specific solvent effects on chain dimensions. Refinements have been made in the design of a light scattering photometer, and

(over)

calibration procedures have been critically evaluated. Melt viscosities of mixtures of polymer fractions appear to depend on the viscosity average molecular weight in a theta solvent rather than a higher molecular weight average. New characterization data have been obtained for the vinyl acetate polymer from emulsion polymerization in the presence of protein. Swelling studies of crosslinked polyethylene indicate no appreciable specific solvent effects for this polymer.

1. Dilute polymer solutions
2. Polymer properties
3. Polymer structure

I. AFSC Project 7342, Task 734203
II. Contract AF 33(616) -6968
III. Mellon Institute, Pittsburgh, Pa.
IV. T. A. Orofino et al
V. Not aval fr OTS
VI. In ASTIA collection